Statistical Analysis of Extreme Climate events in Brandenburg

A thesis approved by the Faculty of Environmental Sciences and Process Engineering at the Brandenburg

University of Technology in Cottbus-Senftenberg in partial fulfilment of the requirement for the award of the academic degree of Doctor of Philosophy (Ph.D.) in Environmental Sciences

by

Master of Science

Ni An

From Shenyang, Liaoning, VR. China

Supervisor: Prof. Dr. rer. nat. Eberhard Schaller

Supervisor: Prof. Dr. rer. nat. habil. Ralf Wunderlich

Day of the oral examination: 08.05.2015

Table of Contents

List of tables

List of figures

1 Introduction

It is a common sense nowadays that the increase of anthropogenic greenhouse gases has caused the general climate changes since the last century. In the report of IPCC (IPCC, 2007), it is estimated that on the global scale for the next two decades a warming of about 0.2K per decade can be expected on the basis of the SRES (Special Report on Emission Scenarios) emission scenarios (Nakicenovic et al., 2000). Even if the concentrations of all greenhouse gases remained on the same level as 2000, a further warming of about 0.1K per decade can still be expected. The updated 100-year linear trend from 1906-2005 shows a global mean temperature increase of 0.74K (IPCC, 2007). For many land regions even a higher increase of the annual mean temperature is estimated. This anthropogenic induced climate change persists over all scales, global and regional and for all atmospheric observables. On a regional climate model about 200km for example, the largest warming in Europe is likely to happen in the northern part in winter and in the Mediterranean area in summer (Christensen et al., 2007). Annual precipitation is estimated to increase in most of northern Europe and decrease in most of the Mediterranean area. For Germany, the changing tendencies are even more obvious. For example, an increase of 1K in temperature and 9% in precipitation from 1901-2000 have been stated (Schoenwiese et al., 2006).

These changes occur not only in the mean values but are also noticed in the extremes as well. There is an increasing concern about temperature extremes which are expected to become more frequent, longer and more severe (Mehl et al., 2004). Extremes of daily precipitation are very likely to increase as well throughout Europe (Boberg et al., 2008). These kinds of climate changes especially in extreme values can have considerable socio-economic influences in different aspects, such as agriculture, industry and flood-risk management. It has been reported that there have been more frequent and destructive floods in Germany during the last two decades than recorded, such as floods in 1997 and 2010 in the river of Oder (Disse et al., 2001; Bronstert 2003 and Kreibich et al., 2009). It is obviously important to study the climate changing pattern, adjust to adapt to them and prevent severe damages on economics and human life.

Currently different climate models are applied to simulate the climate conditions on a global scale and regional scales. They have the potential to provide climate information on both mean and extreme conditions (Beniston et al., 2006). From time

series analysis of observations, it is known that climate change signals can be significantly different on spatial scales in the order of tens of kilometers (Panitz et al., 2010). Therefore, a climate model with a fine resolution of 0.5° or less is required which the COSMO-CLM model used in this paper can provide. The CLM model is a three-dimensional non hydrostatical model, forced by global scenarios using ECHAM5-MPIOM (Boehm et al., 2006). This model solves prognostic equations for wind, pressure, air temperature, different phases of water, soil temperature and soil water content (Panitz et al., 2010). Further details on CLM can be found on the web-page of the CLM community (http://www.clm-community.eu/).

The CLM model has been validated for different purposes. For example, the simulated precipitation discharge and observed discharge using a soil and water integration model driven by COSMO-CLM in Germany were in good agreement (deviation within ±10 %) in the period of 1961-2000 (Huang et al., 2013). The model has been applied to other regions besides Europe, eg. in Asia (Zhong et al., 2013; Meng et al., 2013 and Tang et al., 2013) and Africa (Panitz et al., 2013 and Lutz et al., 2013). The current studies are mainly focused on mean values and the evaluation results over several regions reveal that the CLM presents an overestimation in mean precipitations and a cold Bias in mean temperatures (Rockel et al., 2008; Berg et al., 2011 and Panitz et al., 2010). However, very few studies have assessed the performance on the extreme climate events and the evaluation results on extreme events may not always coincide with that of the mean values.

For example, a preliminary comparison is carried out using the observation record from German weather service (Deutscher Wetterdienst, DWD) in Cottbus compared with simulated results in the grid cell in the same location. According to the simulation run of C20_2, the average annual temperature in 1961-2000 is 8.1°C which is 1K smaller than the observed of 9.1°C. However, although the simulations present an underestimation at most of the values and the mean value, the analysis on the extreme low values showed opposite results. Table 1.1 shows the differences between the simulations and observed data at different percentages in 40 years in Cottbus 1961-2000.

Table 1.1 Sorted daily 2m temperature in Cottbus 1961-2000

	OBS. T [°C]	CLM 20_1 [°C]	CLM 20_2 [°C]	CLM 20_3 [°C]
0	-20.0	-17.1	-18.0	-16.8
1%	-9.9	-8.1	-8.4	-7.2
5%	-3.8	-3.2	-3.4	-2.5
10%	-0.9	-0.8	-1.0	-0.5
50%	9.4	8.6	8.3	8.7
90%	19.3	17.6	17.6	17.8
95%	21.4	19.7	19.7	19.8
99%	24.5	23.6	23.3	23.8
100%	30.7	30.7	30.6	30.2

The table presents the daily mean temperature of 30 years from 1961-2000, with the observation record in the second column and the results for 3 simulations in the other columns. In climate analysis, the extreme conditions are always considered to be the lowest or highest 5 percentile of a distribution. In this comparison, the lowest 5 percent of the data presents an overestimation with all 3 simulations and the lower the values are, the larger differences they have. For the rest of the distribution, the underestimation is obvious, as well as at extreme high temperatures. The simulations underestimate at extreme high conditions and overestimate the temperatures at extreme cold conditions, which can also be seen as an underestimation of the intensity of the coldness.

With precipitation simulations, according to the preliminary analysis there is an overestimation in annual values in all the simulation runs over the period of 1961-2000. Figure 1.1 shows the sorted precipitation simulation results in Cottbus. The x axis represents the lowest to the highest value in 40 years.

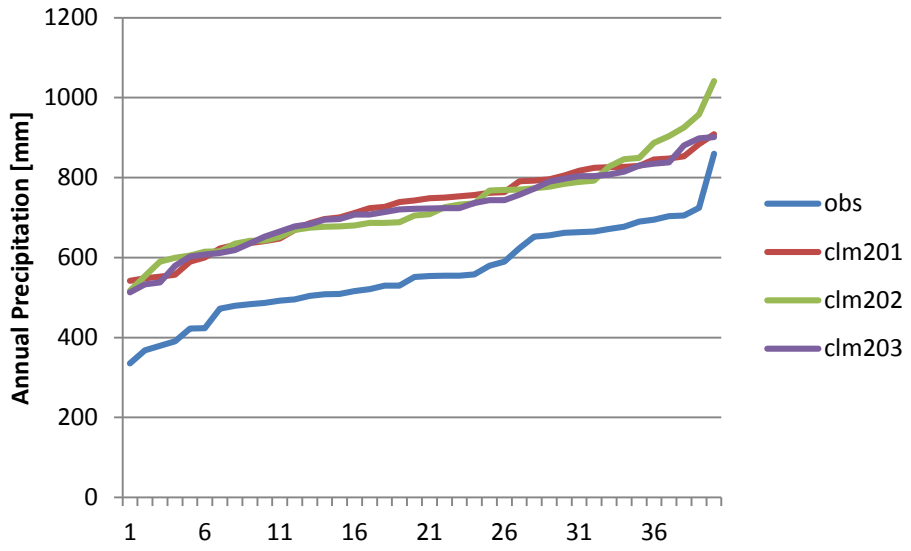

Figure 1.1 Comparison of the sorted annual precipitation in Cottbus 1961-2000

The observed precipitation records (represented by blue line in the figure) is much lower than the simulations (represented by the other 3 colors), the average difference is about 200mm/a. One reason of the overestimation in annual values lies in the fewer dry days in the simulated results, seen in the figure 1.2.

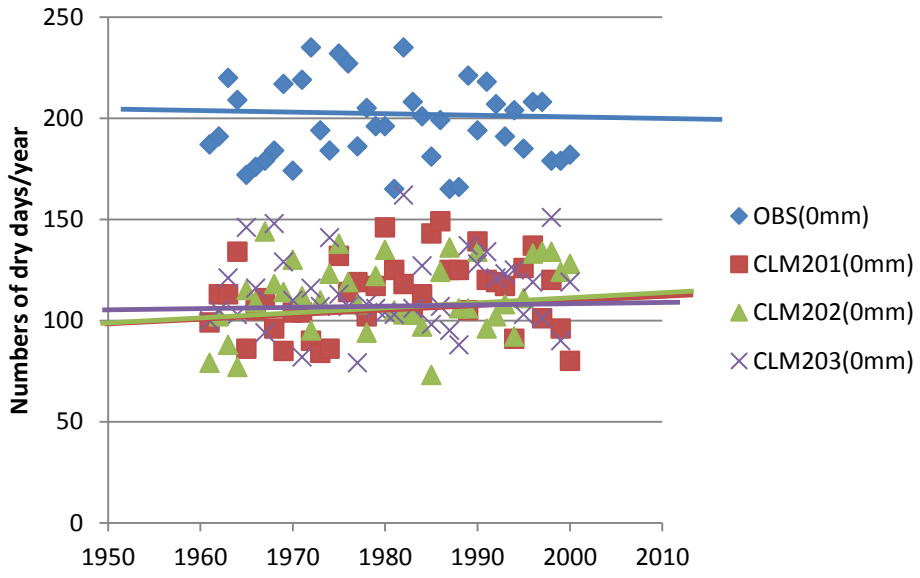

Figure 1.2 Numbers of dry days per year in Cottbus from 1961-2000

In the period of 1961-2000 in Cottbus, the observed record shows around 200 dry days per year with zero precipitation, while in simulations there are only about 100-150 dry days. This is due to the sensitivity and complixity of the model that collects detailed information that can cause precipitation, and forms into data with very small values that in reality should be 0. This difference on the dry days has not been solved yet, but the research carries on. Except for the overestimation on the dry days, the precipitations are higher below the 95 percentile in the simulations and lower above the 95 percentile, seen table 1.2.

Table 1.2 Sorted daily precipitation values in Lindenberg 1961-2000

	OBS. Prec. [mm]	CLM 20_1 [mm]	CLM 20_2 [mm]	CLM 20_3 [mm]
0	0	0	0	0
1%	0	0	0	0
5%	0	0	0	0
10%	0	0	0	0
50%	0	0.6	0.6	0.6
90%	4.7	6.5	6.4	6.3
95%	7.7	9.6	9.2	9.3
99%	17.2	16.7	17.5	16.6
100%	171.7	87	65.9	86.3

In the upper 10 percent of the daily precipitation, the simulations present higher values than the observation, the differences are up to 2mm, indicating an overestimation on precipitation extremes. Meanwhile, the single highest precipitation event in this period was a 171.7mm/d. The study on the extreme precipitation will reveal if this kind of extreme large amount of precipitation will occur in the next century or how often will it occur.

The preliminary analysis shows that the model has a tendency of overestimating the extreme precipitation and underestimating on the intensity of extreme temperatures. In this thesis the evaluation of model performance is therefore mainly focused on extreme conditions. From the distributions of the daily temperature and precipitation, the highest 5 percent and lowest 5 percent are selected and analyzed as extremes. The comparison with corresponding observation records in the period of 1961-2000 is carried out. Through analysis on the distinct behaviors of the distributions, a bias correction method will be invented correspondingly and used on the simulation

projections untill the end of the century. The climate signals therefore will be reanalyzed with the corrected simulated data. Except for the daily extreme values, the detailed climate information simulated by the CLM provides the possibility to study the change on diurnal temperature range or daily temperature difference (daily maximum temperature minus daily minimum temperature). This parameter has drawn more attentions because of the correlation to Forbush deceases (Dragic et al., 2011) and chronic obstructive pulmonary disease death (Song et al., 2008). The simulations will reveal whether the diurnal temperature will change with the increase of temperature. Apart from daily values, the analysis on seasonal temperatures and monthly precipitations will also be conducted to demonstrate that the bias correction method can be used for different time ranges and analyzing purposes.

The investigated area is Brandenburg located in the Northeast of Germany. The comparison is made between the simulated results of the CLM models and the observation data provided by the dwd. The descriptions of the data and the parameters are presented in chapter 2. In chapter 2, the modeling techniques are also introduced and the two different bias correction methods are compared, one of which is a distribution oriented method involving the creation of a transfer function used in this paper. Chapter 3 is a brief introduction on the basic concepts in statistics and the empirical distributions. The transfer functions are created with the software Easyfit, which will be presented in chapter 3 as well. Once the transfer functions are generated, the corrections will be made and the results will be shown in chapter 4. The correction is firstly carried out on the historical runs of 1961-2000. After the correction is proven to be effective on historical runs and also have positive results on testifying runs of 1972-2008, the correction will be used on the projections until 2100. The conclusions will be generalized in chapter 5.

2 Description of data

2.1 Observation and simulation data sets

The investigated period is from 1960-2000 as the historical runs and 2001-2100 as the projections. In order to reveal the climate changing pattern, long term climate conditions must be studied. Commonly a time period of at least 10 years must be enfolded. In this study, 30 year time series are selected as the analysis time range, which will be demonstrated in chapter 2.1.2 as well.

2.1.1 Research area and observation data

The investigated area is Brandenburg, which is one of the sixteen federal states of Germany with the capital of Potsdam. It is located in the east of the country surrounding Berlin, the national capital of Germany. It is known for its well-preserved natural environment. The land structure map is shown in figure 2.1. It is constructed mostly with old and young Moraine highland and between them lie the lowlands as Rhinluch , the Havellaendisches Luch and a chain of lakes. The Oder and Elbe rivers form a part of the eastern and western border. The main rivers are the Havel and the Spree which flows through the wetland region called Spreewald in the southeast.

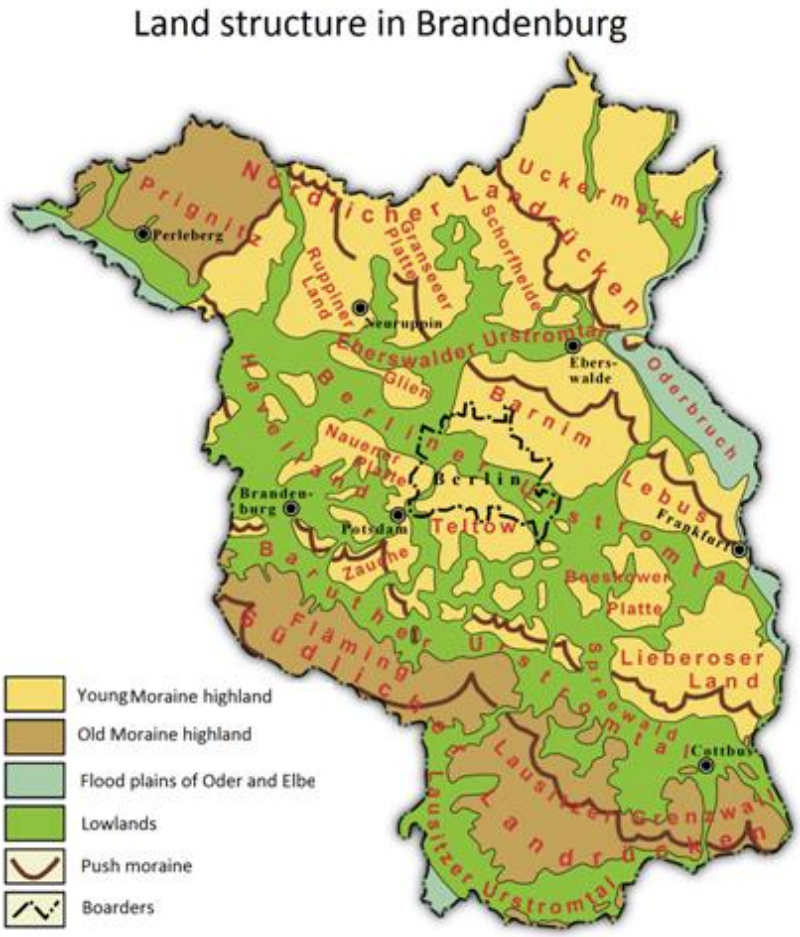

Figure 2.1 Land structure in Brandenburg

sourece:http://de.wikipedia.org/wiki/Brandenburg

Brandenburg is located in the transition zone from oceanic climate in Western Europe to the continental climate in the east (Hendel et al., 1994). Due to the relatively small height differences, the climatic differences within the state are small. Since it is located in a relatively dry region and characterized by mainly sandy soils, Brandenburg is vulnerable to climate change impacts (Holsten et al., 2009). According to the data of the German Weather Service, the average annual temperature has significantly increased during the last decades as seen in figure 2.2. The average annual temperature of the period from 1960-1990 is 8.7°C and in the period of 1971-2000 is 9.0°C, increased by 0.3K.

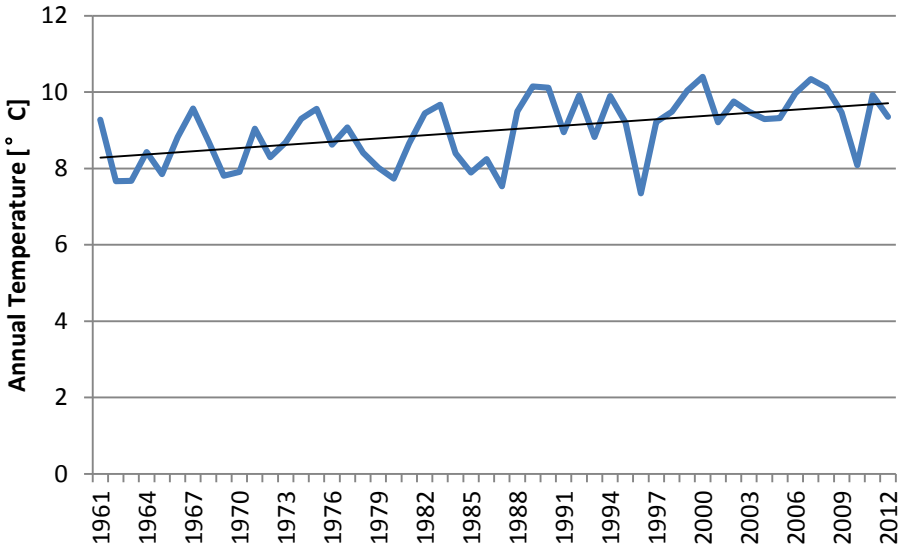

Figure 2.2 Average annual temperature from 1960-2012

Source:http://www.dwd.de/bvbw/appmanager/bvbw/dwdwwwDesktop?_nfpb=true&_pageLabel=_dwdwww_klima_umwelt_klimadaten_deutschland&T82002gsbDocumentPath=Navigation%2FOeffentlichkeit%2FKlima__Umwelt%2FKlimadaten%2Fkldaten__kostenfrei%2Fdaten__gebietsmittel__node.html%3F__nnn%3Dtrue (DWD,2014)

Brandenburg is famous for its landscapes with the lakes, moors and abundance of water stands, but in contrast is the situation of low precipitation as compared with other regions. The average annual precipitation since 1960 is 570mm and much lower compared to the annual average of Germany of 800mm.

There are 72 stations with records dated from 1960 or earlier in Brandenburg, but most of them are exclusive stations measuring precipitation. 12 of them are Climate weather stations with both temperature and precipitation measurements. However, due to the incomplete records, only 7 of the 12 can be chosen as analysis objects. The detailed records information of stations in the network of dwd can be found in the following table 2.1.

Table 2.1 Data records information of stations in Brandenburg in the network of dwd (*represents the station investigated with temperature and precipitation records)

Stations location	Period used		Parameters			
			Tmin	T 2m	Tmax	Prec.
Neuruppin *	1960	2010	×	×	×	×
Angermuende*	1947	2009		×		from 1951
Potsdam*	1893	2010	×	×	×	×
Tempelhof*	1948	2010	×	×	×	×
Lindenberg*	1947	2010	×	×	×	from 1951
Cottbus*	1951	2009	×	×	×	×
Wittenberg*	1947	2008		×		from 1951
Zehdenick	1949	2009		missing 1991		from 1951
Doberlug-Kirchhain	1949	2009		missing 1991		from 1951
Muencheberg	1949	2009		missing 1981,1991,2001		from 1951
Woldegk	1951	1990		From 1979		×
Berlin-Schoeneiche	1951	2009				×
Altdoebern	1969	2005				×
Zahna	1951	2002				×
Treuenbrietzen	1951	2009				×
Schoenewalde	1951	2001				×
Seelow	1951	2005				×
Ogrosen	1975	2005				×
Ruhland	1951	2005				×
Ruednitz	1951	2009				×
Penkun	1951	2005				×
Peickwitz	1951	2003				×
Hoyerswerda	1951	2005				×
Spremberg-Klaeranlage	1951	2005				×
Bahnsdorf	1973	2005				×
Dahme	1951	2005				×
Drebkau	1951	2009				×
Eberswalde	1951	2005				×
Friedrichswalde	1951	2009				×
Grambow	1951	2003				×
Herzberg	1931	1998				Untill 1998
Luckenwalde	1951	2001				×
Lieberose	1951	2009				×

Annaburg	1951	2005				×
Beeskow	1951	2009				×
Burg/Spreewald	1951	2000				×
Storkow	1951	2005				×
Frankfurt/Oder	1951	2009				×
Fuerstenwalde	1951	2009				×
Fuerstlich Drehna	1951	2009				×
UEbigau	1951	2005				×
Velten	1951	2005				×
Elsterwerda	1951	2009				×
Guben	1951	2005				×
Haselberg	1951	2009				×
Hohenbucko	1951	2009				×
Jueterbog	1951	2009				×
Kyritz	1951	2009				×
Maerkisch Buchholz	1951	2001				×
Petkus	1951	2009				×
Paewesin	1951	2005				×
Prenzlau	1951	2009				×
Rathenow	1951	2009				×
Rutenberg	1951	2009				×
Fuerstenberg	1951	2009				×
Gartz/Oder	1951	2005				×
Bran-Goerden	1951	2007				×
Brueck-Goemnigk	1951	2009				×
Hohenreinkendorf	1951	2009				×
Karstaedt/Prignitz	1951	2009				×
Lenzen	1951	2009				×
Meyenburg	1951	2009				×
Neutornow	1951	2009				×
Wittstock	1951	2009				×
Bredereiche	1951	2003				×
Goeritz	1951	2003				×
Hirschfeld	1951	2005				×
Hoppenrade	1951	2005				×
Kemlitz	1951	2005				×
Koenigshorst	1951	2001				×
Loewenberg	1951	2005				×
Neustadt-Kampehl	1951	2001				×

Among the 72 stations, except Woldegk and Herzberg which do not have long enough record to 2000, 70 stations keep the records required for the analysis in precipitation in the period of 1960-2000. At four of the 12 stations, the temperature records suffer from incomplete data. Both Zehdenick and Doberlug-Kirchhain records do not include the data of 1991. In station Muencheberg, the records of 1981, 1991 and 2001 are missing. The records of Woldegk start from 1979. Therefore, only 7 stations with intact temperature records can be used for the temperature analysis, namely Cottbus, Lindenberg, Neuruppin, Tempelhof, Potsdam, Wittenberg and Angermuende. Two stations of the seven, namely Wittenberg and Angermuende only keep measurements of daily mean temperature, thus it is not possible to compare the daily temperature difference records with simulations. Therefore, the diurnal temperature range (daily maximum temperature minus daily minimum temperature) analysis is restrained within the 5 stations, namely Cottbus, Lindenberg, Neuruppin, Tempelhof and Potsdam. All the stations are shown in the following figure 2.3 with the temperature stations circled out. The ones in blue circles are where both temperature extremes and daily temperature differences are investigated and the two in purple circles are only with mean temperature records.

2.1.2 Simulation data and data sets

As mentioned, Brandenburg is covered by 110 grid cells in the model which are marked in red in figure 2.3. For temperature analysis, since there are only 7 stations with records dated from 1960, the comparisons are made between the 7 stations and the grid cells with the center coordinates closest to them. The number of stations with precipitation records are however 70, meaning that it is reasonable to find one station for each grid cell to compare with. Therefore the precipitation analysis will be taken out within 110 grid cells. The coupling of stations and grid cells are listed in table 2.2 with their coordinates.

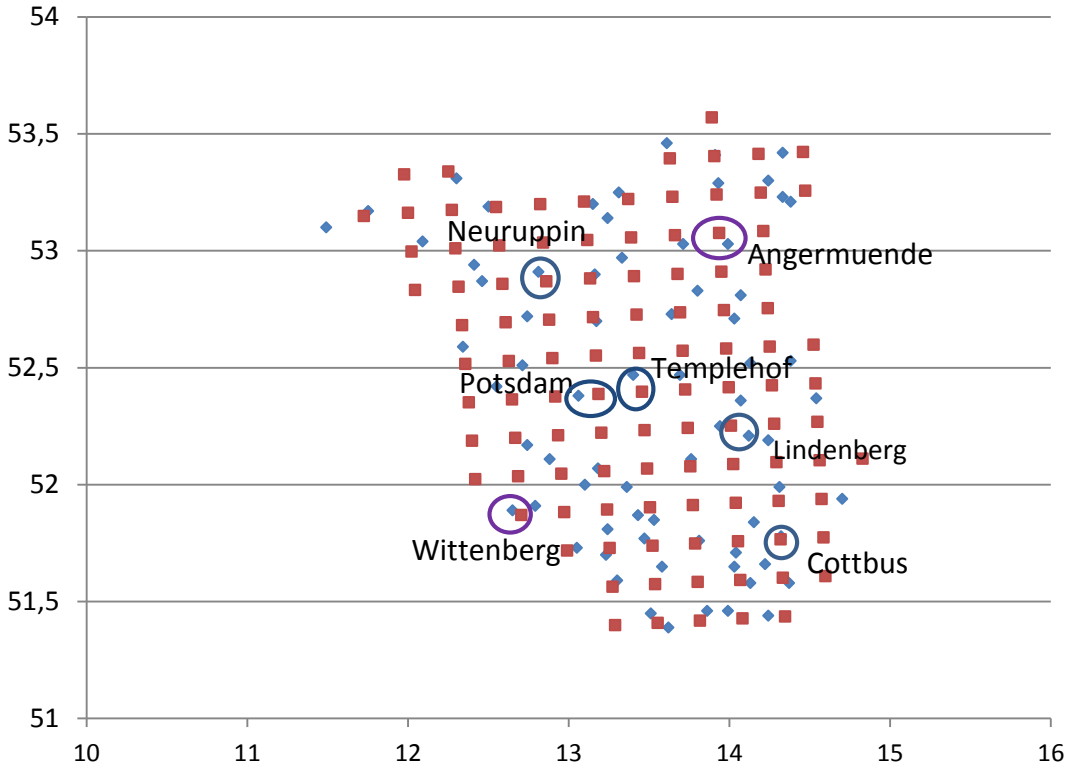

Figure 2.3 Weather stations (blue) and grid cell centers of CLM (red) in Brandenburg

Table 2.2 CLM gird cells and observation stations coupling with coordinates

(*marks those grid cells where both Temperature and Precipitation have been investigated.)

	CLM grid cell	Coordinates		Station	Coordinates	
		°E	°N		°E	°N
1	134_150	12.84	53.03	Neuruppin	12.81	52.91
2*	134_149	12.86	52.87	Neuruppin		
3	132_143	12.97	51.88	Neuruppin		
4	136_150	13.39	53.06	Zehdenick	13.33	52.97
5	136_149	13.41	52.89	Zehdenick		
6	136_148	13.42	52.73	Zehdenick		
7*	138_150	13.94	53.08	Angermuende	13.99	53.03
8	138_149	13.95	52.91	Angermuende		
9*	132_146	12.92	52.38	Potsdam	13.06	52.38
10	135_146	13.19	52.39	Potsdam		
11*	136_147	13.44	52.56	Tempelhof	13.4	52.47
12	136_146	13.46	52.40	Tempelhof		

13	136_145	13.47	52.23	Tempelhof		
14	137_147	13.71	52.57	Berlin-Schoeneiche	13.69	52.47
15*	137_146	13.73	52.41	Berlin-Schoeneiche		
16	138_145	14.01	52.25	Lindenberg	14.12	52.21
17	138_144	14.02	52.09	Lindenberg		
18*	139_142	14.32	51.77	Cottbus	14.32	51.78
19	132_144	12.42	52.02	Wittenberg	12.65	51.89
20	133_144	12.69	52.04	Wittenberg		
21*	133_143	12.70	51.87	Wittenberg		
22	137_141	13.80	51.58	Ruhland	13.86	51.46
23	137_140	13.82	51.42	Ruhland		
24	137_152	13.63	53.40	Friedrichswalde	13.71	53.03
25	137_151	13.65	53.23	Friedrichswalde		
26	137_150	13.66	53.07	Friedrichswalde		
27	137_149	13.68	52.90	Friedrichswalde		
28	135_145	13.20	52.22	Luckenwalde	13.18	52.07
29	135_144	13.22	52.06	Luckenwalde		
30	134_142	12.99	51.72	Annaburg	13.05	51.73
31	139_145	14.28	52.26	Beeskow	14.24	52.19
32	138_153	13.89	53.57	Goeritz	13.91	53.41
33	138_152	13.91	53.40	Goeritz		
34	140_146	14.54	52.43	Frankfurt/Oder	14.54	52.37
35	140_145	14.55	52.27	Frankfurt/Oder		
36	140_144	14.56	52.10	Frankfurt/Oder		
37	138_142	14.05	51.76	Ogrosen	14.04	51.71
38	138_141	14.07	51.59	Ogrosen		
39	137_143	13.77	51.91	Fuerstlich Drehna	13.81	51.76
40	137_142	13.79	51.75	Fuerstlich Drehna		
41	135_141	13.27	51.56	Uebigau	13.3	51.59
42	135_140	13.29	51.40	Uebigau		
43	135_148	13.15	52.72	Velten	13.17	52.7
44	135_147	13.17	52.55	Velten		
45	136_140	13.55	51.41	Elsterwerda	13.51	51.45
46	140_143	14.57	51.94	Guben	14.7	51.94
47	140_142	14.59	51.77	Guben		
48	140_141	14.60	51.61	Guben		
49	141_144	14.83	52.11	Guben		
50	137_145	13.74	52.24	Maerkisch Buchholz	13.76	52.11
51	137_144	13.76	52.08	Maerkisch Buchholz		

52	136_144	13.49	52.07	Petkus	13.36	51.99
53	133_147	12.63	52.53	Paewesin	12.71	52.51
54	132_147	12.90	52.54	Paewesin		
55	136_151	13.37	53.22	Rutenberg	13.31	53.25
56	135_151	13.10	53.21	Fuerstenberg	13.15	53.2
57	135_150	13.11	53.05	Fuerstenberg		
58	130_151	11.72	53.15	Karstaedt/Prignitz	11.75	53.17
59	130_150	11.75	52.98	Karstaedt/Prignitz		
60	131_152	11.98	53.33	Karstaedt/Prignitz		
61	132_152	12.25	53.34	Meyenburg	12.3	53.31
62	132_151	12.27	53.17	Meyenburg		
63	138_148	13.97	52.75	Neutornow	14.07	52.81
64	138_147	13.98	52.58	Neutornow		
65	139_149	14.22	52.92	Neutornow		
66	139_148	14.24	52.75	Neutornow		
67	133_151	12.55	53.19	Wittstock	12.5	53.19
68	134_151	12.82	53.20	Wittstock		
69	131_151	12.00	53.16	Hoppenrade	12.09	53.04
70	131_150	12.02	53.00	Hoppenrade		
71	131_149	12.04	52.83	Hoppenrade		
72	132_149	12.32	52.85	Neustadt-Kampehl	12.46	52.87
73	133_149	12.59	52.86	Neustadt-Kampehl		
74	138_146	14.00	52.42	Muencheberg	14.13	52.52
75	139_147	14.25	52.59	Muencheberg		
76	139_146	14.27	52.43	Muencheberg		
77	136_141	13.54	51.57	Doberlug-Kirchhain	13.58	51.65
78	132_145	12.93	52.21	Treuenbrietzen	12.88	52.11
79	132_144	12.95	52.05	Treuenbrietzen		
80	128_151	11.18	53.12	Lenzen	11.49	53.1
81	129_151	11.45	53.13	Lenzen		
82	132_150	12.29	53.01	Hoppenrade	12.09	53.04
83	133_150	12.57	53.02	Neustadt-Kampehl	12.46	52.87
84	132_146	12.38	52.35	Bran-Goerden	12.55	52.42
85	132_145	12.40	52.19	Bran-Goerden		
86	133_146	12.65	52.36	Bran-Goerden		
87	133_145	12.67	52.20	Brueck-Goemnigk	12.74	52.17
88	133_148	12.61	52.69	Koenigshorst	12.74	52.72
89	134_148	12.88	52.71	Koenigshorst		
90	132_148	12.34	52.68	Loewenberg	13.16	52.9

91	132_147	12.36	52.52	Loewenberg		
92	135_149	13.13	52.88	Loewenberg		
93	135_143	13.24	51.89	Schoenewalde	13.24	51.81
94	135_142	13.25	51.73	Schoenewalde		
95	136_143	13.50	51.90	Dahme	13.43	51.87
96	136_142	13.52	51.74	Dahme		
97	137_148	13.69	52.74	Eberswalde	13.8	52.83
98	138_151	13.92	53.24	Prenzlau	13.93	53.29
99	138_140	14.08	51.43	Peickwitz	13.99	51.46
100	138_143	14.04	51.92	Burg/Spreewald	14.15	51.84
101	139_152	14.18	53.41	Penkun	14.24	53.3
102	139_151	14.20	53.25	Penkun		
103	139_150	14.21	53.08	Penkun		
104	139_144	14.29	52.10	Lieberose	14.31	51.99
105	139_143	14.31	51.93	Lieberose		
106	140_152	14.46	53.42	Grambow	14.33	53.42
107	140_151	14.47	53.26	Hohenreinkendorf	13.47	51.77
108	139_141	14.33	51.60	Spremberg-Klaeranlage	14.37	51.58
109	139_140	14.35	51.44	Spremberg-Klaeranlage		
110	140_147	14.52	52.60	Spremberg-Klaeranlage		

The 110 pairs in the table are all objectives for the precipitation analysis, including daily precipitation extremes and monthly precipitation. The ones marked with stars are where the temperatures are analysis, namely 2, 7, 9, 11, 15, 18, 21 and the corresponding stations are Neuruppin, Angermuende, Potsdam, Tempelhof, Lindenberg, Cottbus and Wittenberg respectively. The temperature analysis includes daily extreme temperatures, daily temperature difference and seasonal temperature.

The analysis includes three time series, which are historical runs from 1960-2000, small part of validation runs from 1972-2008 and the projections from 2001-2100. From the first part, the distribution behaviors of each kind of parameters will be studied and the bias correction methods will be determined and used on simulated data. In the second part, the effectiveness of the bias correction methods is tested and validated on the simulated runs from 1972-2008. For the projections, the correction

will be made and the climate change signals will be reanalyzed. Data sets are consistent within the investigation period in a way of data runs. In the historical runs for example, the time period is 41 years from 1960-2000 and the time range of each data set is 30 years. To maximize the numbers of data sets, 12 data sets of 30 years are drawn from the 41 years, with the first one of 1960-1989, followed by 1961-1990, 1962-1991 untill the last data set of 1971-2000. In the projection simulations, the same kinds of data runs are created as well and there are 71 data sets in the period from 2001-2100. The correction method is determined from the 12 data sets of historical runs and then used on the 71 data sets of the projections.

2.2 Modeling techniques

Although many global Atmosphere-Ocean General Circulation Models (AOGCMs) show a good performance in simulating large-scale patterns of climate parameters, they fail to provide detailed information for smaller scales. To overcome this problem downscaling methods are developed to deduce this information from large scale AOGCMs. Two main techniques exist, statistical downscaling and dynamical downscaling. With statistical downscaling, relationships are derived between large-scale variables of global climate models and locally observed regional climate variables based on a control climate, which is then applied to a projected climate. The main drawback of this method is the assumption of stability of the derived relationship when the climate is changing (Kjellstroem et al., 2007). Dynamical downscaling involves higher-resolution atmospheric regional climate models (rcm) initialized and forced at the boundaries by data from a coarser resolution AOGCMs. Rcm has been shown to be able to reproduce a broad range of climates around the world and therefore is confident in their ability to realistically downscale future climates. The analysis presented here is dynamic downscaling of global AR4 simulations over Europe, consisting of three realizations of the climate of the 20th century, and two realizations of each of the A1B and B1 projections, which were done with the regional climate model CLM.

The CLM model is a non-hydrostatic limited-area atmospheric prediction model first developed in 2001 based on the Local Model (lm), the operational weather forecast model of the Consortium for Small-scale Modeling (COSMO). The consortium was

formed by a number of meteorological services including the German Weather Service and Meteo Swiss. Scientists from BTU are among the first developers and continued to improve and optimize the model ever since. CLM has the same dynamical and physical core as the lm which is an advantage in the development of a common model for research and forecast purposes. Although at that time, many models already existed and were operating to simulate the global climate, CLM has its own advantages. For example, compared to the models operated in hydrostatic mode with grid spacings larger than 10km, the feature of non-hydrostatic allows CLM to simulate horizontal scales down to 1km. CLM is therefore able to meet high resolution regional forecast requirements and capture small scale severe weather events. The equations are discretised on a staggered horizontal grid of type Arakawa C with hybrid terrain following coordinates in the vertical direction (Doms et al., 2009). Moist convection is parameterized by the mass flux convection scheme of Tiedtke (1989). Compared to lm, CLM have many extensions implemented (Boehm et al., 2006), including a time-dependent treatment of boundary data, e.g. vegetation characteristics, soil variables, sea surface temperature and humidity and air tracer.

Besides forecasting, the COSMO model is used for various scientific purposes, such as applications of the model for large-eddy simulations, cloud resolving simulations and studies on orographic flow systems. For example, one of the ongoing projects in Meteorology department at BTU is to study the influences on regional climate if the current mining areas were to be filled with water forming lakes in the future, by changing the configuration of surface coverage. For these applications, the model is therefore applicable to both real data cases and artificial cases using idealized initial data. The model is developed according to above mentioned requirements and therefore possess features (Doms et al., 2009), such as flexible choice of initial and boundary conditions to accommodate both real data cases and idealized initial states, capable of assimilating high-frequency a synoptic data and remote sensing data and use of pure Fortran constructs to render the code portable among a variety of computer systems and so on. More introductions to the model can be found on the home page of COSMO-model (http://www.cosmo-model.org/).

The evaluation presented here is run with CLM version 2.4.6 on a spherical 0.165° grid (approx.18km). In 2006, simulations consisting two climate scenarios (A1B and B1) with two realizations each for the time period 1960-2100 driven by ECHAM5

were performed. Table 2.3 gives an overview of the ECHAM5/MPIOM experiments related to the regional projections described.

Table 2.3 ECHAM5/MPIOM IPCC AR4 forcing for CLM (Hollweg et al., 2008)

Name	Period	Description
EH5-T63L31_OM-GR1.5L40_CTL	2150-2655	Pre-industrial control experiment (CTL).
EH5-T63L31_OM-GR1.5L40_20C_1 (C20_1)	1860-2000	20th century reconstruction (20C3M) with anthropogenic forcing (greenhouse gases, sulfate) initialized in the year 2190 of the CTL.
EH5-T63L31_OM-GR1.5L40_20C_2 (C20_2)	1860-2000	Second realization of 20C3M (yr 2215 of CTL).
EH5-T63L31_OM-GR1.5L40_20C_3 (C20_3)	1860-2000	Third realization of 20C3M (yr 2240 of CTL).
EH5-T63L31_OM-GR1.5L40_A1B_1 (A1B1)	2001-2100	SRES Scenario: A1B (initialized with yr 2000 of 20C_1).
EH5-T63L31_OM-GR1.5L40_A1B_2 (A1B2)	2001-2100	Second. realization (yr 2000 of 20C_2).
EH5-T63L31_OM-GR1.5L40_B1_1 (B11)	2001-2100	SRES Scenario B1 (yr 2000 of 20C_1).
EH5-T63L31_OM-GR1.5L40_B1_2 (B12)	2001-2100	Second realization (yr 2000 of 20C_2).

The first column displays the names of data runs associated with World Data Center for Climate (WDCC). All global experiments are started from model states obtained in a 505-year long integration of the coupled global model with pre-industrial conditions. In that ’control’ experiment (CTL), the concentrations of well-mixed greenhouse gases have been specified at the observed levels of 1860 and sulphate aerosols are not included. This reconstruction is representative for the middle of the 19th century and provides the initial fields for the 20th century AR4 20C3M global ensemble simulations (rows 2 to 4 in table 2.1). Fields from different years of CTL are used to initialize the different 20C3M realizations. The state of each 20C3M global ensemble realization at the end of year 2000 is used to initialize the ipcc AR4 climate projections. Dynamical downscaling of the data from the three 20C3M global ensemble members was performed for the last four decades of the 20th century (1960–2000). These regional simulations will be used as historical runs in the analysis.

Analogously, CLM_C20 provides initial driving fields for the realizations of the regional climate projections A1B and B1. The downscaling was performed for the full 100 years simulation period of the global projections A1B and B1, from 2001-2100.

As described, CLM is using the dynamic approach to downscale the global data, therefore the observed regional climate variables have not played a role in the downscaling and the projections. It is possible to use the observed data in Brandenburg in the past decades to evaluate the performance of the model and the data can be used in the correction method as well. The bias correction method is based on the comparison between the observed data from 1960-2000 and the 3 simulated runs of C20s. To validate the correction effectiveness, the C20 simulations and projections of A1B and B1 are combined to form data sets that cover the period of 1972-2008 in the following sequence: C20_1+A1B1, C20_2+A1B2, C20_1+B11 and C20_2+B12. Afterwards the correction will be used on the projections from 2001-2100.

2.3 Distribution oriented bias correction method

In statistics, there are several forms of bias, such as the commonly mentioned systematic bias which represents external influences that may affect the accuracy of statistical measurements. In this paper, it refers to the bias of an estimator, which is the difference between an estimator's expectation and the true value of the parameter being estimated. For two data sets, simulated and observed for example, the bias is defined as the median value of the differences of simulated values minus observed values. In the example of Temperature analysis, if the bias is negative which is also called cold bias, it means that the simulation showed lower values than the observed records. The bias correction method used in this paper is a distribution oriented method to create a transfer function matching observation and simulation data. This method is based on the assumption that both observed and simulated probability distribution can be well approximated by one kind of empirical distribution. Once this distribution is determined fitting both observed and simulated data sets, the cumulative density functions (CDF) of the two will be in the same form with different parameters. The basic idea is to match the corrected simulation cdf to the observation cdf. To construct a transfer function y=f(x), where x and y are original and corrected

simulated data respectively, the distribution of y must match that of observation. Therefore, the transfer function must obey

$$cdf_{OBS}(f(x))=cdf_{sim}(x). \quad (2.1)$$

This method is developed by Piani in his paper in 2009 for the correction of daily precipitation. The validation of the methods in that paper was carried out that to apply transfer function y=f(x) inferred using simulated and observed daily precipitation from a given time period to simulated data from a different time period and compared with observation. In this paper, the correction is done in a different way. The transfer function is not derived from a single time period or one pair of observation and simulation data set. It is a generalized function from the 12 data sets in the period of 1960-2000. Once the fitted distribution is set, both observation and simulation data sets share the same kind of cdf, only with different parameters. For each data set, two sets of parameters are determined, one for the observation and one for the original simulated data. In the 41 years, there are 12 sets of observation parameters and 12 sets of simulation parameters. The median values of the 12 are taken as representative parameters to construct a general cdf which is used in equation 2.1. The f(x) solved from the equation is the transfer function for the 12 data sets. It is then applied to the 12 sets of original simulated data and compared with corresponding observation data to validate the effectiveness.

In the original method of Piani, the correction is aimed at the daily precipitation with the Gamma distribution. Here however, the precipitation is not the only parameter investigated and one single kind of empirical distribution cannot be fitted to all the data sets due to the distinctive behavior of different distributions. The major step for this method is to choose the fitted distributions for each kind of parameters; extreme temperatures, daily temperature differences, daily precipitation and so on. This step is simplified with the help of Easyfit which can list out all kinds of fitted possibilities with the comparisons of goodness of fit. Certain criteria have to be followed and the chosen distribution must meet following requirements.

1. The chosen distribution must fit to all the data in both the observational and simulated data sets. Since final transfer function is a generalized form of 12 data sets for each parameter, the chosen distribution must fit all the 12 pairs of data sets. For example, in the extreme low temperature analysis, the best fitted

function for data sets 1960-1989 was beta function followed by the second best power function. However the observed data matches best the function of pert and power. The chosen distribution will be power function for the benefits of both kinds of data sets.

2. The parameters of the chosen distribution for the 12 data sets should be relatively stable. Since the median values are used to form a representative cdf, the differences between the 12 sets of parameters should not be large. Otherwise the uncertainty of the transfer function will be increased largely, causing the failure in the correction. For example, the best fitted distribution for the winter temperature distribution should be Burr (4p) with four parameters of k, α, β, γ. However, all the parameters are spread causing the unstable median values seen in table 2.4.

Table 2.4 Unsuccessful fitted distribution Burr for simulated DJF temperature in Lindenberg with unstable parameters

Burr (4p) Lindenberg DJF Temperature				
C201	**k**	**α**	**β**	**γ**
1960-1999	2.75	586.52	1590.8	-1586.8
1961-2000	2.9409	296.36	822.39	-818.15
1962-2001	2.748	1716.5	4636.8	-4632.9
1963-2002	2.6974	271.25	735.41	-731.53
1964-2003	2.8292	156.82	433.05	-428.99
1965-2004	2.6119	320.62	863.2	-859.47
1966-2005	2.885	65.867	185.36	-181.27
1967-2006	2.8375	82.322	231.48	-227.46
1968-2007	0.2134	1.00E+09	9.20E+08	-9.20E+08
1969-2008	0.2865	4.20E+08	4.40E+08	-4.40E+08
1970-2009	2.4862	39495	1.00E+05	-1.00E+05
1971-2000	0.3468	1.20E+09	1.40E+09	-1.40E+09
Min	**0.2134**	**65.867**	**185.36**	**-1.4E+09**
Median	**2.7227**	**453.57**	**1227**	**-1223.14**
Mean	**2.136067**	**2.18E+08**	**2.3E+08**	**-2.3E+08**
Max	**2.9409**	**1.2E+09**	**1.4E+09**	**-181.27**

As shown in the table, because of the wide range of the parameters for this distribution, the median values cannot be the representative values to describe

this distribution. A correction with the median values on the data set of 1971-2000 will be failed due to the large differences in all parameters.

3. The domain of the chosen distribution has to correspond with the range of the actual data. The final representative cdf is based on the median values that may not be able to cover the whole data range. For example, if the General Pareto Distribution is used to fit the extreme low temperature in Cottbus, a distribution with the median values of parameters of -2.51, 26.45°C and -14.87°C can be determined with the domain of -14.9°C to -4.3°C. The actual data of temperature in the set of 1971-2000 is from -20°C to -3.8°C, which has a lower limit than the domain. The values smaller than -14.9°C cannot be calculated with the transfer function. Furthermore, until the end of this century, the range of the temperature is about to change which may lead to a failure in the method. Therefore, the domain of the distribution must be taken into consideration.

The detailed description of the software and the distributions that are chosen to fit different variables and their parameters are introduced in the next chapter.

3 Basic concepts and tools

3.1 Basic concepts

The analysis of extreme climate events not only includes the intensity of the severe situations, but also the frequency, which is the probability or likelihood of occurrence of an event. Probabilities are values between 0% to 100% and the higher the degree of probability, the more likely the event is to happen, or, in the case of climate samples, the greater the number of times such event is expected to happen. To analyze the probability in an intuitive way, in statistics several graphs are commonly mentioned and used.

- Probability density Function

A probability density function (pdf) is a function that describes the relative likelihood for a random variable. The probability of the random variable falling within a particular range of values is given by the integral of this variable's density over that range, meaning, it is given by the area under the density function above the horizontal axis and between the lowest and greatest values of the range. If x is a continuous random value, then the probability density function of x is a function f(x) such that for any two numbers a and b with a≤b

$$\Pr[a \le \mathrm{x} \le b] = \int_a^b f\ (x)dx\,. \tag{3.1}$$

The use of this function in the analysis of climate is to find out the parameter values in any given interval. For example, by temperature analysis, it is able to know what the probability for the temperature in a certain range is. The pdf graph is commonly linked to the histogram, which is a representation of tabulated frequencies shown as adjacent rectangles erected over discrete intervals (bins). When the bin size is finer and finer, the histogram will become a smooth curve which will represent the probability distribution for x.

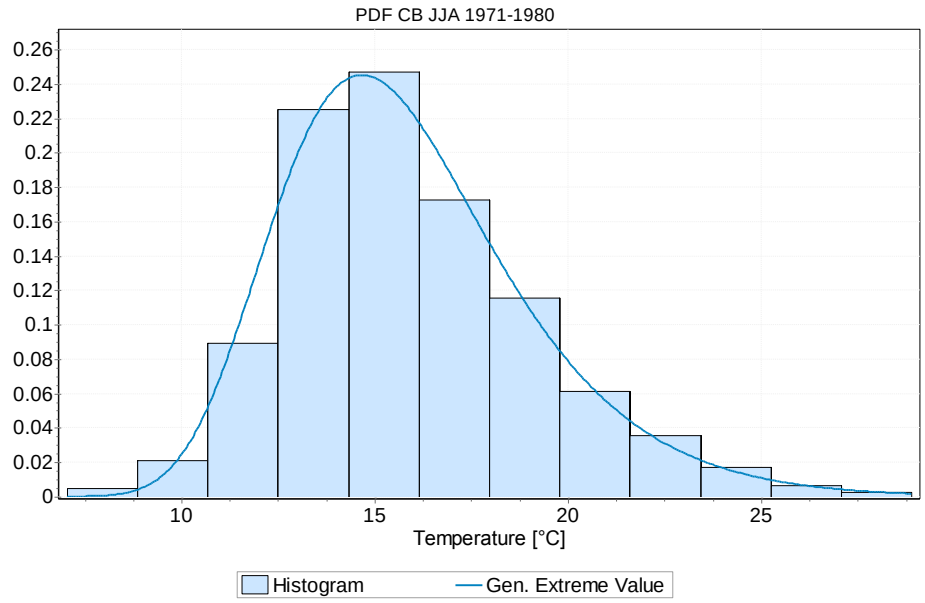

Figure 3.1 Histogram and pdf of JJA daily temperature in Cottbus 1971-2000

- Cumulative distribution Function

To study the extreme climate events, a more comprehensive way is by analyzing the cumulative distribution function (cdf), which describes the probability that a real-valued random variable x with a given probability distribution will be found at a value less than or equal to x. In the case of a continuous distribution, it gives the area under the probability density function from minus infinity to x. Hence, the expression of cdf is

$$\Pr\left[-\infty < x < b\right] = \int_{-\infty}^{b} f\,(x)dx\,. \tag{3.2}$$

In the same example of summer temperature, the cumulative distribution function can tell the probability of temperature smaller or equal to a certain value. For example, the cdf graph is shown in figure 3.2 for the same distribution as in figure 3.1.

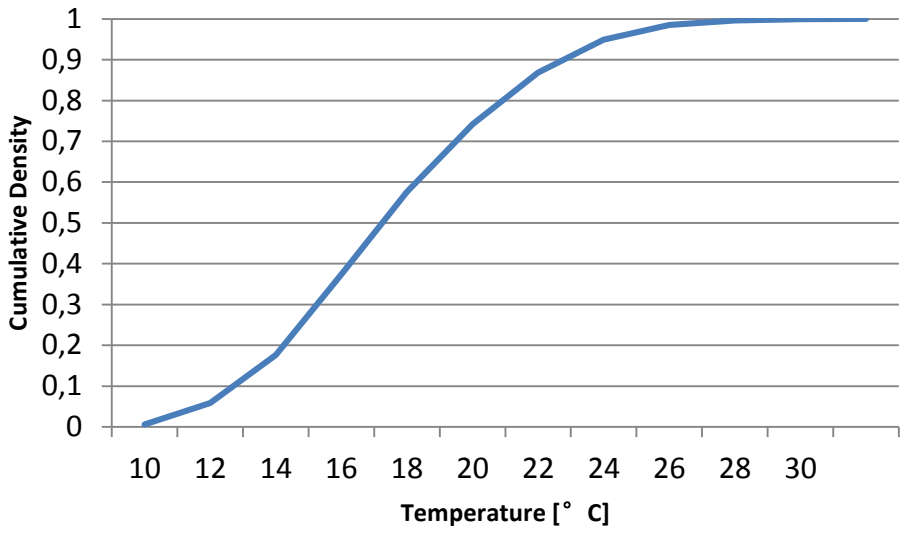

Figure 3.2 Cdf of JJA daily temperature in Cottbus 1971-2000

The temperature ≤ 22°C has a probability of 0.87, indicating that 87% of the time (2401 days) in the 30 years of 1971-2000, the temperature in summer is not more than 22°C. However, to study the extreme climate events, it is also important to know the probability of events greater than a value. Here as, the temperature higher than 22°C is 1-0.87=0.13, meaning 13% of the time, the temperature will be higher than 22°C. Similarly, the probability for temperature lower than 24°C is 0.95 considered as the 95 percentile data. Histogram, pdf and cdf are three graphs that are commonly used in the later analysis.

3.2 Easyfit and goodness of fit

The basic idea is to find an empirical distribution that fits both observed and simulation data and match the cdf of the corrected data to that of the observed. The techniques of distribution fitting used commonly in literature are parametric methods, by which the parameters of the distribution are calculated, such as method of moments, method of L-moments and maximum likelihood method or regression method using a transformation of the cumulative distribution function so that the linear relation is found between the data sets (Ritzema et al., 1994). In this paper, with the help of software Easyfit, the analysis is much easier. All the possible fitted

distributions can be found with different parameters measuring the goodness of fit. Figure 3.3 and table 3.1 show a part of the distributions fitted and their goodness of fit.

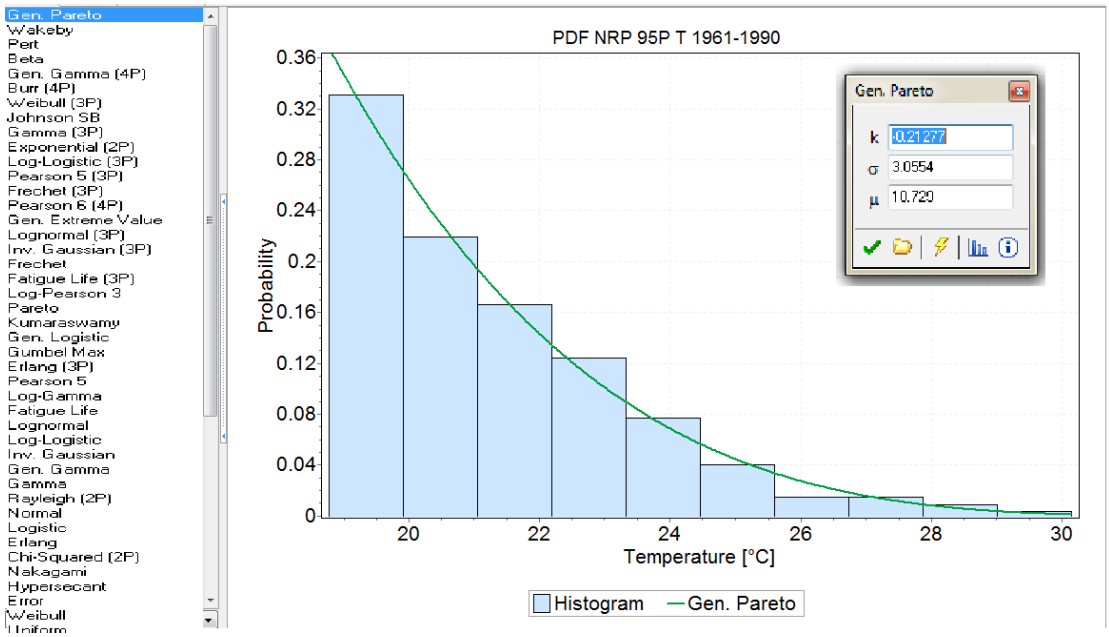

Figure 3.3 A part of distributions fitting with Easyfit: Neuruppin simulated 95p Temperature in 1961-1990

Table 3.1 Goodness of fit for different distributions for Neuruppin simulated 95p temperature in 1961-1990

Goodness of Fit - Summary

#	Distribution	Kolmogorov Smirnov		Anderson Darling		Chi-Squared	
		Statistic	Rank	Statistic	Rank	Statistic	Rank
25	Gen. Pareto	0.019	1	0.35019	1	4.2491	2
61	Wakeby	0.01917	2	7.6079	23	N/A	
51	Pert	0.02504	3	0.37259	2	3.6833	1
1	Beta	0.02615	4	4.4886	18	N/A	
23	Gen. Gamma (4P)	0.03634	5	0.74738	3	7.3807	4
3	Burr (4P)	0.03911	6	1.0791	4	9.1966	6
63	Weibull (3P)	0.0392	7	1.0921	5	9.2021	7
31	Johnson SB	0.04359	8	1.421	7	5.942	3
20	Gamma (3P)	0.04671	9	1.375	6	8.2231	5
14	Exponential (2P)	0.05415	10	2.3189	8	12.636	8

Once the data are input into the program, distribution fitting can be analyzed with all the possible results listed in the left side of figure 3.3. For example, for extreme daily temperatures in 1961-2000 in Neuruppin, the simulated data set can be fitted to General Pareto distribution, Wakeby, Beta and so on. The parameters of each distribution are also calculated shown in the right side box in the same figure. Meanwhile, the goodness of fit comparisons between these distributions can also be found out, with the results expressed in Kolmogorov-Smirov test, Anderson Darling and Chi-Squared which are 3 typical indicators of goodness of fit. The Kolmogorov–Smirnov statistic quantifies a distance between the empirical distribution function (edf) of the sample and the cumulative distribution function of the reference distribution, or between the empirical distribution functions of two samples. If the empirical distribution function is F_n, the KS statistics of a given cumulative distribution function $F(x)$ is

$$D_n = \sup_x |F_n(x) - F(x)| \tag{3.3}$$

where $\sup_x$ is the supremum of the set of distances.

The Anderson Darling test also measures in the distance between the two, but belongs to the quadratic edf and is based on the distance of

$$A = n\int_{-\infty}^{\infty} \frac{\left(F_n(x)-F(x)\right)^2}{F(x)\left(1-F(x)\right)} dF(x). \quad (3.4)$$

The results of the chi-squared test are evaluated by the chi-squared distribution. It is used to assess the goodness of fit by comparing the X^2which resembles a normalized sum of squared deviation between observed and theoretical frequencies.

The value of the test-statistics is

$$X^2 = \sum_{i=1}^{n} \frac{(O_i-E_i)^2}{E_i} \quad (3.5)$$

where

X^2= Pearson's cumulative test statistic, which asymptotically approaches a X^2.

O_i= ith observation;

E_i= an expected (theoretical) frequency, asserted by the null hypothesis;

n =the number of variables.

The determination of the best fitted distribution is combining the results of the 3 tests, with K-S test serving as primary criteria. For the sample data in table 3.1, the best fitted distribution will be Generalized Pareto Distribution with the K-S test statistic of 0.019 ranking number 1, Anderson Darling statistic of 0.35 and Chi-squared of 4.2591 as the best fitted distribution.

3.3 Chosen Empirical distributions

Several distributions are compared and three are chosen for the description of analyzed data sets, as shown in table 3.2.

Table 3.2 Chosen distributions for the analyzed paramaters

Analyzed data	Chosen Distribution
95 P Temperature	Generalized Pareto Distribution (GPD)
5P Temperature	Power distribution
95P Precipitation	GPD

Monthly Precipitation	GEV
Winter Temperature (DJF)	Generalized extreme distribution (GEV)
Summer Temperature (JJA)	GEV
Daily Temperature difference	GEV

The three chosen distributions are Generalized Extreme value distribution (GEV) for daily temperature difference (T_{diff}) and seasonal daily temperature (T_s), Generalized Pareto Distribution (GPD) for daily extreme temperature (95P T),extreme precipitation (95P Prec.) and monthly precipitation ($Prec_{m.}$) and Power distribution for extreme low daily temperature (5P T).

- Generalized Extreme Value Distribution (Seen in figure 3.4)

Generalized Extreme Value Distribution is a single family that combines the more commonly known Gumbel, Frechet and Weibull families, having the cumulative distribution function of the form

$$f(x) = \begin{cases} exp\left(-(1+kz)^{-\frac{1}{k}}\right) k \neq 0 \\ exp(-exp(-z)) \quad k = 0 \end{cases}$$

$$where\ z \equiv \frac{x-\mu}{\sigma}. \tag{3.6}$$

The distribution has three parameters: a location parameter μ; a scale parameter σ; and a shape parameter k. It defines the set of x, where $1 + k\,(x-\mu)/\sigma > 0$.

The 3 subsets of the GEV are type I Gumbel, type II Weibull and type III Frechet. When the parameter k=0, the distribution is called Gumbel, k>0, $x>\mu-\sigma/k$, the GEV is Frechet and k<0, $x<\mu-\sigma/k$, it is Weibull, shown in figure 3.4.

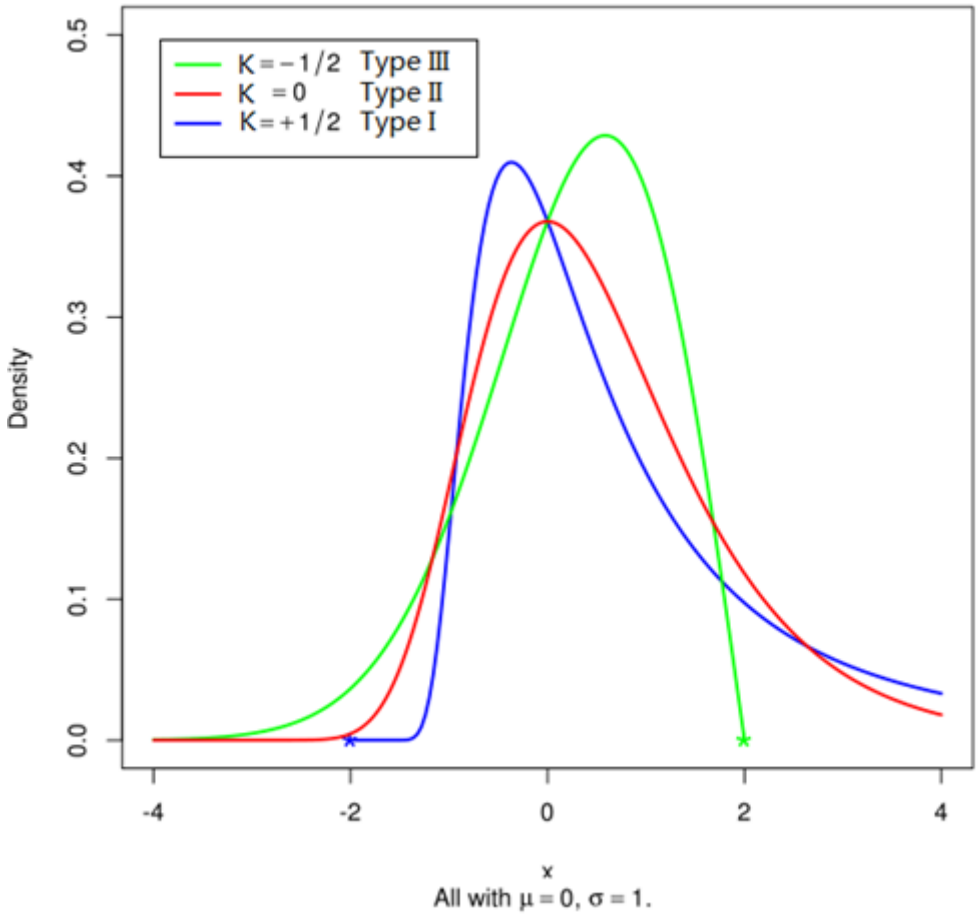

Figure 3.4 Pdf of GEV distribution with different parameters

The GEV family is a unification of the original three families, which greatly simplifies statistical analysis and implementation (Katz et al.,1999). It is not necessary to make a priori judgement about which family should be adopted, because with the different values of k, the data themselves determine the most appropriate type of tail behavior (Coles et al.,2001). The shape of this distribution function fits to the distribution line of seasonal temperature and daily temperature difference and as well as the daily temperature in a decade or 30 years which are not studied in this paper. The function fits to the aim of studying the extreme conditions. With this function, it is possible to find out the possbility of the occurrence of a single event and also, to determine the value of certain probability (95 percentile temperature).

- Generalized Pareto Distribution

The standard cumulative function is defined as equation 3.7

$$f(x) = \begin{cases} 1 - \left(1 + k\frac{(x-\mu)}{\sigma}\right)^{-\frac{1}{k}} & k \neq 0 \\ 1 - exp\left(-\frac{(x-\mu)}{\sigma}\right) & k = 0 \end{cases} \quad (3.7)$$

where the domain is x≥μ for k >0, μ≤x≤μ-σ/ k for k <0. It is specified by three parameters: a location parameter, μ; a scale parameter, σ; and a shape parameter, k The function line shape is shown in the figure 3.5 below

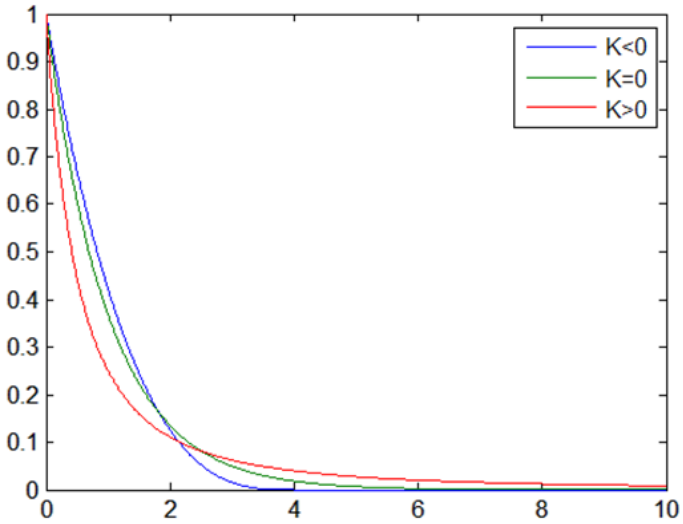

Figure 3.5 Cdf of GPD with different k values

The GPD is often used to model the tail of another distribution, in this case GEV distribution. GPD too has 3 forms: k<0, Beta function, k=0, Exponential, and k>0, Pareto. If the daily temperature of 30 years can be described with the GEV distribution, the upper 5 percentile in the tail part can be well approximated by the GPD, where the parameter k is equal to the corresponding GEV distribution (Cole et al., 2001). The GPD in this paper is used to model the data set of 95 percentile of daily temperature, and 95 percentile of daily precipitation in 30 years.

- Power function

The power function is rather a well known and simple function with the cumulative function in equation 3.8. It is used to fit the distribution of extreme low temperature distributions (5p T).

$$F(x) = \left(\frac{(x-a)}{b-a}\right)^{a} \quad (3.8)$$

Domain: a<x<b

3.4 Transfer function

Once the distributions are chosen for each kind of analyzed parameters, the transfer function can be solved with the equation 2.1.

$$cdf_{OBS}(f(x))=cdf_{sim}(x) \quad (2.1)$$

The Cumulative density function of GPD and GEV are different as shown in equation 3.6 and 3.7, but the transfer function solved is the same

$$f(x) = \left[\left(1 + k_s \times \left(\frac{x-\mu_s}{\sigma_s}\right)\right)^{\frac{k_o}{k_s}} - 1\right] \times \frac{\sigma_o}{k_o} + \mu_o \quad (3.9)$$

Where k_o, μ_o and σ_o, are parameters of the observation distribution and k_s, μ_s and σ_s are the parameters of the simulation distribution

The transfer function of the power distribution fitted for 5p temperature is different shown in equation 3.10.

$$f(x) = \left(\frac{x-a_s}{b_s-a_s}\right)^{\frac{\alpha_s}{\alpha_o}} \times (b_o - a_o) + a_o \quad (3.10)$$

Where a_o, b_o and α_o are the parameters for observation distributions; a_s, b_s and α_s are the parameters for simulation distributions

The parameters for both distributions are the median values obtained from the 12 data sets that have been analyzed. The transfer functions may have the same expression, but with different parameters, they have slightly different behavior. In figure 3.6, the transfer functions f(x) are shown.

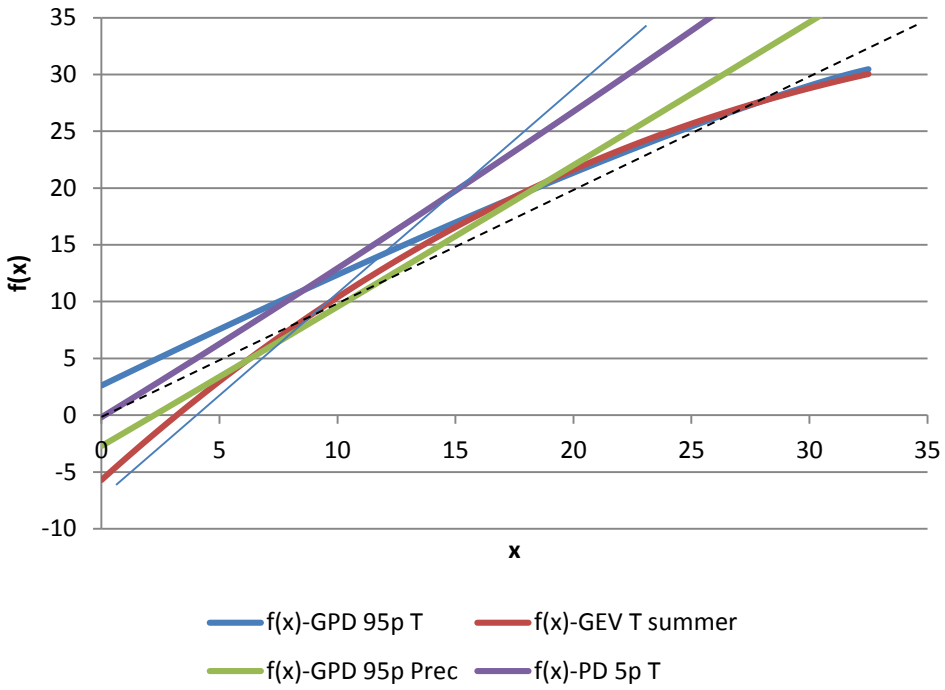

Figure 3.6 Transfer function of 95p T, 5p T, summer T and 95p Prec. (Cottbus)

In general, the transfer function is a non-linear function and the distribution depends on the different parameters. For example, in the figure 3.6, the blue line and the red line represent the extreme temperature and seasonal temperature transfer functions of Cottbus. The transfer function of 95p T and the summer temperature has a skewness of -0.15 and -0.46 respectively. As for the extreme precipitation, the function tends to be more linear, with a skewness of 0.014. The power function related f(x) has a skewness of 0.05.

3.5 Sensibility analysis and parameters

The parameters μ, σ and k are the indicators of the behavior of a distribution. To analyze how the differences in parameters reflect on the distributions, sensitivity studies are carried out, which in this case, are to keep two out of three parameters unchanged and change the third to test how the outcomes will be altered. The main concern is how often extreme high or low events will occur, and thus the results are interpreted in a cumulative density function graph to demonstrate the changes on the probability. In figurers 3.7 to 3.9, 3 parameters of a generalized extreme distribution

are tested. The tested data sets are created according to the real data sets of summer temperature. The analysis is to change k from -0.05 to -0.2 and σ and μ remains 3°C and 15 °C respectively and the similar tests are done with the other two parameters. The changing range of the parameters is summarized from the actual diversifications of observed and simulated distributions of seasonal daily temperature.

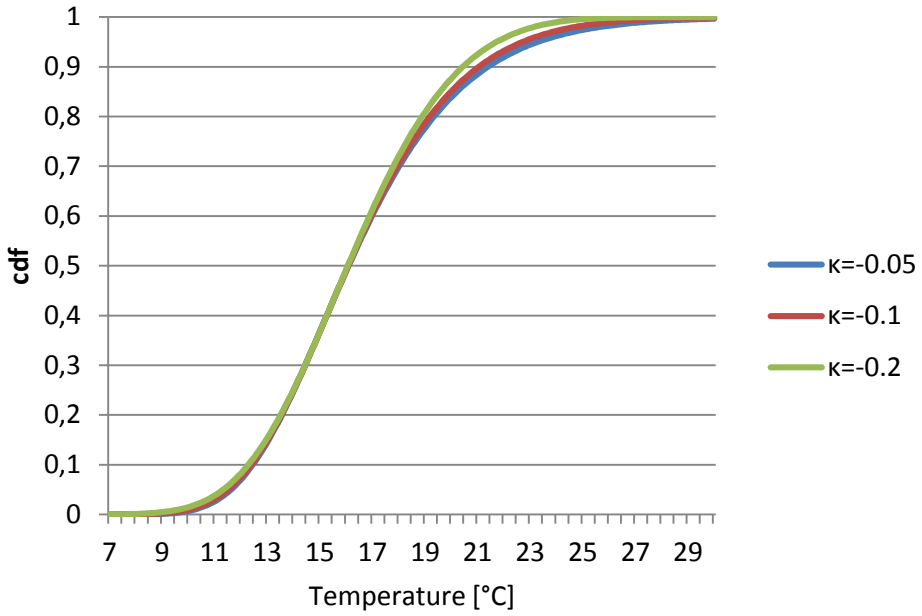

Figure.3.7 Sensitivity analysis of k in GEV distribution σ=3°C; μ=15°C (sample sets based on cdf of JJA temperature)

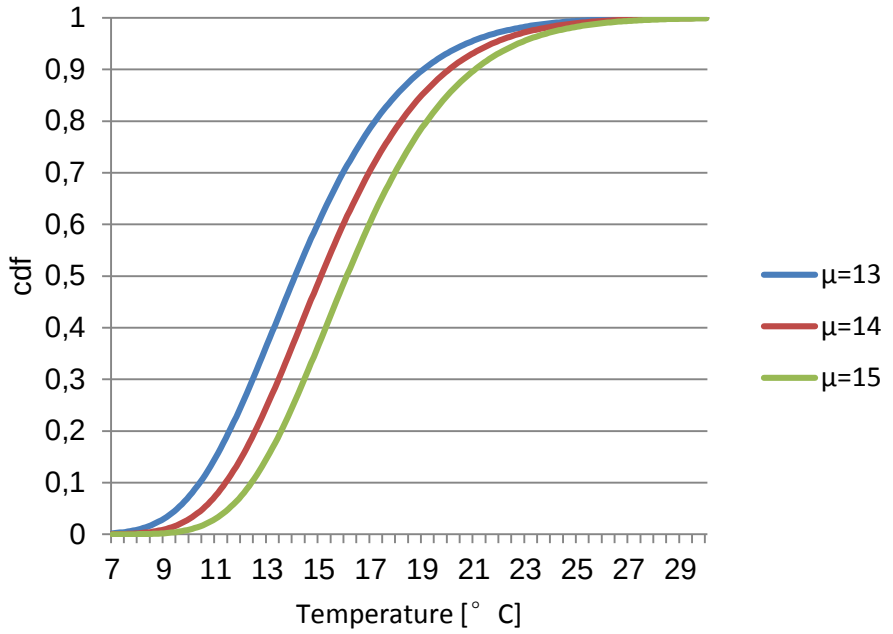

Figure 3.8 Sensitivity analysis of μ in GEV distribution (k=-0.1; σ=3 °C)

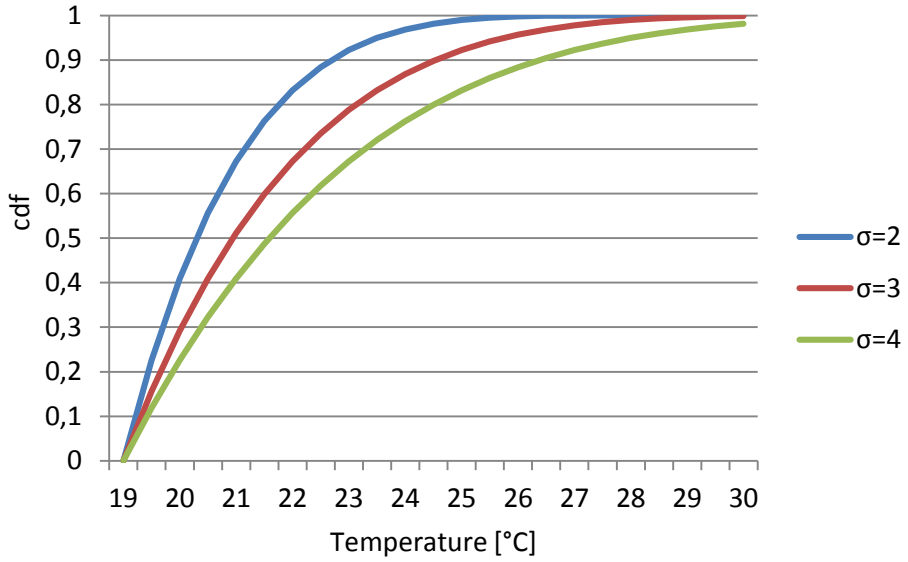

Figure 3.9 Sensitivity analysis of σ in GEV distribution (k=-0.2; μ=19 °C)

Table 3.3 Variation of the probability as a function of the GEV distribution parameters k, μ [°C] and σ [°C]

T>21°C	k=-0.05	k=-0.1	k=-0.2
	0.11	0.10	0.07
	σ=2	σ=3	σ=4
	0.03	0.10	0.18
	μ=13	μ=14	μ=15
	0.04	0.07	0.10
T≤12°C	k=-0.05	k=-0.1	k=-0.2
	0.07	0.07	0.08
	σ=2	σ=3	σ=4
	0.02	0.07	0.13
	μ=13	μ=14	μ=15
	0.25	0.15	0.07

The analysis indicates that the variation of k within the range of -0.05 to -0.2, the distribution will not result a great change. The difference is observable in the tail part. For example, in the sample set of seasonal daily temperature, the probability of T equal to or less than 21°C is 0.89 when k is -0.05 and 0.93 when k is -0.2. Thus the probability of a temperature higher 21 is 11% and 7% respectively as shown in table 3.3. It indicates that the cdf value of a temperature higher than a certain value will increase as the increase of k. The location parameter μ is approximately equal to the median value of the distribution, and the increases on μ will shift the distribution lines to the right in figure 3.8. The result on the probability change on the same value (T>21°C) is an increase of 3 percent by one unit on μ. σ change the scale of the distribution, for extreme high values, the probability of T higher than 21°C increase by 7 percent and for lower values, the probability decreases with the increase of sigma. In summary, among the 3 parameters, μ and σ have larger influences on the results. For the tail part (extreme high values), the probability increase with greater parameter values of μ and σ. Changes on k however only show influences when the difference is large enough.

Another distribution used for fitting the sample sets is the Generalized Pareto Distribution, which as mentioned can be considered as the tail part of the GEV. The

changes on parameters k, σ, μ have the similar impacts as the GEV, seen in figure 3.10 to 3.12. The sample sets are created based on distributions of extreme daily temperature (95p T).

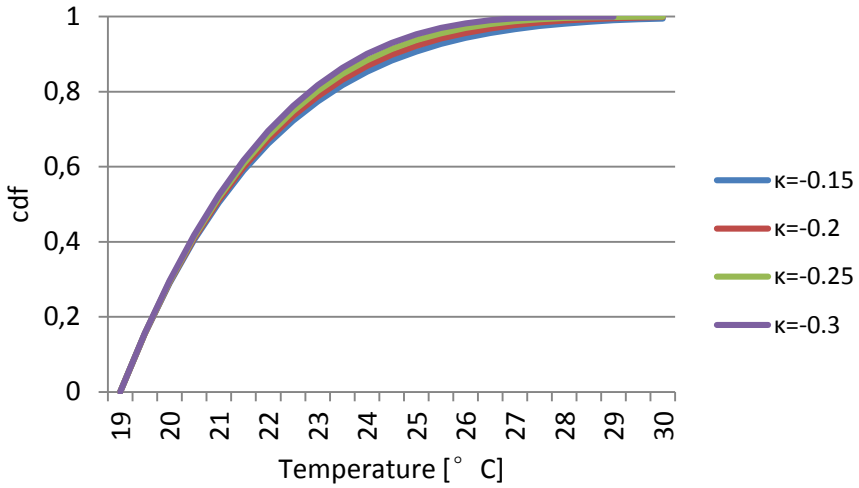

Figure 3.10 Sensitivity Analysis for k in the General Pareto Distribution with σ=3°C and μ=19 °C (sample sets based on 95pT)

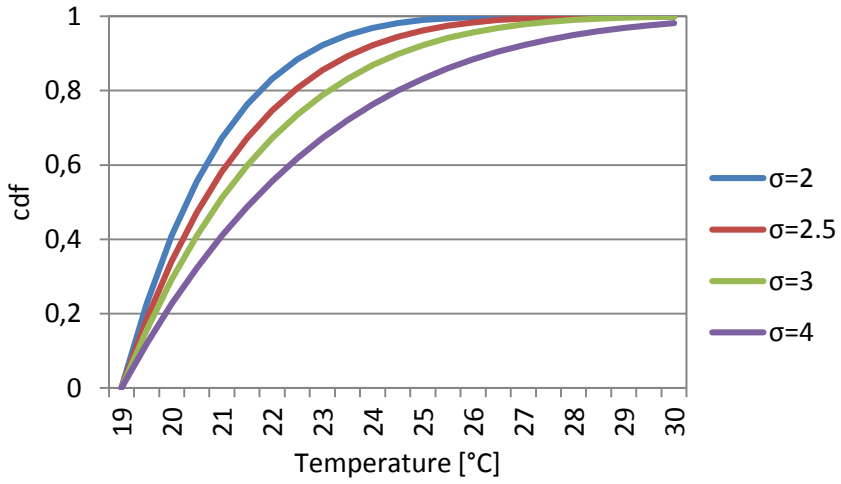

Figure 3.11 Sensitivity Analysis for σ in the General Pareto Distribution with k=-0.2 and μ=19 °C

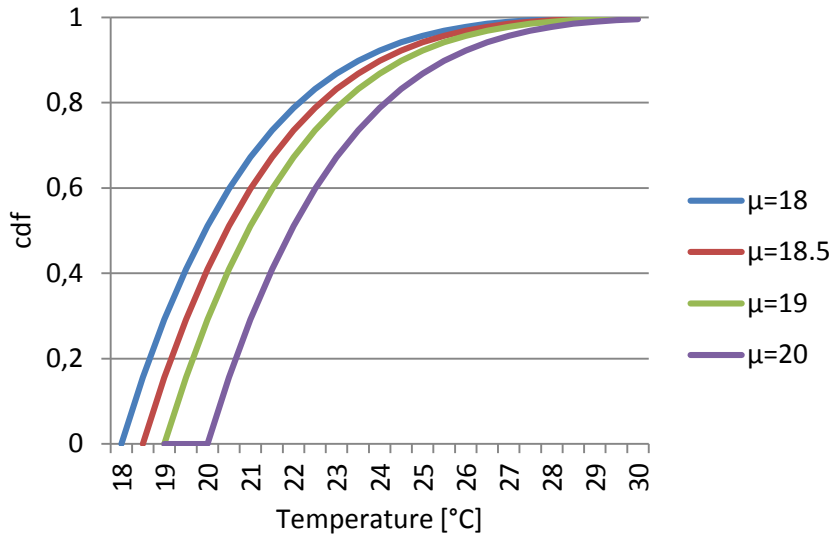

Figure 3.12 Sensitivity Analysis for μ in the General Pareto Distribution with k=-0.2 and σ=3 °C

Similar as the results of GEV test, the small change on parameter k within 0.1unit does not affect the probability results in a large scale (change within 0.01) and the increases on σ and μ shifted the distribution functions to the right, meaning for an extreme condition of temperature higher than certain value, the probability will be higher. The probability changes on temperature higher than 25°C with the different parameter values are shown in table 3.4. For example, a change on μ from 19 °C to 20 °C with other parameters remain the same, the probability of temperature higher than 25°C in the 95 percentile temperature of 30 year will be increased from 8% to 13%. However, if the change is small, e.g. from 18 °C to 18.5 °C, the probability change will be 2%.

Table 3.4 Variation of the probability as a function of the GPD distribution parameters k, μ [°C] and σ [°C]

T>25°C	k=-0.15	k=-0.2	k=-0.25	k=-0.3
	0.09	0.08	0.06	0.05
	σ=2	σ=2.5	σ=3	σ=4
	0.01	0.04	0.08	0.17
	μ=18	μ=18.5	μ=19	μ=20
	0.04	0.06	0.08	0.13

The results on the sensitibity analysis are important in 3 ways. Firstly, as explained in the correction method, the parameters taken as the generalized (representing) function for both observed and simualted data are median values of 12 data sets in the period of 1960-2000. The sensitivity analysis defines the impacts of the uncertainty on the transfer function. It shows whether the differences between the individul parameter sets and the median values will make a dramatic difference on corrected results. For example, in table 3.5 the median parameters determination of GPD is presented. The parameters are from GPDs fitted to observed and simulated extreme daily temperature distributions in Lindenberg during 1960-2000. The values taken to produce the transfer function are median values of 12 data sets, with number 1 representing the data set of 1960-1989 and number 2 representing the data set of 1971-2000.

Table 3.5 Parameters of GPD fitted to the extreme daily temperature (95p T) in Lindenberg in 1960-2000.

	Observed			Simulated		
data set	k	σ (°C)	μ (°C)	k	σ (°C)	μ (°C)
1	-0.306	2.686	20.758	-0.206	2.595	18.795
2	-0.316	2.679	20.803	-0.198	2.628	18.691
3	-0.310	2.661	20.851	-0.192	2.605	18.719
4	-0.282	2.602	21.010	-0.195	2.640	18.743
5	-0.294	2.594	20.972	-0.188	2.593	18.791
6	-0.259	2.639	21.018	-0.190	2.611	18.823
7	-0.273	2.644	21.165	-0.203	2.689	18.887
8	-0.272	2.634	21.153	-0.214	2.701	18.948
9	-0.273	2.619	21.209	-0.196	2.662	18.900
10	-0.276	2.626	21.204	-0.185	2.639	18.942
11	-0.243	2.506	21.220	-0.183	2.663	18.881

12	-0.231	2.502	21.231	-0.186	2.670	18.916
MIN	**-0.316**	**2.502**	**20.758**	**-0.214**	**2.593**	**18.691**
MEDIAN	**-0.275**	**2.630**	**21.086**	**-0.194**	**2.640**	**18.852**
MEAN	**-0.278**	**2.616**	**21.050**	**-0.195**	**2.641**	**18.836**
MAX	**-0.231**	**2.686**	**21.231**	**-0.183**	**2.701**	**18.948**

The differences of k between median values and the 12 values are less than ±0.05, which according to the sensitivity analysis results very small impacts on the distribution behavior. The differences of σ and μ are within ±0.13 and ±0.33 respectively. Since the differences are small, the median values can be representative for the 12 sets. This also explains one of the reasons that GEV and GPD are chosen as fitted distributions, which is due to relatively small uncertainties.

Secondly, a relative relationship between data sets can be roughly analyzed through the parameters. In the following figures, all the parameters of the data sets in the 7 stations analyzed are compared. Since GPD fitted to 95P T, 95P prec and monthly Prec. can be seen as the tail part of GEV fitted to Tdiff and seasonal daily T, the parameters from the two kinds of distributions are in the same range. Thus in figure 3.13-3.23, the same kind of parameters for GEV and GPD are presented in one figure, with figure 3.13-3.16 presenting k, figure 3.17-3.20 presenting μ and figure 3.21-3.24 presenting σ. The parameters for each kind data set are median values obtained from the 12 data sets in 1960-2000. For each parameter, the results for 7 observed and 3 modelled distributions are shown. For example, figure 3.13 to figure 3.16 are showing the shape parameter k for observed, C20_1 simulated, C20_2 simulated and C20_3 simulated data sets respectively. For the extreme low temperature 5P T however, the fitted distribution is power which has a totally different cdf function and therefore different parameters, α,β and γ. The results for 5P T are shown in figure 3.24.

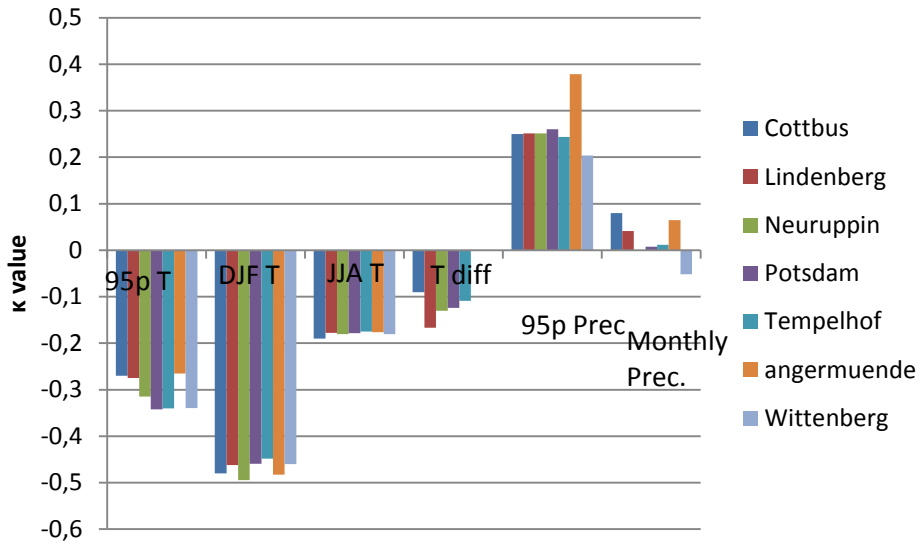

Figure 3.13 Parameter k for observed data sets (95pT, Seasonal daily T, Tdiff, 95p Prec and monthly Prec.) at 7 stations

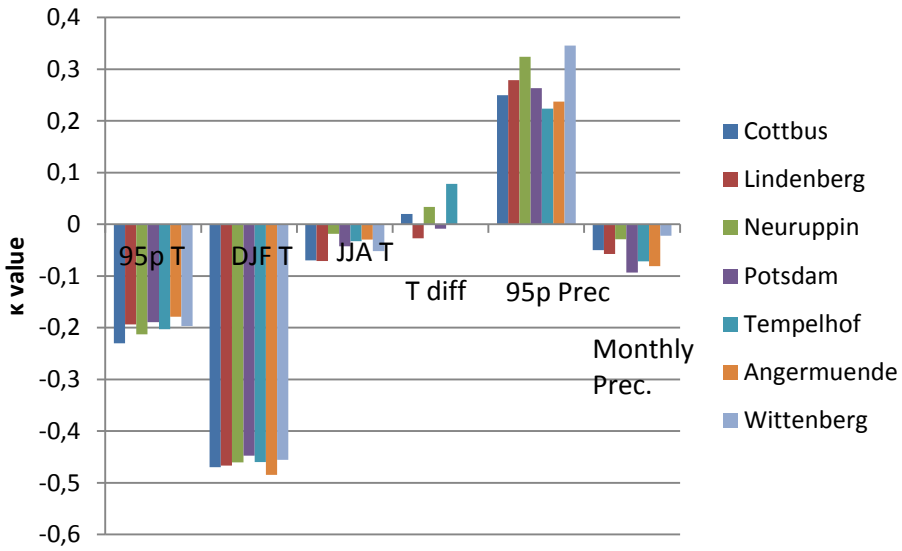

Figure 3.14 Parameter k for C20_1 simulated data sets (95pT, Seasonal daily T, Tdiff, 95p Prec and monthly Prec.) at 7 stations

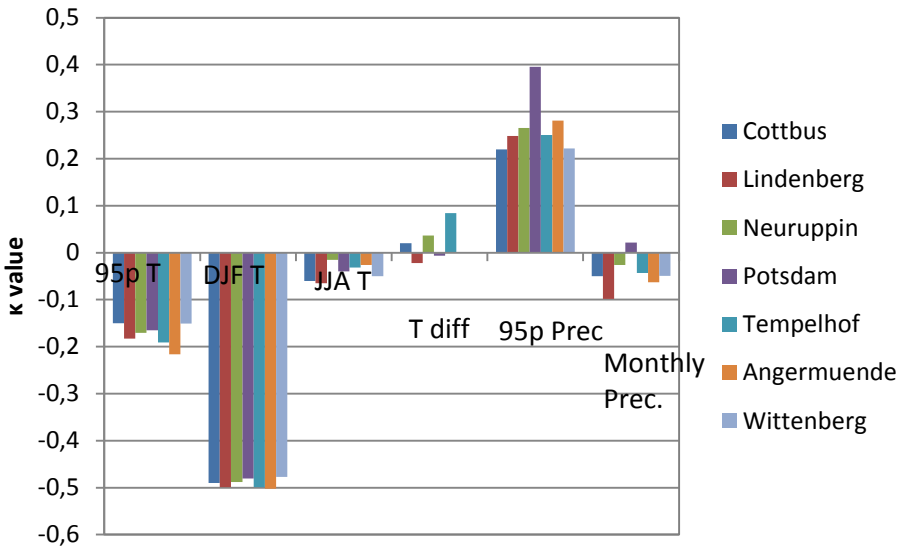

Figure 3.15 Parameter k for C20_2 simulated data sets (95pT, Seasonal daily T, Tdiff, 95p Prec and monthly Prec.) at 7 stations

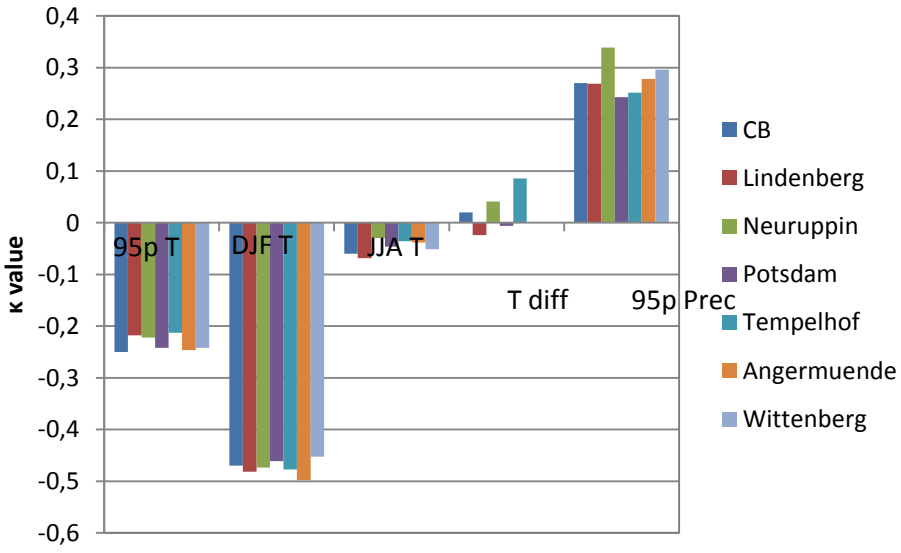

Figure 3.16 Parameter k for C20_3 data sets (95pT, Seasonal daily T, Tdiff, 95p Prec and monthly Prec.) at 7 stations

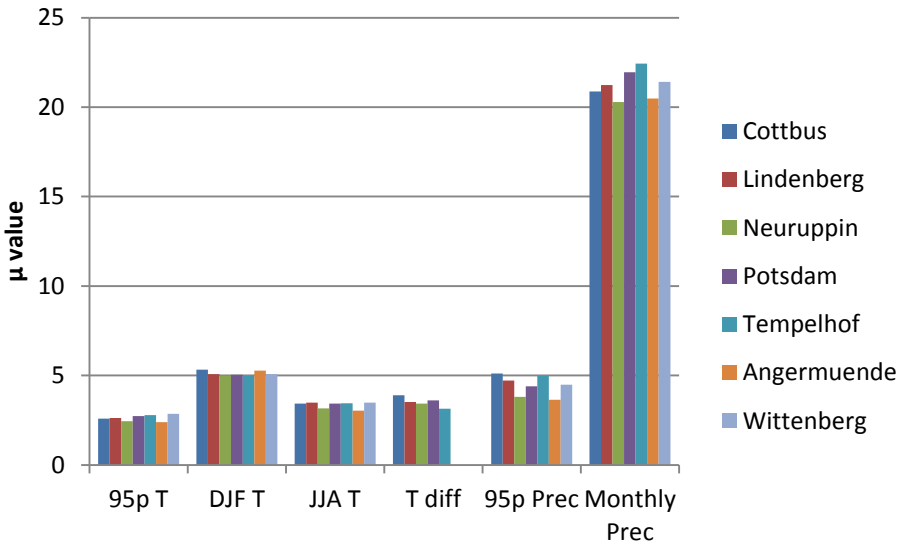

Figure 3.17 Parameter µ for observed data sets (95pT, Seasonal daily T, Tdiff, 95p Prec and monthly Prec.) at 7 stations

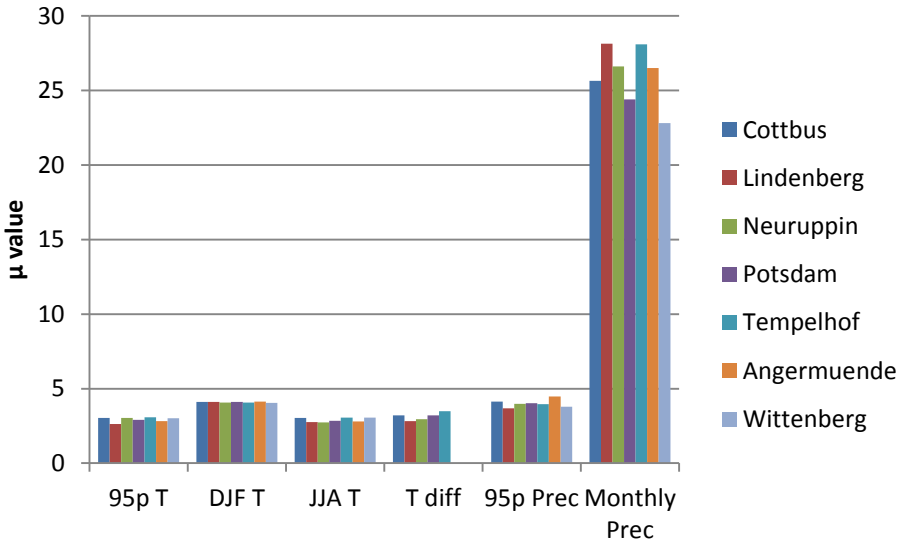

Figure 3.18 Parameter µ for C20_1 simulated data sets (95pT, Seasonal daily T, Tdiff, 95p Prec and monthly Prec.) at 7 stations

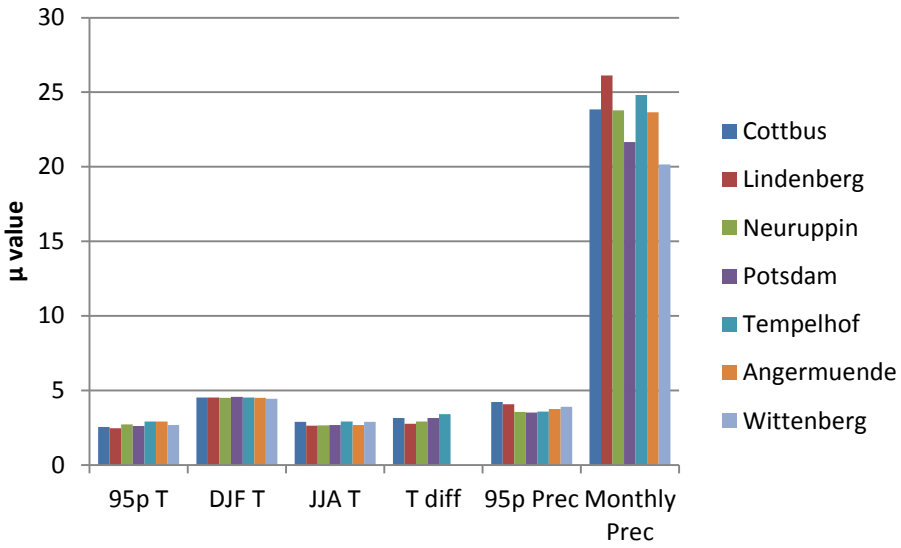

Figure 3.19 Parameter µ for C20_2 simulated analyzed data sets (95pT, Seasonal daily T, Tdiff, 95p Prec and monthly Prec.) at 7 stations

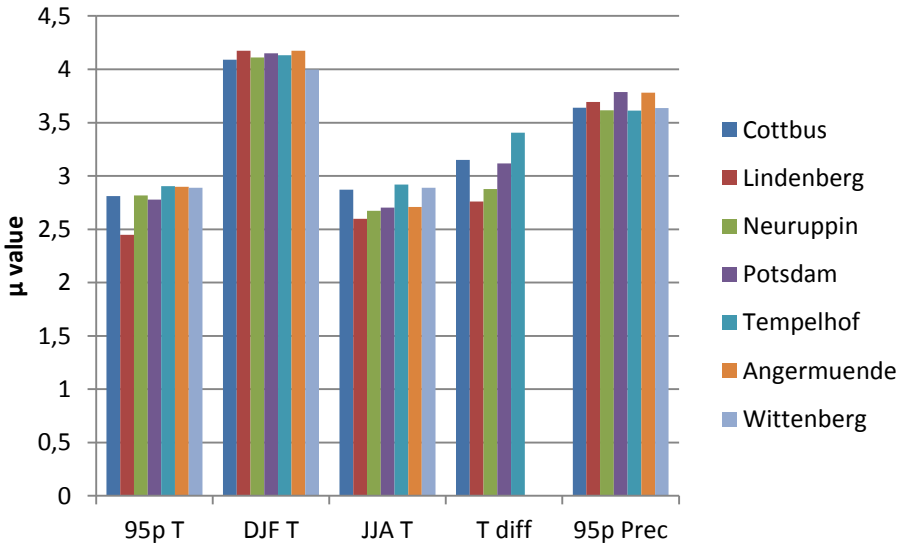

Figure 3.20 Parameter µ for C20_3 simulated data sets (95pT, DJF T, JJA T,Tdiff, 95p Prec and monthly Prec.) at 7 stations

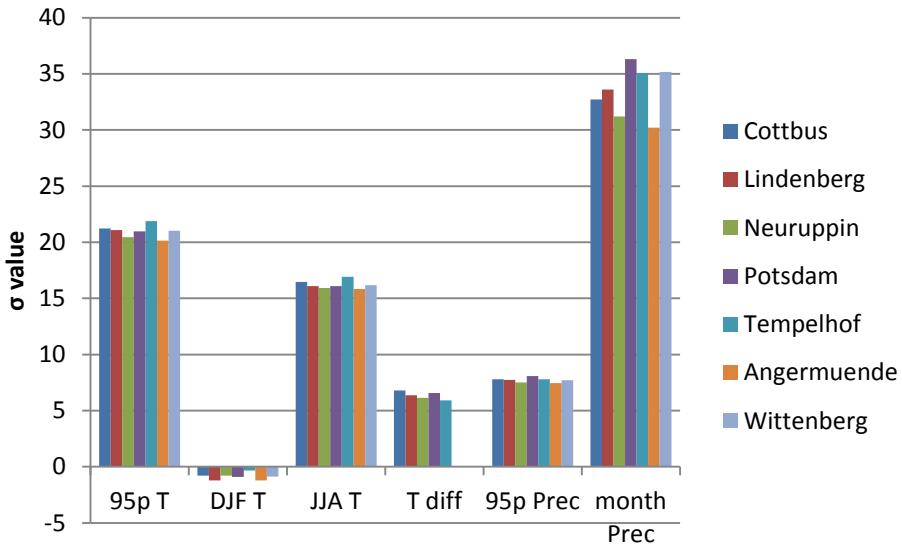

Figure 3.21 Parameter σ for observed data sets (95pT, Seasonal daily T, Tdiff, 95p Prec and monthly Prec.) at 7 stations

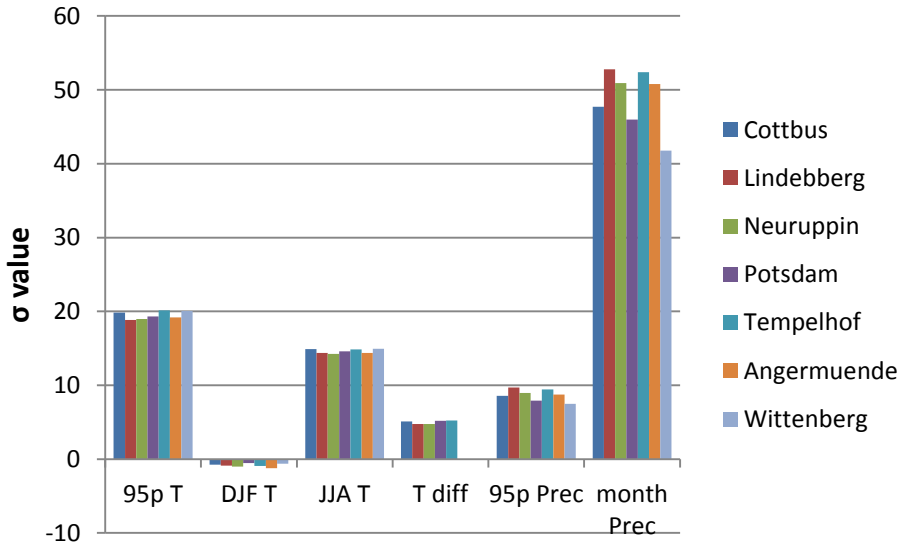

Figure 3.22 Parameter σ for C20_1 simulated data sets (95pT, Seasonal daily T, Tdiff, 95p Prec and monthly Prec.) at 7 stations

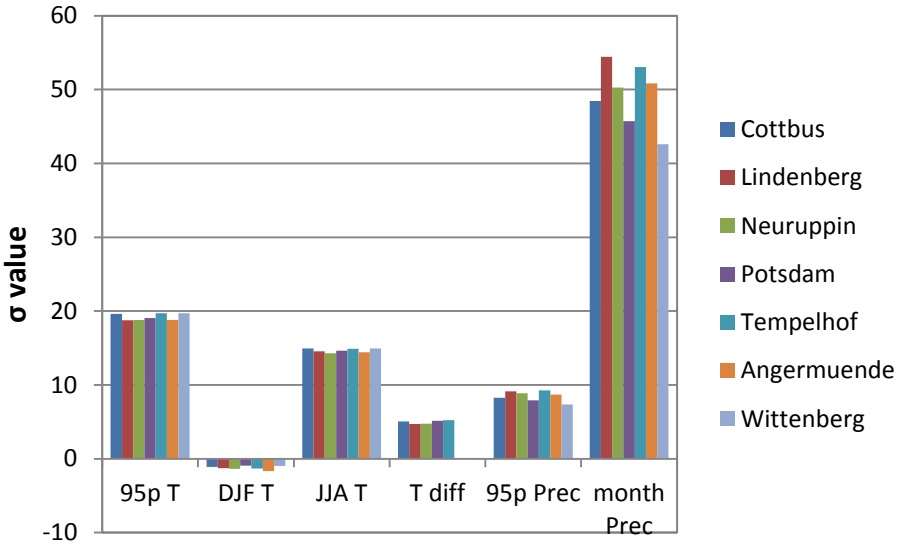

Figure 3.23 Parameter σ for C20_2 simulated data sets (95pT, Seasonal daily T, Tdiff, 95p Prec and monthly Prec.) at 7 stations

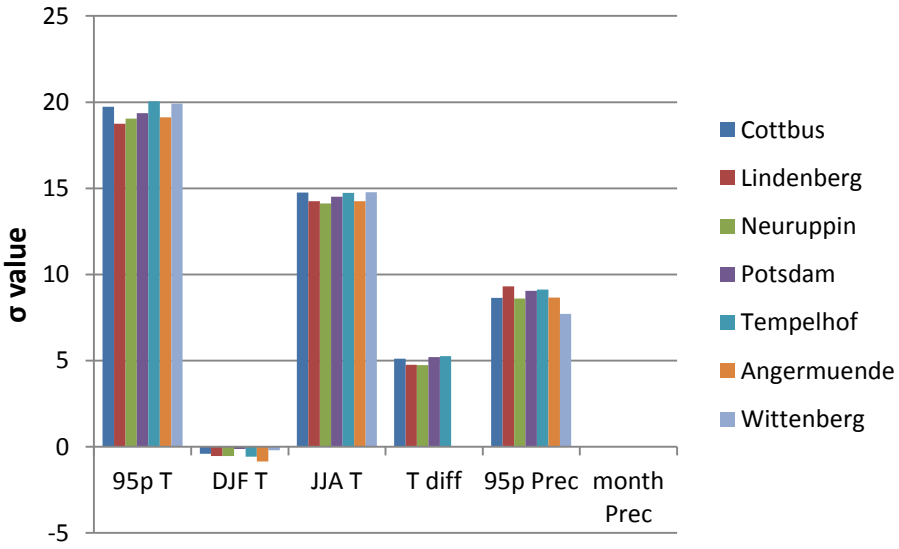

Figure 3.24 Parameter σ for C20_3 data sets (95pT, Seasonal daily T, Tdiff, 95p Prec and monthly Prec.) at 7 stations

In each of the above figures, there are seven parts of colored bars, which are representing parameters for extreme daily temperautre (95pT), winter daily temperature (DJF t), summer daily temperautre (JJA t), daily temperature difference

(Tdiff), extreme daily precipitation (95P Prec.) and monthly Precipitation. The different colors representing different analyzed stations namely Cottbus, Lindenberg, Neuruppin, Potsdam, Templehof, Angermuende and Wittenberg, among which Angermuende and Wittenberger do not possess the data for daily temperature difference analysis. For different parameters, the scales are different. For example, the mean value of a GPD is

$$X_{mean}=\mu+\frac{\sigma}{(1+\kappa)} \tag{3.9}$$

In the data sets approximated by GPD, the k is in the range of ±0.1 to ±0.3 and μ is around 2 to 4, so the mean value is very close to the parameter σ. From figure 3.20-3.24, the mean values of each kind of distribution can be estimated. For example, the mean values of winter daily temperature are around -2 to -1 degrees and in summer, they are around 15 degrees. There are also slight differences between different locations. The monthly precipitation for example in Lindenberg is more than 50mm and in Angermuende, the values is around 42mm. Yet the climate condition in Brandenburg is relatively unanimous, there are not great differences between locations in the daily temperature and precipitations. There are however differences between observed and simulated data in all kinds of parameters. For example, the σ for 95pT in observed sets are between 20-21 and the ones in simulated data are between 19-20. The comparisons are better illustrated with figure 3.25 of parameters of power distributions for 5P T. in this fiture, the 7 parts of bars represent the locations and different colors represent the data sets, observed or simulated. For example, β in simulated sets are smaller than β in observed sets in most of stations except for Neuruppin and Tempelhof. The job in the correction is to obtain a distribution with a new set of parameters that fits the observed sets better than the original simulated data.

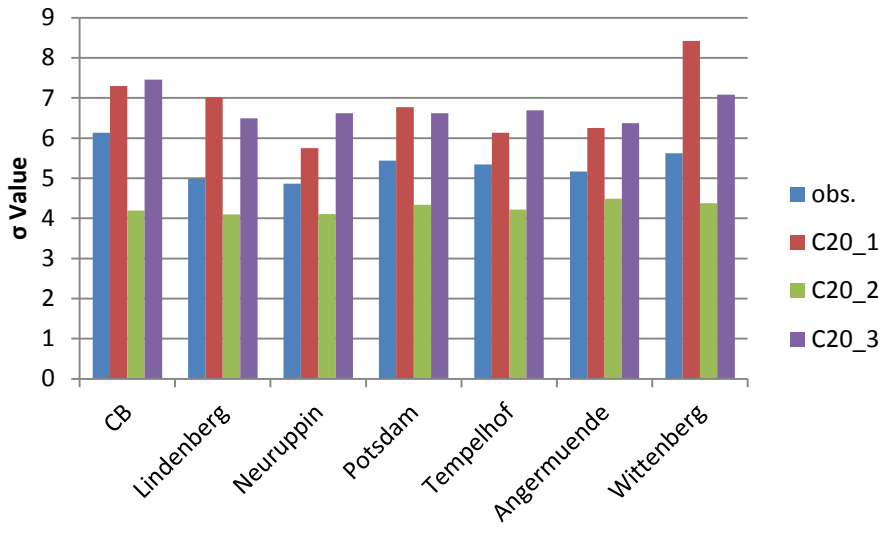

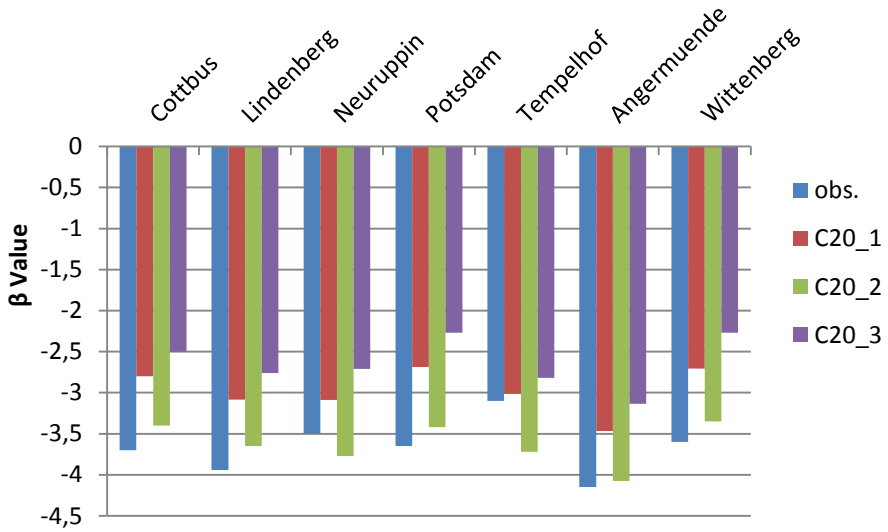

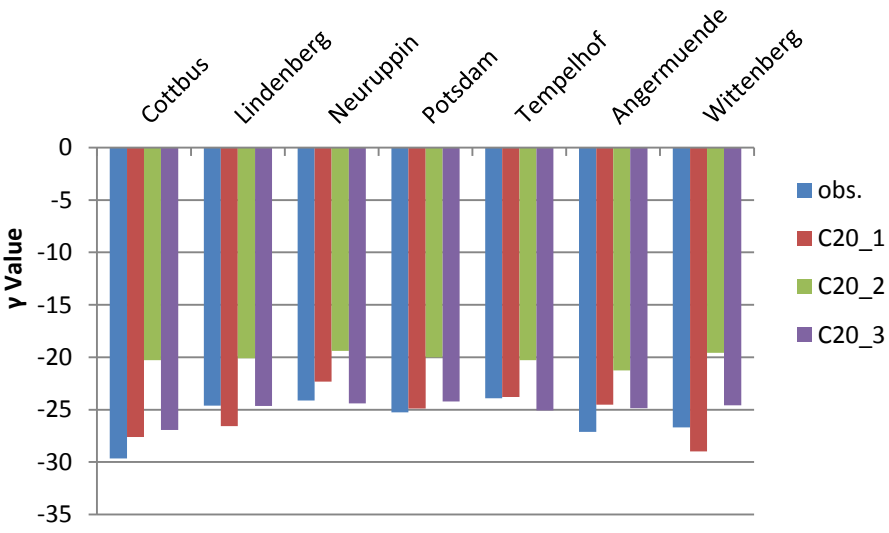

Figure 3.25 Parameters for Power distr. 5pT at 7 stations (σ,β,γ)

Through the analysis of the parameters, another issue worth discussing is if the parameters can be exchanged in locations or generalized a common set of parameters for an area. Two stations such as Lindenberg and Cottbus, which share a similar behavior in climate, thus a similar set of parameters in observed cases, is it fair to exchange the parameters or use one set of parameters representing the whole area, saving the efforts on determing the parameters for each grid point. An experiment of exchaning the parameters between Lindenberg and Cottbus has been conducted with the hope that with the parameters from others, the bias correction will still be effective. However, the goals are not achieved as expected seen in figure 3.26 Correction of extereme temperature simulated by C20_1 in Cottbus with parameters from observation and C20_1 in Lindenberg.

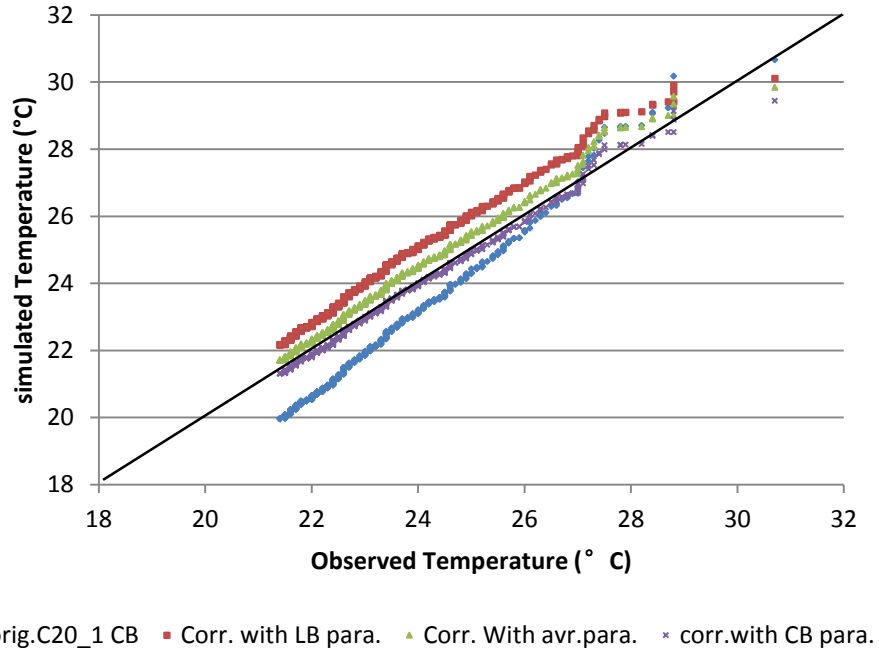

Figure 3.26 Correction of C201 Cottbus with parameters from Lindenberg.

In the figure 3.26, the dots show the agreement of the observed and simulated values at the same percentile with the x axis representing observed and y representing simulated data. If the two data sets are coinciding well, then the dots should be lying on the central line. The colors of blue, red, green and purple represent the relationships of observed data with original C20_1 simulated data in Cottbus,

corrected simulation data with parameters from Lindenberg, corrected simulation data with the avereage parameters of Cottbus and Lindenberg and lastly the corrected simulations with Cottbus C20_1 parameters. Obviously the red line does not appear to be a good matching of observed and corrected. Before correction, at the same percentile, the simulated data are lower than observation and the average difference between the two is -1.1K. After corrected with parameters from Lindenberg ovservation and C20_1, the corrected simulated data (in red) is higher than the observation of Cottbus about averagely 1.0K which is not a result that is desired. When correcting the simulated with the average parameters of Cottbus and Lindenberg (both observed and simulated mean values), the results are more satisfied, shown in green line. The average difference after correction is reduced to 0.4K. However, the bias then is changed to a warm one rather than a cold one as original. The correction with the observed and simulated parameters with its own data sets of Cottbus has with not doubt the best results (in purple). The median difference after correction is -0.1K. This experiment suggests that the parameters exchanging between two locations entirely will not make a satisfying correction even the locations are close to each other. It is not reasonable to correct simulated results from one location with parameters from another location. However, the analysis also suggests that an average values of several sets of parameters can be used to one location. The correction will reduce the median difference between the observed and simulated data. That is to say that in an area which includes several stations, one of them does not possess the data required for correction, it is also a solution to apply the average parameters to that one to correct. Of course the results will not be as good as the correction with its own parameters. In the results analysis parts in this paper, the corrections are all made by the parameters obtained from the observed and simulated data sets of its own locations to ensure the most accurate correction.

4 Results analysis

The analysis will be introduced in 3 parts. First is a bias correction on historical runs of 1960-2000 and as discussed before, 12 data sets will be created and analyzed. The model data are from simulation runs of C20_1, C20_2 and C20_3. Second part is a combination of C20 simulations and the projections to validate the effectiveness of the correction in the period of 1972-2008. The last part is the analysis on the projections from 2001-2100, including A1B1, A1B2, B11 and B12 and the climate change signals will be reanalyzed.

In each part, the results on bias correction include temperature analysis and precipitation analysis. For temperature, 7 stations are analyzed and the parameters include daily extremes, daily difference and seasonal temperatures. The main parameters are the extreme daily temperatures, which is the highest 5 (95p) or lowest 5 (5P) percentile daily values from a sorted distribution in 30 years. In one set of daily temperature of 30 years, the total value amount is 10957 or 10958 and therefore, in an extreme daily temperature data set, there are 5 percent of the total which are 548 values. The daily temperature difference is daily maximum temperature minus daily minimum temperature and as said, in a 30 year period, the data size is 10957 or 10958. To demonstrate that the bias correction method is suitable for variety of data sets, the seasonal daily temperatures are drawn, which is summer temperatures of June, July and August, and winter temperatures of December, January and February. The data size of JJA months and DJF months are 2760 and 2707 respectively. For precipitation, all the 110 grid cells in the model are analyzed, coupled with the closest observation station. The daily precipitation extremes are the highest 5 percent of the 30 year daily values, which makes the data size 548 as well. As for monthly temperature, the data set is consisted of 12 monthly summarized precipitation values each year, and the total values are 360 in 30 years. The description of parameter data sets and the researched stations are listed in table 4.1.

Table 4.1 Description of analyzed data parameters and stations

	Parameters	Data	No. of Analyzed stations	Data size
T	Extreme Daily Temperature (95pT & 5pT)	Top/low 5 percent of the daily T in a 30 year period	7 stations*	548
	Daily Temperature Difference	Daily max T minus min. T in 30 years	5 stations	10957 or 10958
	Seasonal Temperature	Daily temperature of 3 months (JJA or DJF) in 30 years	7 stations*	2760 (JJA) 2707 or 2708 (DJF)
Prec.	Extreme daily precipitation (95pPrec)	Top 5 percent of the daily prec. in a 30 year period	110 grid cells	548
	Monthly Precipitation	Monthly Prec. Sum	110 grid cells	360

*7stations with complete temperature records: Cottbus, Lindenberg, Neuruppin, Tempelhof, Potsdam, Wittenberg and Angermuende

4.1 Bias correction on historical runs

The bias correction method described in chapter 3 is relied on the transfer function which is determined by both the observed and simulated data. For this purpose, the correction is first made on the historical runs of C20 series of those grid points/stations with complete weather record to compare. The corrections are made on 5 kinds of parameters: Extreme temperature, extreme precipitation, monthly precipitation, seasonal temperature and daily temperature differences. The results are presented in the following paragraphs.

4.1.1 Extreme Temperature

In this part, the extreme daily temperature in 30 years are compared and corrected with the transfer function. As described chapter 3 from the data of daily temperature in the period of 1960-2000, 12 data sets of 30 years, e.g. 1960-1989, 1961-1990 and 1962-1991. With the exception of Neuruppin where the temperature record starts from 1961 and therefore, for Neuruppin, there are 11 data sets of 30 years. For the 95 percentile daily temperature (95PT) and the extreme low temperature (5PT), the fitted distributions are General Pareto distribution and power distribution respectively. Fig 4.1 is the results comparison of one data set 1965-1994 in simulation C201 from the 7 investigated stations. The highest 5 percent values taken from total daily values in the 30 years are ranking from lowest to the highest and compared with observation data. The x axis represents the ranking of the values, in total 548 values and y axis represents the temperature differences in K (CLM-OBS). In Lindenberg, during the period of 1965-1994, the original simulated data (blue line) shows an obvious underestimate compared to the observation data. There is an average of -2K difference between the simulated and observation in this data set of 95PT and for all the other data sets the difference is approximately the same, which means the simulation demonstrates a cold bias of 2K. After analyzing the distributions, the transfer function is created and applied to the original simulated data, the new corrected data are obtained, shown in figure 4.1 in red line. The corrected data shows a much smaller difference compared to the original data. The corrected bias is -0.01K. The other 6 stations have the similar result that bias is minimized.

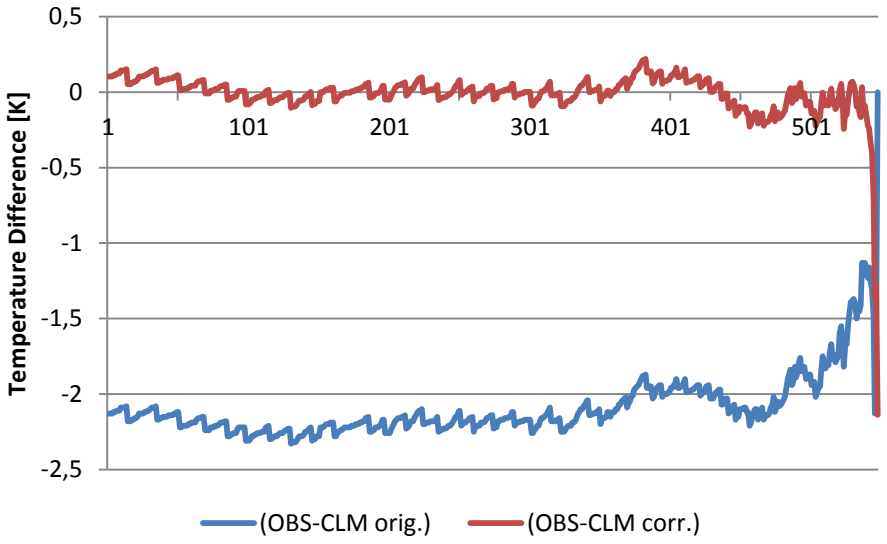

Figure 4.1 95P Temperature difference in Lindenburg (1965-1994)

The relationship between the observation and simulated data are shown in figure 4.2. In the figure, the x axis is the temperature values of certain quantiles of observation and y axis is that of the simulated data. The points correspond to the respective 1st, 2nd, … and 99th quantiles of the temperature value of 95PT and therefore represents the relationship between observation and simulated data.

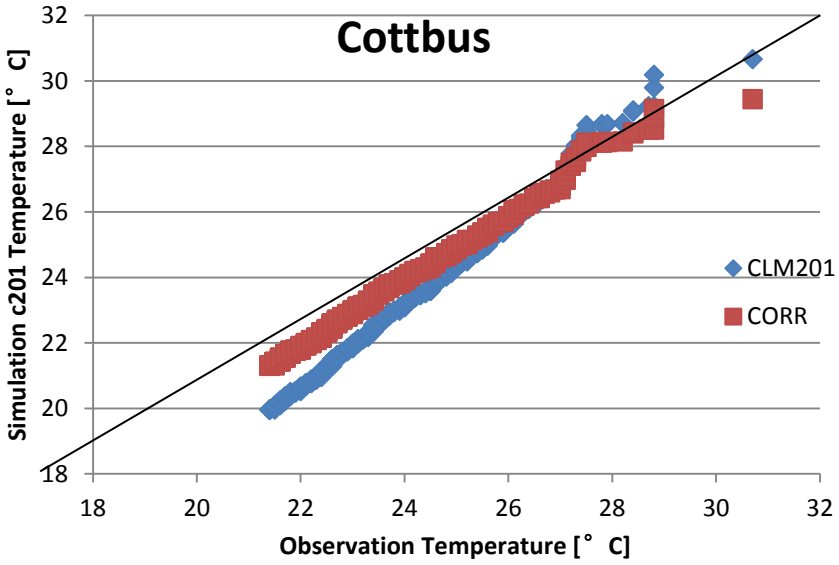

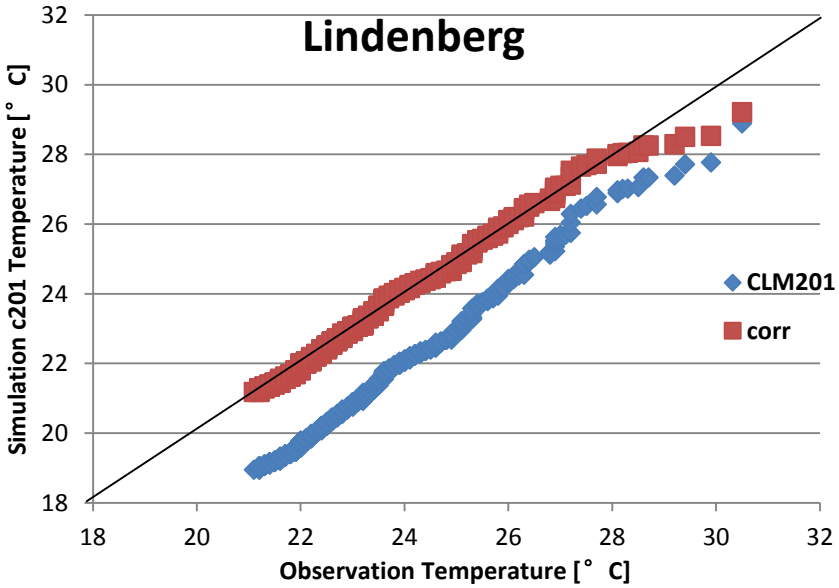

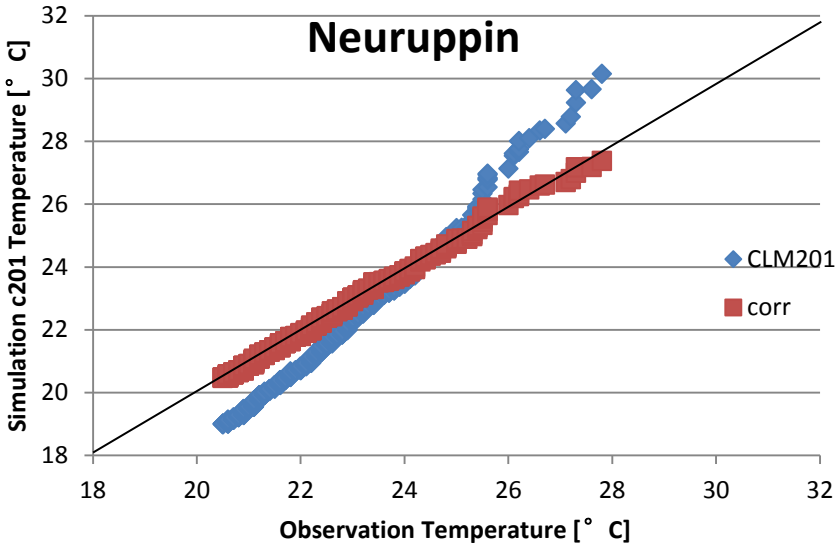
Neuruppin
Simulation c201 Temperature [° C]
Observation Temperature [° C]
CLM201
corr
32
30
28
26
24
22
20
18
18
20
22
24
26
28
30
32

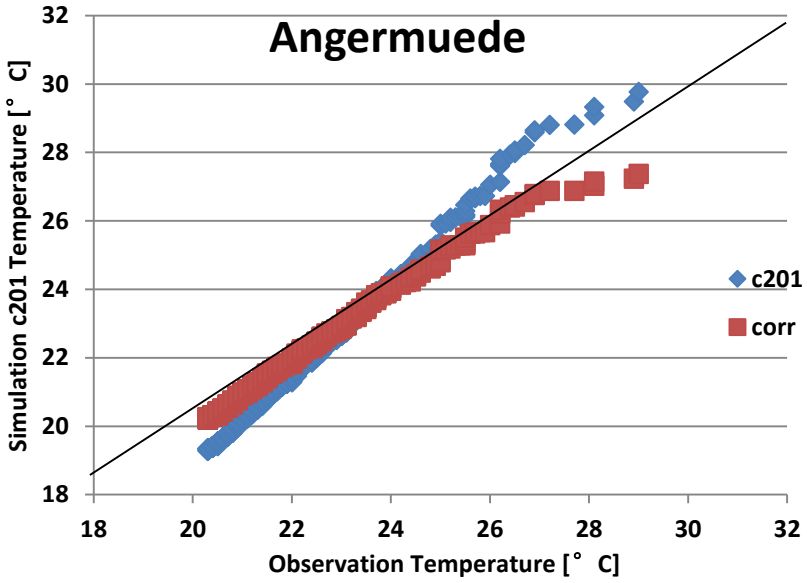
Angermuede
Simulation c201 Temperature [° C]
Observation Temperature [° C]
c201
corr
32
30
28
26
24
22
20
18
18
20
22
24
26
28
30
32

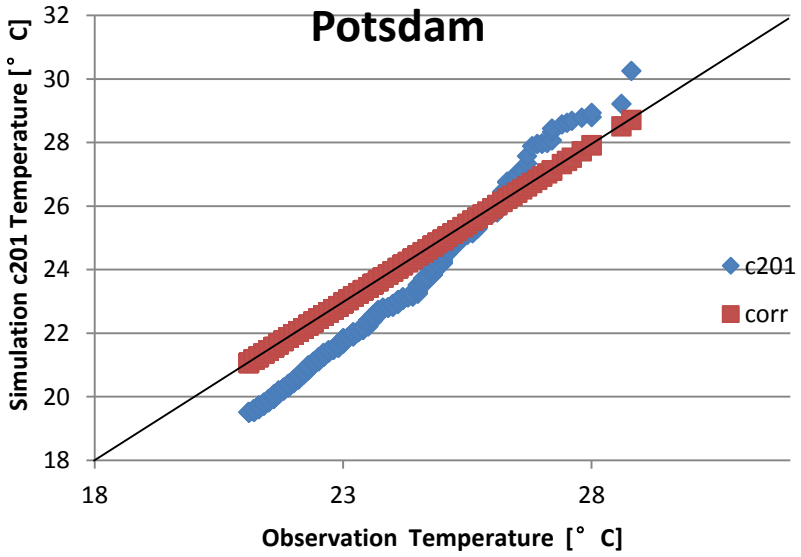
Potsdam
Simulation c201 Temperature [° C]
Observation Temperature [° C]
c201
corr
32
30
28
26
24
22
20
18
18
23
28

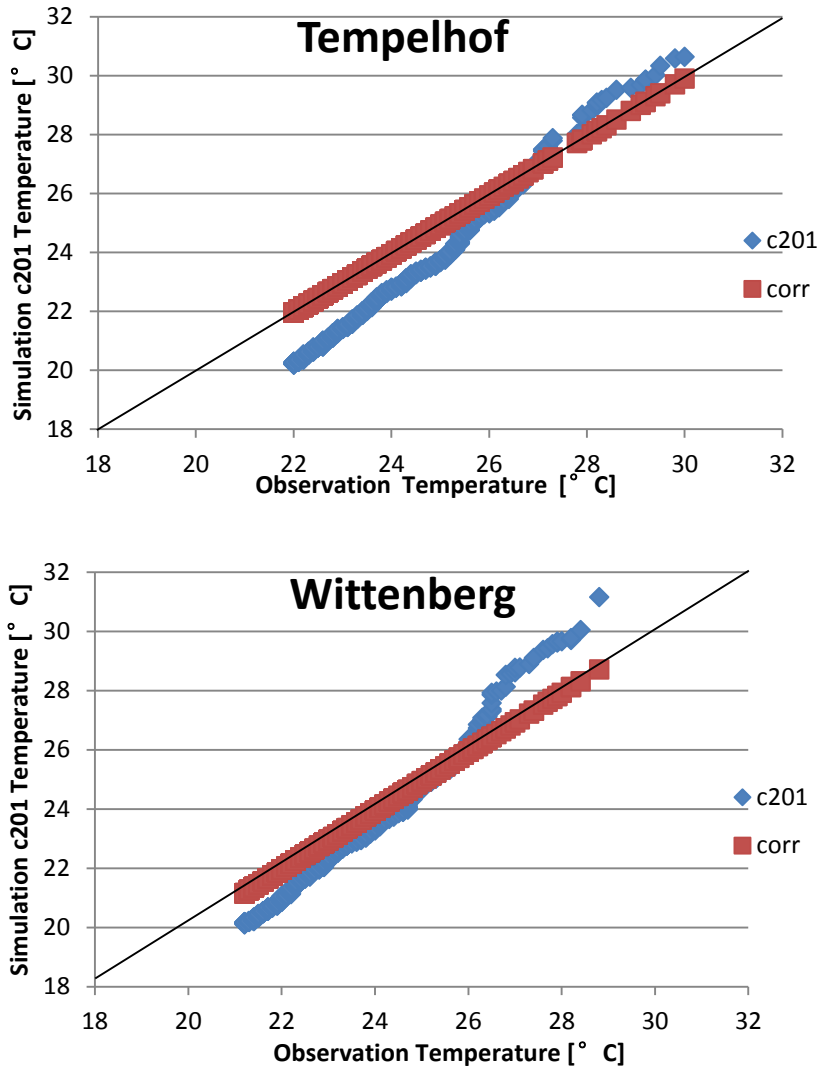

Figure 4.2 Relationship between 95pT observation and simulated data in C20_1 of 7 stations (1971-2000)

In figure 4.2, the blue and red dots represent the observation data vs original simulation data and the observation data vs. the corrected data respectively. Before correction, simulation data (blue) show a pattern of underestimation at lower points and overestimation at higher points, with an exception of Lindenberg showing underestimate in all values. For example the first graph of Cottbus 1971-2000, as 50 percentile values of the two data sets, the observation value is 23.1°C whereas the same value of original simulated data is 21.9°C. This underestimation remains until higher percentiles as well but the difference is smaller. For 95 percentile values, the observed value is 27°C and the simulated data is 26.8°C. Only with a few values with extreme high percentile, the simulated data coincide with the observed and even

present higher values. This pattern is the same with other 6 analyzed stations and with simulation runs with slightly difference of the turning point. The correspondence of the corrected data and the observation data are much improved, represented by the red points, only with a slightly underestimate in the extreme values in Lindenberg and Angermuende. With the same percentile in the distribution, the observed and corrected simulated data have approximately the same values, which is to say the two distributions have the same behavior. In the sense of representing reality better, this bias correction method is successful for the extreme high temperature.

For the extreme low temperature in figure 4.3, the original simulated data indicate an overestimate on temperature values (blue dots). After correction the differences are less obvious.

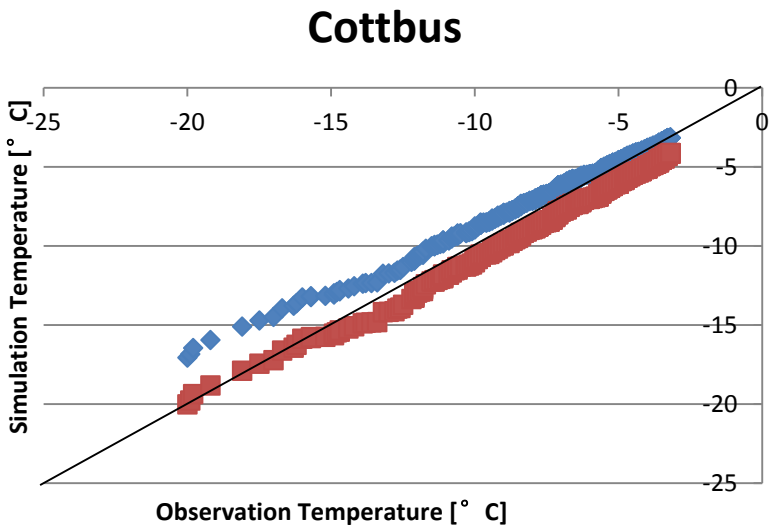

Lindenberg

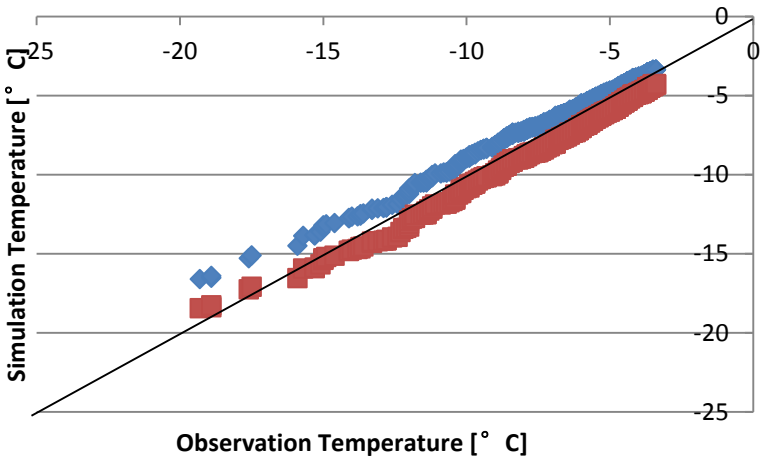

Neuruppin

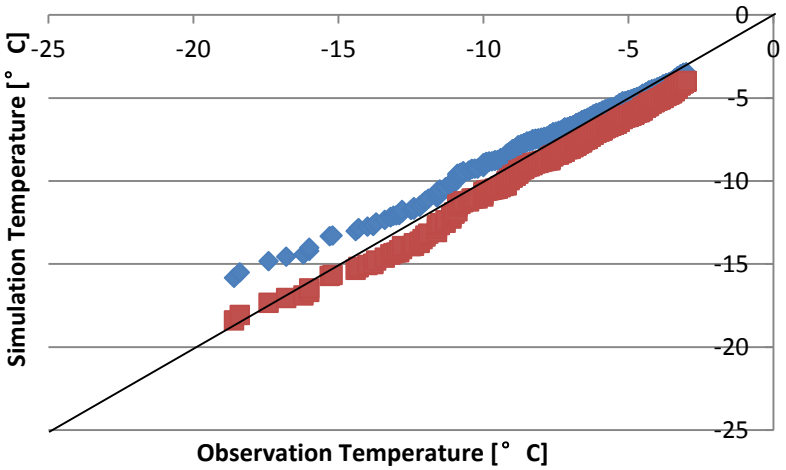

Angermuende

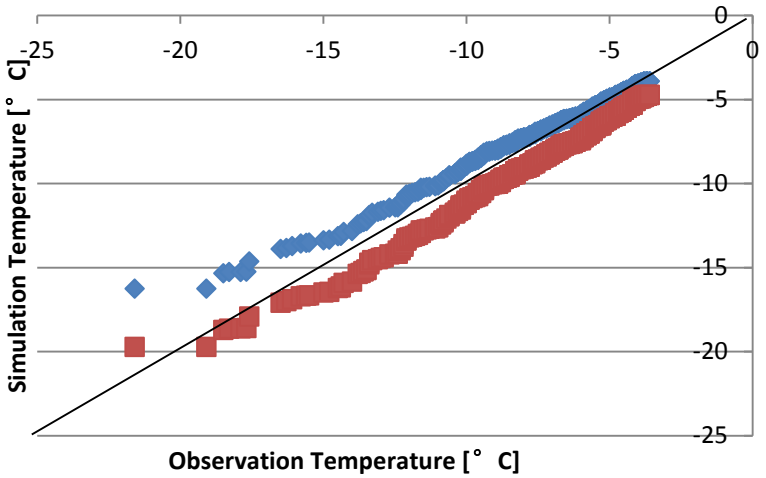

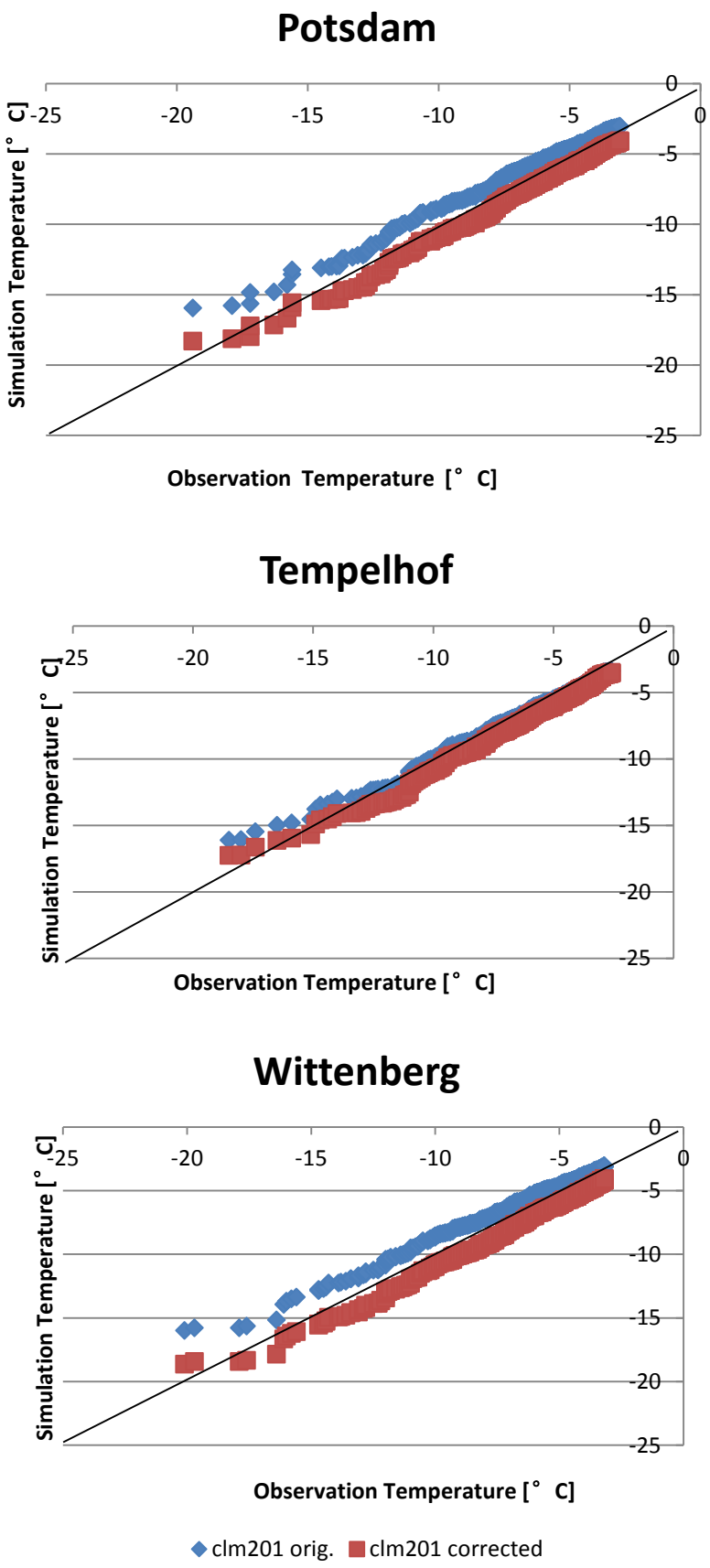

Figure 4.3 Relationship between 5pT observation and simulated data in C20_1 of 7 stations (1971-2000)

The figure 4.3 showed one data set from each station, the period of 1971-2000. The more general and detailed numerical results are shown in table 4.2 which is the median bias (simulation-observation) value of the total 12 data sets from one station. For 95pT, in all the 3 simulation runs, there is a cold bias of 1-2K, which after correction is diminished to less than 0.1K. The extreme low values have achieved the similar results, only with a warm bias reduced to less than 0.1K.

Table 4.2 Bias correction results of all the simulated runs and stations

		C20_1		C20_2		C20_3	
		orig. bias (K)	corr. bias (K)	orig. bias (K)	corr. bias (K)	orig. bias (K)	corr. bias (K)
95P T	CB	-1.02	-0.08	-1.02	-0.08	-1.44	-0.08
	LB	-2.16	-0.03	-2.33	-0.03	-2.38	-0.02
	NRP	-0.99	0.02	-1.39	-0.02	-1.13	-0.08
	ANG	-0.61	-0.01	-0.97	0.05	-0.67	0.01
	PD	-1.37	0.02	-1.84	0.03	-1.44	0.07
	TPH	-1.33	0.05	-1.93	0.05	-1.63	0.01
	WTB	-0.73	-0.01	-1.30	0.00	-0.86	0.03
5P T	CB	1.32	-0.11	0.44	-0.04	1.73	-0.06
	LB	1.21	-0.03	0.40	0.00	1.54	-0.05
	NRP	0.92	-0.10	-0.01	-0.07	1.29	-0.09
	ANG	1.16	-0.13	0.55	0.01	1.57	-0.07
	PD	1.33	-0.01	0.38	-0.01	1.75	-0.03
	TPH	0.26	-0.09	-0.61	-0.57	0.58	0.01
	WTB	1.38	-0.11	0.53	-0.04	1.81	-0.06

In general, the correction using the transfer function on the original simulated data established a positive result. The bias, warm or cold, is reduced from 1-2K to less than 0.1K in most of the cases, with some exceptions of -0.11 (CB C20_1), -0.13 (ANG C201) and -0.57(TPH C20_2). The correction is successful in all the data sets in different simulation runs and in all the analyzed 7 stations.

4.1.2 Daily Temperature Difference

Daily temperature difference is the difference between the maximum temperature and minimum temperature within one day. The original simulated results showed obvious lower values compared to the observation values. Table 4.3 shows the average daily temperature difference of the 12 data sets in 1960-2000. The correction is carried out in 5 stations with full records in 3 simulation runs. The original daily temperature difference is approx. 7-8K, and the original simulation results are approx. 5-6K. After correction the results are improved and represent the observation better. For example, the original simulation value of c20_1 in Cottbus is 6.12K and afterwards, the value is corrected to 7.96 K, which is closer to the observation value of 8.1K.

Table 4.3 Daily Temperature difference correction results, 1960-2000

	OBS(K)		CLM orig. (K)	CLM corr. (K)
CB	8.1	C20_1	6.12	7.96
		C20_2	6.04	7.97
		C20_3	6.11	7.99
LB	7.5	C20_1	5.68	7.47
		C20_2	5.60	7.45
		C20_3	5.67	7.48
NRP	7.3	C20_1	5.71	7.24
		C20_2	5.67	7.21
		C20_3	5.69	7.24
TPH	7	C20_1	6.26	6.80
		C20_2	6.19	6.79
		C20_3	6.30	6.85
PD	7.7	C20_1	6.22	7.70
		C20_2	6.19	7.71
		C20_3	6.20	7.67

The probability of occurrence of a certain event is also improved, shown in the cumulative density function in figure 4.4. Before correction the cumulative density is

underestimated at all points, and afterwards, the corrected simulation line and observation are almost coincided.

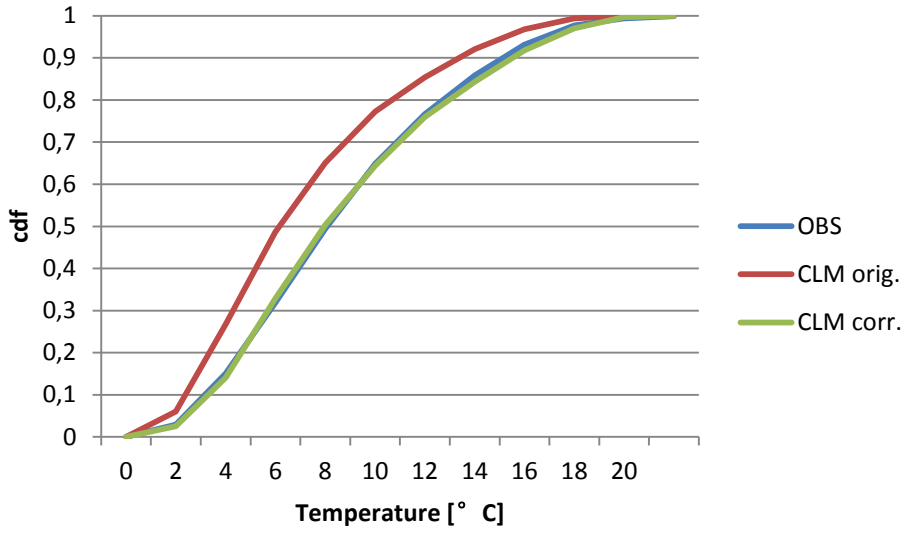

Figure 4.4 Cdf of daily temperature differences correction in Cottbus 1971-2000 in C20_1

4.1.3 Seasonal Temperature

As explained in chapter 4, the fitted distribution for both summer and winter data is generalized extreme value distribution. The correction results are shown in the table 4.4 below. According to the observation records, the average daily temperature value in summer for the 12 data sets of 30 years is between 16.8°C -18.1°C, with the highest value location Tempelhof and lowest Neurrupin. The simulation results however present lower values of the range between 15°C-16°C. The original results showed a cold bias of 1-2K, which is reduced to less than 0.5K after correction. This correction has successfully positive results for all simulations of all the 7 researched stations. The bias is minimized and the corrected simulation values can represent the real climate conditions better than originally.

Table 4.4 Summer Temperature correction results, 1960-2000

		JJA Daily T value [°C]			Bias (CLM-OBS) [K]	
		OBS. T	CLM T	Corr. T	Orig.bias	Corr.bias
CB	201	17.6	15.93	17.60	-1.65	0.02
	202	17.6	15.87	17.56	-1.71	-0.02
	203	17.6	15.75	17.62	-1.83	0.04
LB	201	17.2	15.33	17.27	-1.89	0.05
	202	17.2	15.40	17.24	-1.82	0.02
	203	17.2	15.11	17.23	-2.12	0.00
NRP	201	16.9	15.17	16.95	-1.77	0.01
	202	16.9	15.15	16.92	-1.79	-0.02
	203	16.9	15.05	16.97	-1.89	0.03
TH	201	18.1	15.86	18.05	-2.22	-0.03
	202	18.1	15.84	18.03	-2.24	-0.05
	203	18.1	15.70	18.03	-2.39	-0.05
PD	201	17.3	15.56	17.22	-1.69	-0.04
	202	17.3	15.51	17.21	-1.74	-0.04
	203	17.3	15.44	17.26	-1.82	0.01
WTB	201	17.3	15.95	17.33	-1.38	0.00
	202	17.3	15.90	17.33	-1.43	0.00
	203	17.3	15.75	17.34	-1.58	0.01
ANG	201	16.8	15.32	16.85	-1.51	0.02
	202	16.8	15.26	16.76	-1.58	-0.08
	203	16.8	15.14	16.81	-1.70	-0.03

For winter (DJF) daily temperatures, the observed average daily temperature bias in 30 years is between 0.5-1.3K. Although the difference is small, most of them are still positive value, indicating a warm bias on contrary to the summer temperature. The simulation results after correction shows an average bias of -0.11-1.12K, seen in table 4.5.

Table 4.5 Winter Temperature correction results

	DJF T correction	Bias orig.[K]	Bias corr.[K]
Cottbus	C201	0.62	-0.05
	C202	0.72	-0.06
	C203	0.12	0.00
Lindenberg	C201	0.24	-0.02
	C202	0.33	-0.03
	C203	-0.29	-0.01
Neuruppin	C201	0.50	-0.60
	C202	0.67	-0.54
	C203	0.01	-0.60
Templehof	C201	1.12	0.18
	C202	1.22	0.18
	C203	0.65	0.19
Potsdam	C201	0.20	-0.03
	C202	0.29	0.13
	C203	-0.37	0.10
Wittenberg	C201	0.27	-0.13
	C202	0.36	-0.09
	C203	-0.22	-0.02
Angermuende	C201	0.57	-0.14
	C202	0.69	-0.14
	C203	0.15	-0.13

The corrections are successful in some stations like Cottbus and Lindenberg, where the corrected biases are reduced to less than 0.1K. In other stations, the corrections are not very effective, especially when the original biases are already low, such as in Potsdam, where the original bias is around 0.2-0.3 and the corrected values are around 0.1. The main reason lies in the range of the temperature distribution. As discussed before, the simulations present a higher value at cold conditions (minus C temperatures) and lower values at warm conditions (positive C temperatures). In the

case of DJA daily temperatures, the observed temperature records for 30 years in Cottbus for example locate between -20°C to 14°C. The model results for all 3 simulations have smaller range of -17°C to 10°C. In this case, the differences calculated as simulated minus observed are not large in values. This is one of the limitations of this method that when the original bias is already small, the correction does not achieve expected results. In one special case of Neurrupin, the bias correction results are even in the wrong direction. The original biases are 0.01-0.67K and afterwards the biases are around -0.6K. The reason probably lies in the choice of the empirical distribution. The correction of 5P T is done with the transfer function determined by the power distribution. For Neurrupin, the power distribution is not the best fitted choice and causing the failed bias correction.

However, the bias is not the only parameter that indicates the different behaviors of two distributions. Since the spread range of the two distributions is different, the possibilities of a certain temperature occurrence are different. In figure 4.5 for example, shows the winter temperature distributions of period 1961-1990 in Cottbus. The original simulation results showed a lower possibilities of occurrence of extreme temperatures (-20°C to -5°C and 10°C to 15°C) and higher possibilities with median temperature values (-5°C to 5°C). This difference is corrected by the transfer function and the results are marked green in the figure below. The line showing possibilities of corrected simulation values are closer to the observation values. For example, the occurrence probability of temperature 10°C in observation records is 15%, but the original simulation showed a much lower probability of 10%. After correction, this value is elevated to 16%, which is closer to the observation reality. Although the difference is smaller, the same pattern happens in the extreme low temperature range and the reverse pattern happens in the median range.

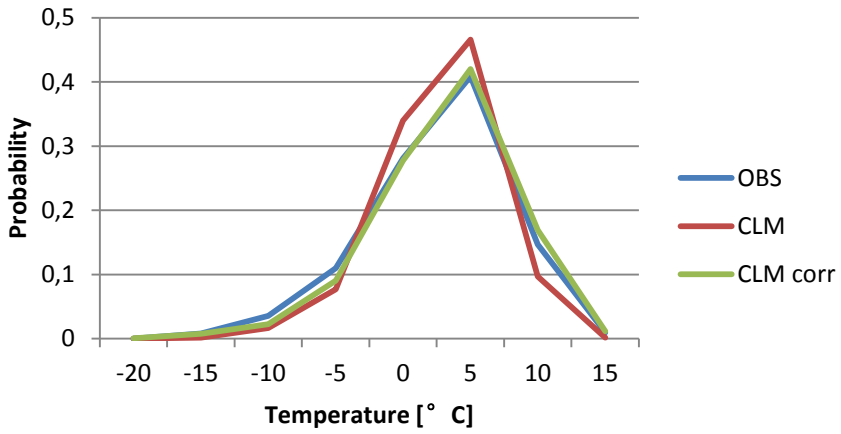

Figure 4.5 Pdf of DJF Temperature correction in Cottbus C20_1 1961-1990

Other 7 stations behave similar with the example of Cottbus. With the DJF daily temperature correction, the distribution of simulation value sets are modified and improved, representing the real climate conditions better than the original simulations.

4.1.4 Extreme precipitation

After analyzing the distribution behaviors of both observation and simulation, the fitted distribution for both is Generalized Pareto distribution. Since the precipitation records are more complete in the observation stations in Brandenburg, it is possible to analyze all the grid cells in model with corresponding stations with full records.

The observed 95 percentile precipitations distribute from 7mm/d up to the maximum 171.7mm/d, with a median value of 10-11mm/d approximately. The simulated data C201 however has a range from 8 to 246mm/d and a median of 11-13mm/d. the figure 4.6 is a part of QQ plot of the 95 percentile precipitation in Neurruppin in the period of 1971-2000. The blue dots represent the original model data vs. observation and the red ones are corrected vs. observation. The figure indicates that before correction simulated data have higher values than observation data, which means an overestimation. A QQ plot comparison is listed in table 4.6.

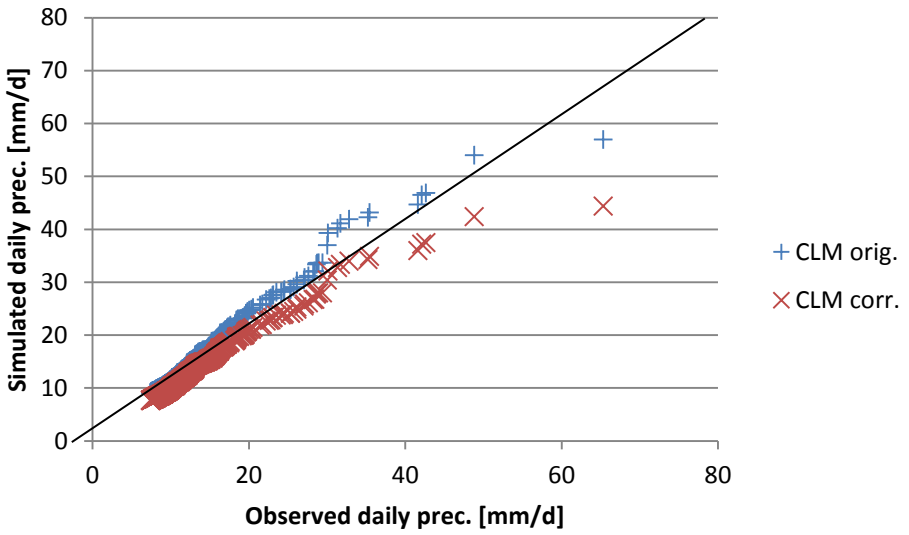

Figure 4.6 Neuruppin extreme precipitation correction results 1971-2000, C20_1

*The maximum values of the daily precipitation are 83mm/d in observation data and 228mm/d in model. The ranges of axis are adjusted for the purpose of better illustration. In the Figure, 1 set of the highest values are not included.

Table 4.6 Correction results of extreme precipitations in different stations in C20_1 data set of 1971-2000

	Cottbus[mm]			Lindenberg[mm]			Neuruppin[mm]		
Percentile[%]	OBS	orig.	*corr.*	OBS	orig.	*corr.*	OBS	orig.	*corr.*
1	8.0	8.6	*7.8*	7.8	9.6	*7.6*	7.5	9.1	*7.6*
5	8.2	8.7	*7.9*	7.9	9.8	*7.9*	7.6	9.4	*7.9*
10	8.4	9.0	*8.3*	8.2	10.0	*8.1*	7.9	9.5	*8.0*
50	11.6	11.4	*11.3*	11.3	12.3	*11.0*	10.4	12.1	*10.4*
90	24.7	21.7	*24.1*	23.2	21.0	*21.7*	18.4	22.9	*19.6*
95	32.2	27.6	*31.6*	27.9	27.5	*29.5*	24.5	28.6	*24.1*
99	45.4	38.6	*45.5*	43.0	50.2	*55.4*	41.6	44.7	*36.0*
	Angermuende[mm]			Potsdam[mm]			Tempelhof[mm]		
	OBS	orig.	*corr.*	OBS	orig.	*corr.*	OBS	orig.	*corr.*
1	7.3	8.8	*7.5*	7.9	8.1	*8.3*	7.9	9.3	*7.6*
5	7.4	8.9	*7.6*	8.0	8.2	*8.4*	8.0	9.5	*7.9*
10	7.6	9.2	*7.8*	8.3	8.4	*8.6*	8.2	9.8	*8.3*
50	10.2	12.0	*10.2*	11.1	10.7	*11.1*	11.5	12.4	*11.6*
90	20.0	23.1	*21.5*	21.4	21.0	*22.3*	23.6	21.7	*23.6*
95	25.6	28.9	*28.5*	28.3	28.4	*30.3*	28.4	25.5	*28.7*
99	44.7	52.2	*62.5*	43.7	49.1	*52.6*	41.4	40.0	*48.3*

The original simulation shows an overestimation most of the time and the amount of overestimation increases with the higher original values. In the lower half of the distribution, the difference between observed and simulated values are not more than 2mm and these differences are increased in the higher half. For the top 10 percent of the extreme precipitation, the differences can be up to 3-4mm. However, for some extreme high values as 99 percentile in Cottbus and Tempelhof, the simulated values appear to be lower than the observed ones. Despite of these rare cases, the simulations have an overall overestimation compared to the observation data for all the data sets and forming an average bias, which is significantly reduced after correction.

Since the full precipitation records are well preserved and the stations spread over whole investigated state, it is possible to find a comparative observation site for each grid point in Brandenburg and map out the precipitation bias results in the state. The bias before and after correction are marked with different colors in figure 4.7 and figure 4.8. In figure 4.7 with the original bias, more stations are presenting the color of light green to dark yellow, which indicates a bias between 0.75 to 3mm/d. For example, Neurrupin has a bias of 1.7mm and Tempelhof 0.85 in the C 201 simulation in the period of 1971-2000. For some stations in the west particularly, the bias can be up to more than 3 mm. The mean bias of all the 110 grid points before correction is 1.24mm. After correction, this value is reduced to an average of 0.11mm. The points in figure 4.8 appearing more green color with an occasional blue dots indicating the corrected bias more in the range of ±0.75mm. The Neurrupin grid point bias is lowered from 1.7 to 0.04mm. The only exception in the Figure 4.8 of corrected bias is the one grid point in blue dot in the center with a bias of -3mm. Compared with the above figure, the original bias of the same grid point is less than 0.75mm, which indicates one of the defects of this method is the failure at correction of those data sets where the original bias is already very small. Other light blue dots in the second figure show the same results that when the original bias is small (in this case, less than 1mm), the corrected method will not be proven as effective as expected. This shortcoming will be more obvious in the following corrections of winter temperature.

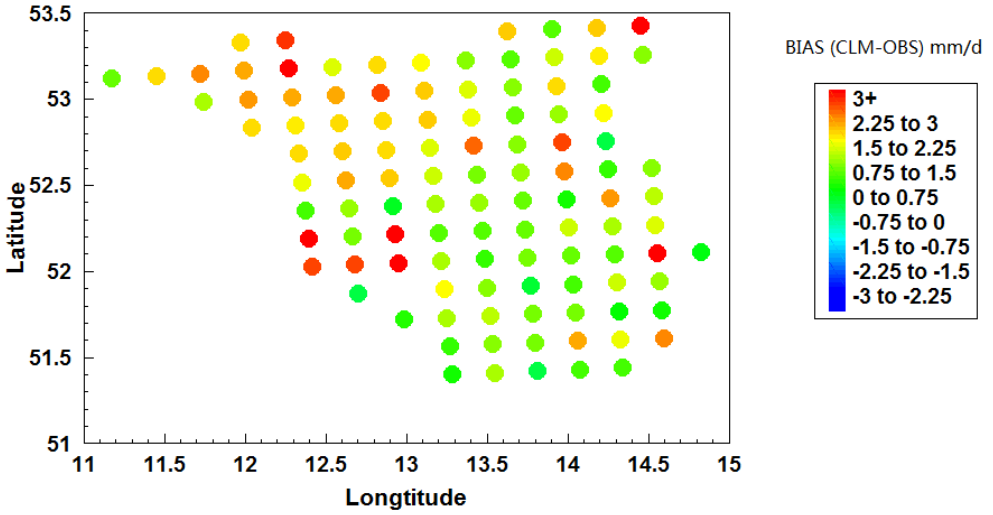

Figure 4.7 Original Extreme precipitation bias over Brandenburg

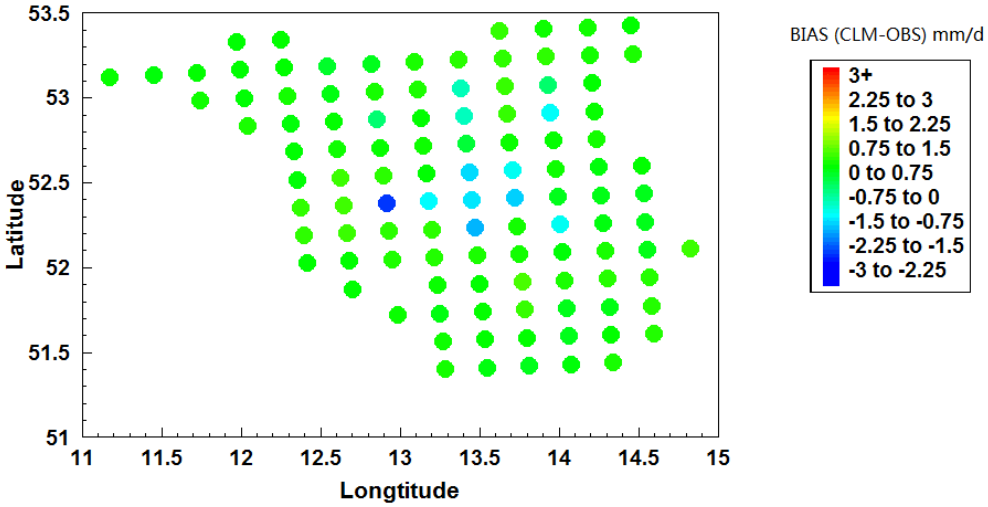

Figure 4.8 Corrected extreme precipitation bias in Brandenburg

In general, these two figures comparison show the correction method is able to reduce the differences to 0.75mm/d (most of the cases down to 0.1mm/d), satisfactorily achieved the goal of minimizing the bias of extreme climate events.

4.1.5 Monthly Precipitation

Monthly Precipitation represents the total precipitation of each month and for a data set of a 30year period, there are 360 values. As daily precipitation results analysis, the monthly precipitation simulation results appear to have an overestimation as well in the data set of 1971-2000 of Cottbus seen in figure 4.9 for example, the original data of CLM have higher values at most points (red line vs. blue line) with a median difference of 15mm. After the transfer function which is created by the General Pareto distribution that fits both observation and simulation data, is applied to the CLM data, the corrected data show a smaller difference. In figure 4.9, the two lines (blue and green) are almost coinciding.

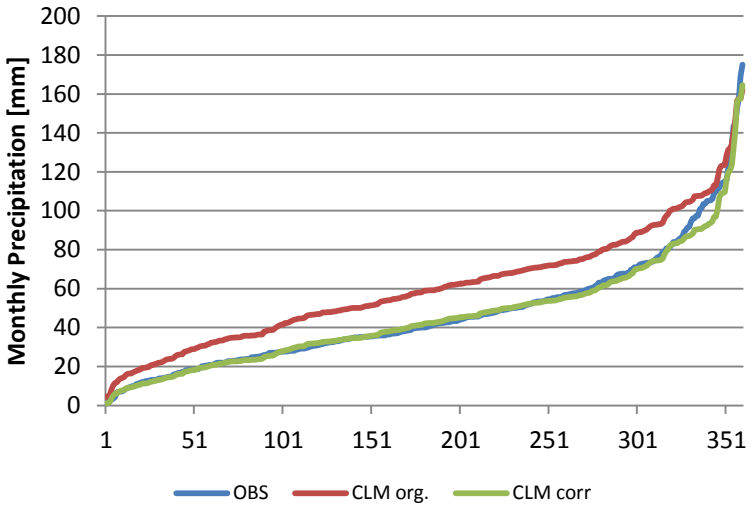

Figure 4.9 Monthly Precipitation correction Cottbus 1971-2000, C201

Values with same percentile comparison are seen below table 4.7. In this table, it states that the differences between model and observed data are not always constant; therefore, it would not be accurate to use the same amount of deduction in the whole distribution. With this transfer function, the corrected results can represent the reality much better at almost all percentiles.

Table 4.7 Percentile comparison Monthly Precipitation correction Cottbus 1971-2000, C20_1

Percentile	OBS	CLM orig.	CLM corr.	Bias orig.	Bias corr.
5	11.1	18.1	10.4	7.0	-0.7
10	14.8	23.9	14.5	9.1	-0.3
50	40.1	59	42.2	18.9	2.1
90	85.9	102	84.2	16.1	-1.7
95	105.4	110.3	93.6	4.9	-11.8
99	152.7	156.6	156.0	3.9	3.3

The original simulated data present higher values at all the percentile. The difference is distinct, especially in the median range of the data set, the difference is up to 19mm. At lower and higher range of the data set, the difference is smaller (4-7mm), but still a clear overestimation. After correction, this difference is reduced, most of the cases down to 1-2mm, with the exceptions of extreme high values.

The figure 4.10 and 4.11 show the overview of bias correction results in Brandenburg. Comparing these two graphs, it is reasonable to generalize that the bias of monthly precipitation is positively reduced. In the upper figure with the original bias, all the grid points show a dark blue to purple colors, indicating the bias are more than 12mm, even with some stations of more than 40mm. After correction in the lower figure, the map is presenting light blue to green color, indicating the bias is controlled within 2mm, with occasional exceptions of 7-10mm. The blue points in the southeast corner in the second map represent higher biases even after correction. Compared to the original map of biases, the grid points which have larger biases after correction are those with even bigger biases in the beginning. The original biases were more than 30 mm and after correction although more than 5mm, are still reduced. Data used in the map is the set of 1971-2000 of simulation c201.

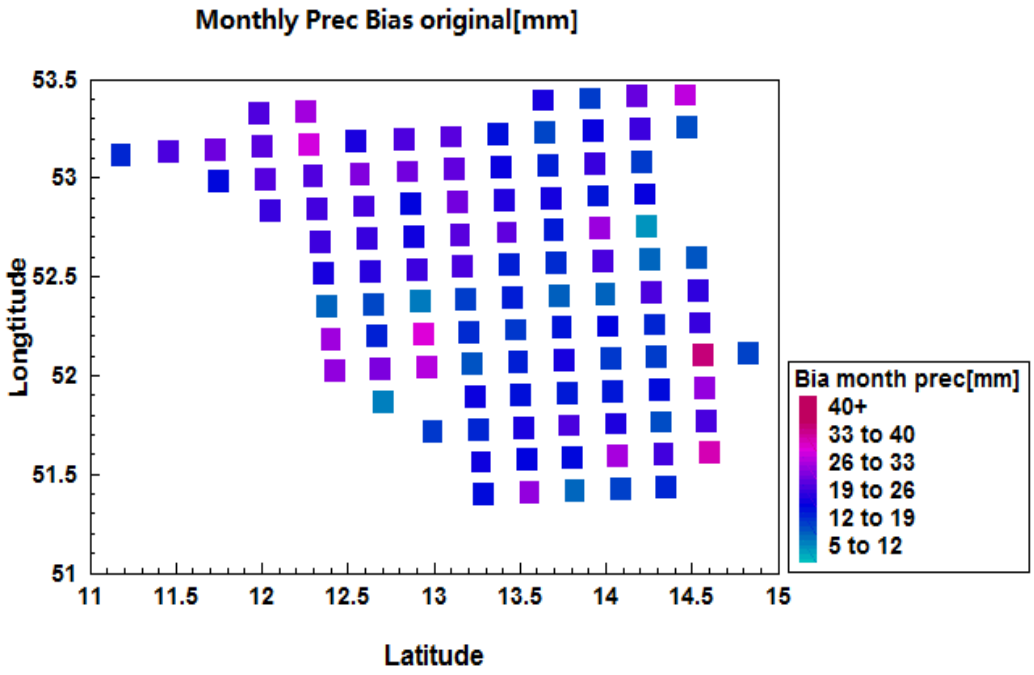

Figure 4.10 Monthly Precipitation bias before correction Brandenburg 1971-2000

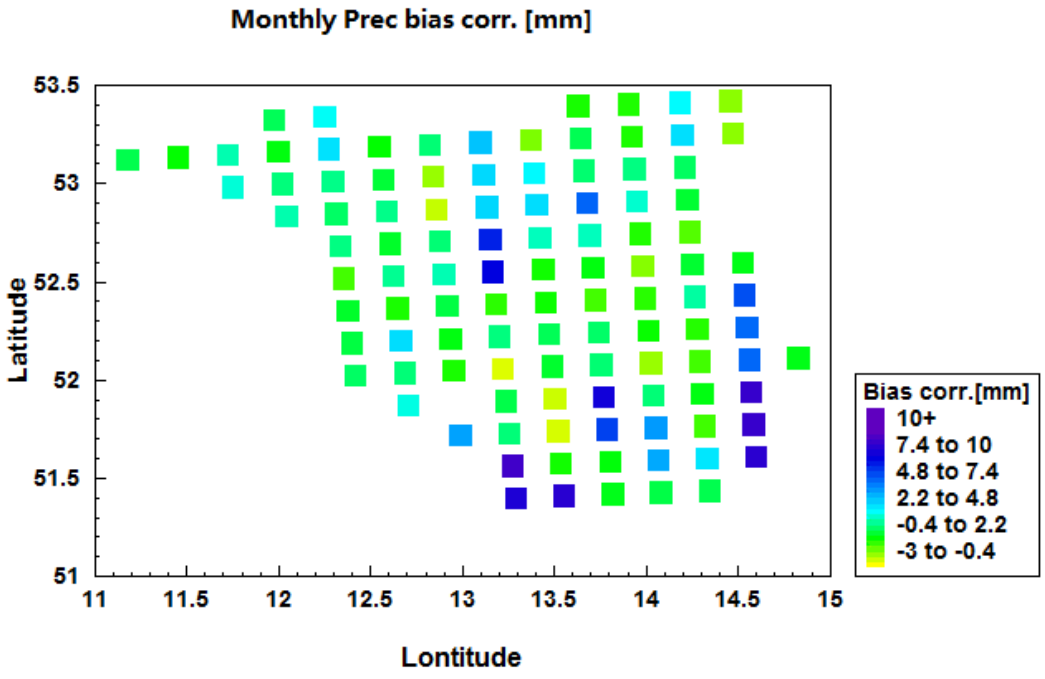

Figure 4.11 Monthly Precipitation bias after correction Brandenburg 1971-2000

In summary, this distribution oriented correction method is proved to be effective at all kinds of parameters corrections. The Transfer function helps to improve the accuracy of simulation and make the simulated values represent the reality better. With the parameters that are determined during the correction of simulation of past decades, the transfer function can be used on the future projections. From the positive satisfying results, it is safe to generalize that the correction on the projections can also be effective and represent the future reality better than before.

4.2 Test and Testify

Chapter 4.1 demonstrates that the bias method of transfer function is able to diminish the bias on the historical runs, from which the parameters of the transfer function are obtained. In this chapter, the results of experiments on simulations including parts of projections are presented. These "testifying runs" are simulated data from 1972 to 2008, consisting of C20 series data and projections data. A1B1 and B11 are combined with C20_1 simulations and A1B2 and B22 are combined with C20_2. The transfer functions obtained from C20 series are used to the test runs and compared with the observed data to test the effectiveness. The results presented are mainly the corrections on extreme temperatures. In figure 4.12, the corrections on the data set of 1979-2008 in Cottbus are shown in colored lines, observed line in blue, original simulated line in red and corrected line in green.

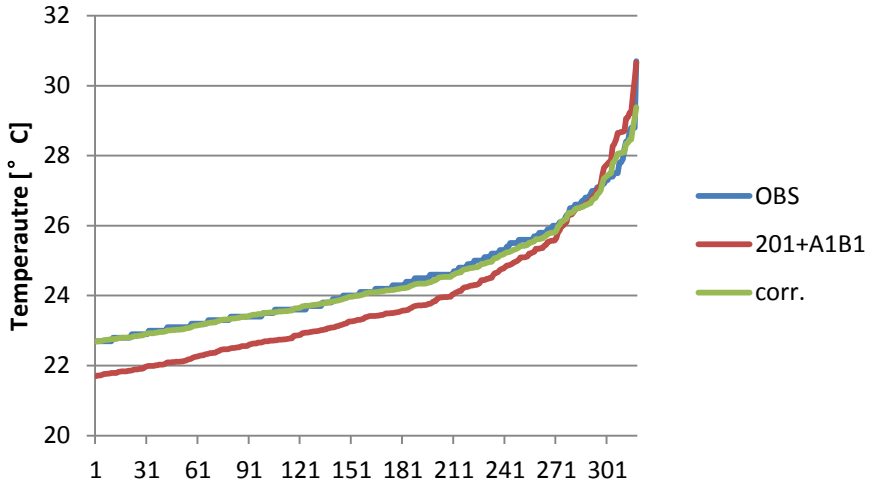

Figure 4.12 Correction on extreme temperature Cottbus 1971-2008

The difference is distinctive before the correction, that the simulated data same as C20 runs, presented an underestimation in values. After correction the difference is not obvious that the two lines are almost coincided with each other. This is the difference on one data set, and with other 7 data sets, the difference remains and therefore a bias is formed. The average difference of the 8 sets of observed and simulated data is listed as original and corrected bias in table 4.8.

Table 4.8 Correction on extreme temperature results in bias

bias 95PT	Simulations	ORIG [K]	CORR[K]
CB	C201+A1B1	-0.78	-0.08
	C202+A1B2	-0.65	-0.09
	C201+B11	-0.94	-0.37
	C202+B12	-1.09	-0.23
LB	C201+A1B1	-2.11	0.03
	C202+A1B2	-2.24	0.12
	C201+B11	-2.35	0.03
	C202+B12	-2.50	-0.12
NRP	C201+A1B1	-1.01	-0.08
	C202+A1B2	-0.93	0.29
	C201+B11	-1.10	-0.06
	C202+B12	-1.22	0.11
PD	C201+A1B1	-1.15	0.13
	C202+A1B2	-1.20	0.54
	C201+B11	-0.99	0.26
	C202+B12	-1.35	0.44
TPH	C201+A1B1	-1.22	-0.09
	C202+A1B2	-1.37	0.39
	C201+B11	-1.02	0.05
	C202+B12	-1.48	0.28
ANG	C201+A1B1	-0.53	0.02
	C202+A1B2	-0.59	0.34
	C201+B11	-0.37	0.13
	C202+B12	-0.74	0.24

The original bias of the 6 stations is a cold bias and around -0.5 to -2.5K, with the highest bias in Lindenberg and lowest in Angermuende. After correction, the biases

are eliminated to less than 0.5K, most of the time less than 0.3K. Similar results as the historical runs are that when the original bias is already small, as in Angermuende less around 0.5K, the correction is not very obvious, eg. C202+A1B2 bias is changed from -0.59K to 0.34K.

In summary, the test runs prove that even if the transfer function is not generated from the data needed to be corrected, it can be still effective. Since the test runs are consisted partly from projections, it is reasonable to apply the correction on projections for future as well.

4.3 Projections Analysis

The correction method is applied to the 71 data sets in the time period of 2001-2100, with the first data set of 2001-2030 and last one of 2071-2100 to study the possible climate changing trend. The transfer function parameters on A1B1 and B11 are generated from C20_1 and A1B2 and B12 are obtained from C20_2. As the results presented in chapter 4.1, the corrections on the projection runs are also including extreme conditions (temperature and precipitation), monthly precipitation, seasonal temperature and daily temperature difference.

4.3.1 Extreme Temperature Projections

Figure 4.13 to figure 4.15 show the comparison of uncorrected and corrected results of different percentiles of extreme high temperature (95p T) with original data above and corrected data below. To reveal results of correction and the climate changing pattern, from each of the 71 data sets of the extreme temperature, a value corresponding to a certain percentile is selected, namely 95 percentile, 50 percentile and 5 percentile and put together in one map. For example, the first figure is the original 95 percentile of extreme daily temperature in Cottbus in next century, where the y axis is the temperature in [°C], and the numbers of 2001, 2002 … 2071 stand for the 30 year data set of 2001 to 2030, 2002 to 2031 until 2071 to 2100 and different colors represents the 4 projections.

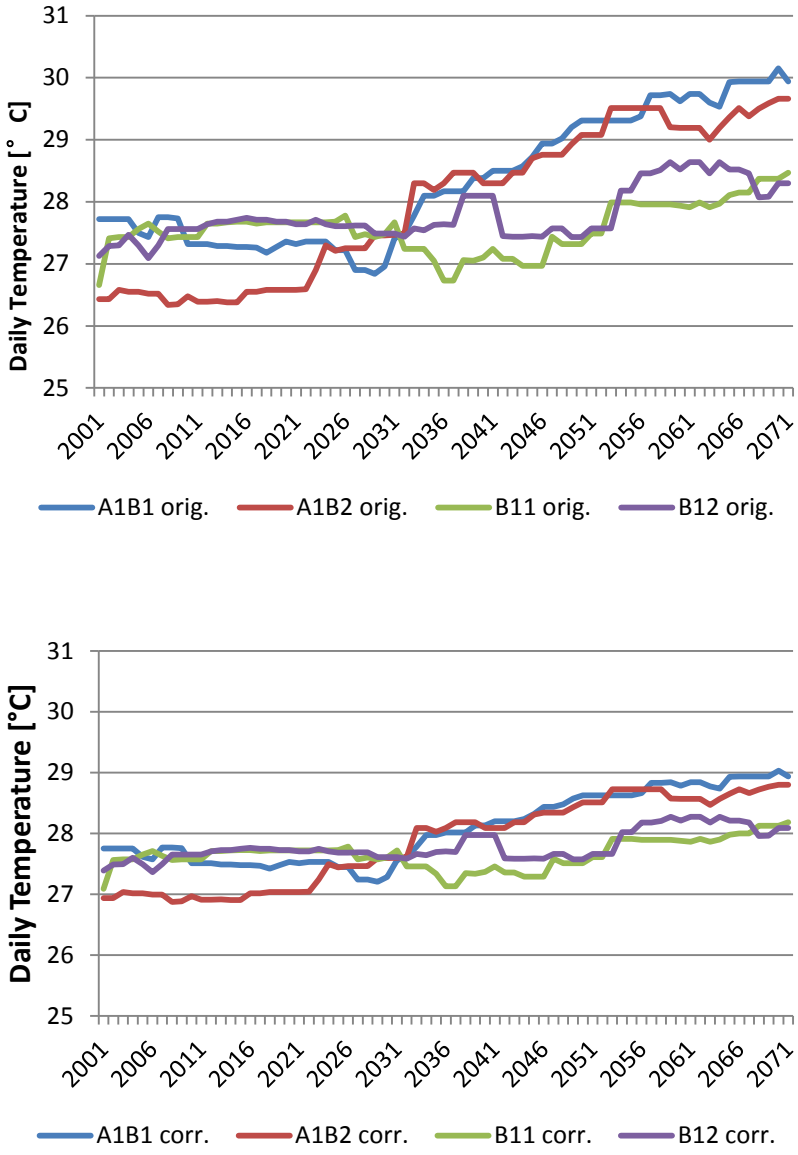

Figure 4.13 Correction comparison of 95P extreme temperature (95P T) in Cottbus 2001-2100

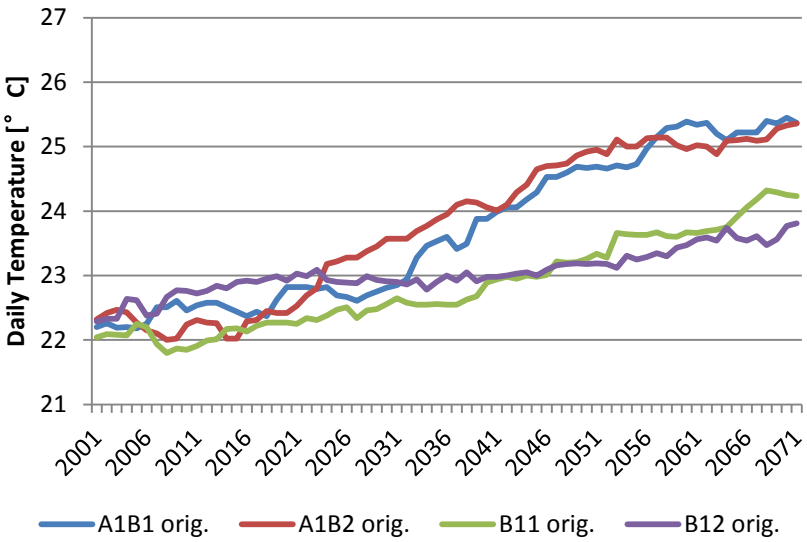

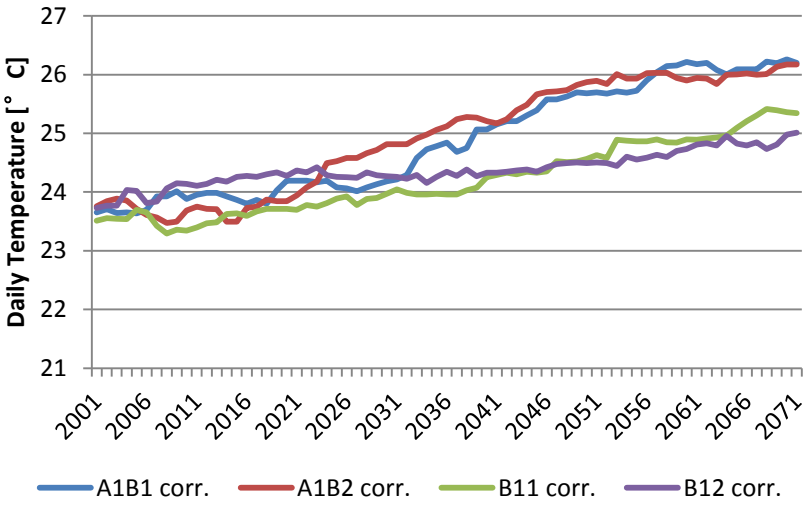

Figure 4.14 Correction comparison of 50P extreme temperature (95P T) in Cottbus 2001-2100

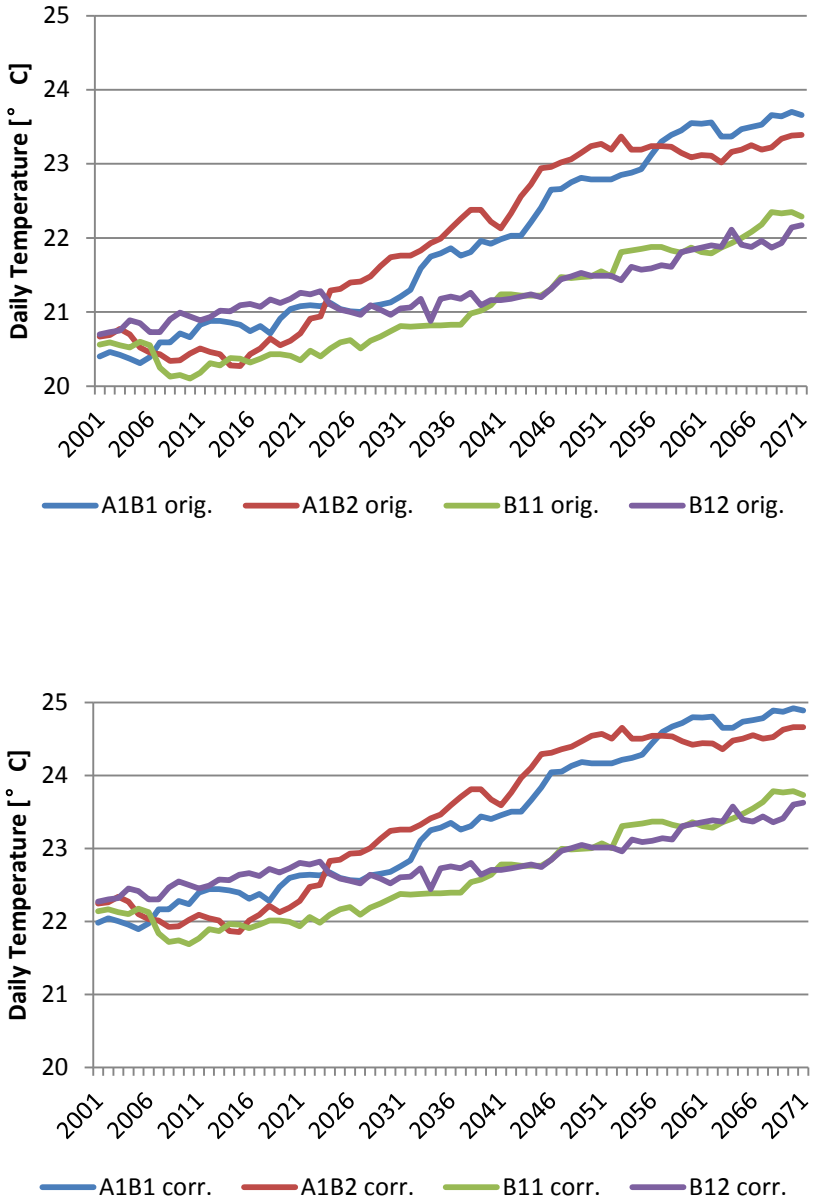

Figure 4.15 Correction comparison of 5P extreme temperature (95P T) in Cottbus 2001-2100

Several conclusions can be generalized from the figure. Firstly, the extreme temperatures over the next century are increasing as predictions in other studies, with projections A1B1 and A1B2 even higher and increased stronger than B11 and B12. The median values of the extreme high temperature for Cottbus are increased from the 22.2 degrees of period 2001-2030 to the 25.3 degrees of 2061-2090 in the projection of A1B1. After correction, this changing tendency is the same, but the values of daily

temperature are higher. The same median value after corrected is 23.6 to 26.2 degrees. The lower part of the extreme temperature shows the same pattern. The values are all elevated by 1-2 degrees. The 5 top percentages of extreme high values show slightly decreased values. In general, the extreme temperature events after correction are more severe in values. The correction however does not change the relationships between different projections. After correction, the fact that the A1 scenarios cause higher extreme temperature than B1 remains the same.

The correction does not only change intensity of the extreme temperature values, it also changes the occurrence frequencies. Figure 4.16 is the cumulative density graph of 95 percentile temperature of A1B1 in cumulative density function of extreme temperatures in Cottbus. The blue and red lines represent the 95 percentile temperature in 2001-2030 and 2071-2100 respectively and the solid and dashed lines stand for the original and corrected values. Through comparison between the first 30 year period and last in the century, the changing tendency of extreme temperatures can be generalized. It is obvious that the latter two data sets show higher cumulative density than the other 2. For example, in the extreme temperature range, the ratios of temperatures larger than 25°C in 2001 is 17%(1-83%), and the same value in 2071 is 58%(1-42%), which indicates a higher possibility of temperatures ≥25 over 40% at the end of the century. The correction enlarges this increase even more. Possibility of temperature ≥25 after correction in 2001 is 22%, 5 percent higher than the original simulated value and the same value in 2071 after correction is 70%. The change between the beginning to the end of the century after correction is 48%, which is more than the 41% of the original values. After correction, the occurrence of the high temperature in 95pT is more frequent and in the next century, this increasing tendency becomes more severe.

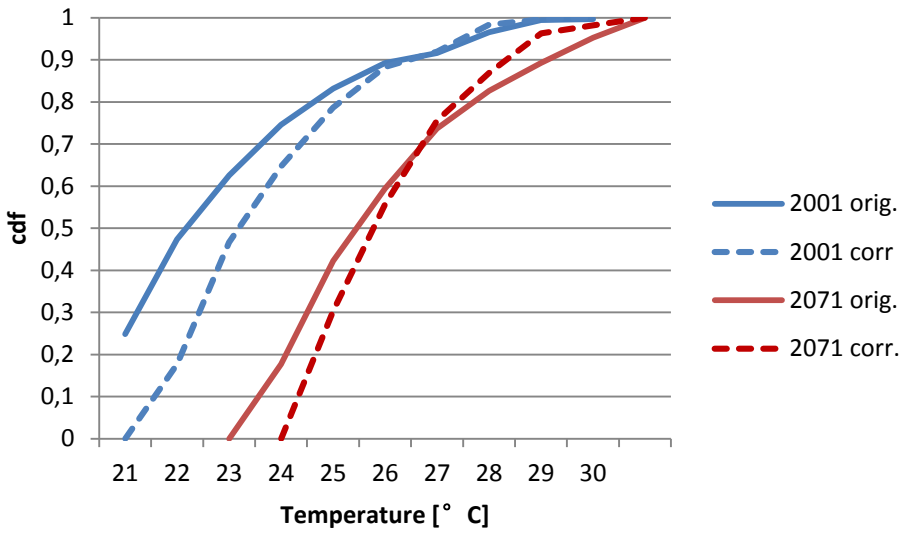

Figure 4.16 Cdf of corrected projections extreme temperatures Cottbus in A1B1 2001 data set and 2071 data set

The correction of the extreme low temperature (5pT) is shown in figure 4.17-4.19. The extreme cold temperatures in both figures show the pattern of strong increasing in the next century, for example, 50 percentile of the low temperature is around -5 degrees in the beginning of the century and in the end this value is increased up to -1 to 0°C. The correction does not change the increasing pattern not the relationships between the projections but the level of the coldness in values. For example the 50 percentile of 5pT of A1B1 before correction, the values in the beginning of the century lie around -5.5 degrees and after correction these values are decreased to -6.7 degrees. At the end of the century, the extreme low temperature is increased to -1 and the same with the corrected values. Changes in other projections have a similar pattern: original B11 increased from -5.5 to -1 and corrected increased from -7 to -1. These changes in the levels of increasing are even more obvious in the 95p of 5Pt, where the original temperature range of -3 to 0 is altered to -4 to 1. After correction, the exteme low temperature is still increasing in the next century, but they are increased with a higher intensity.

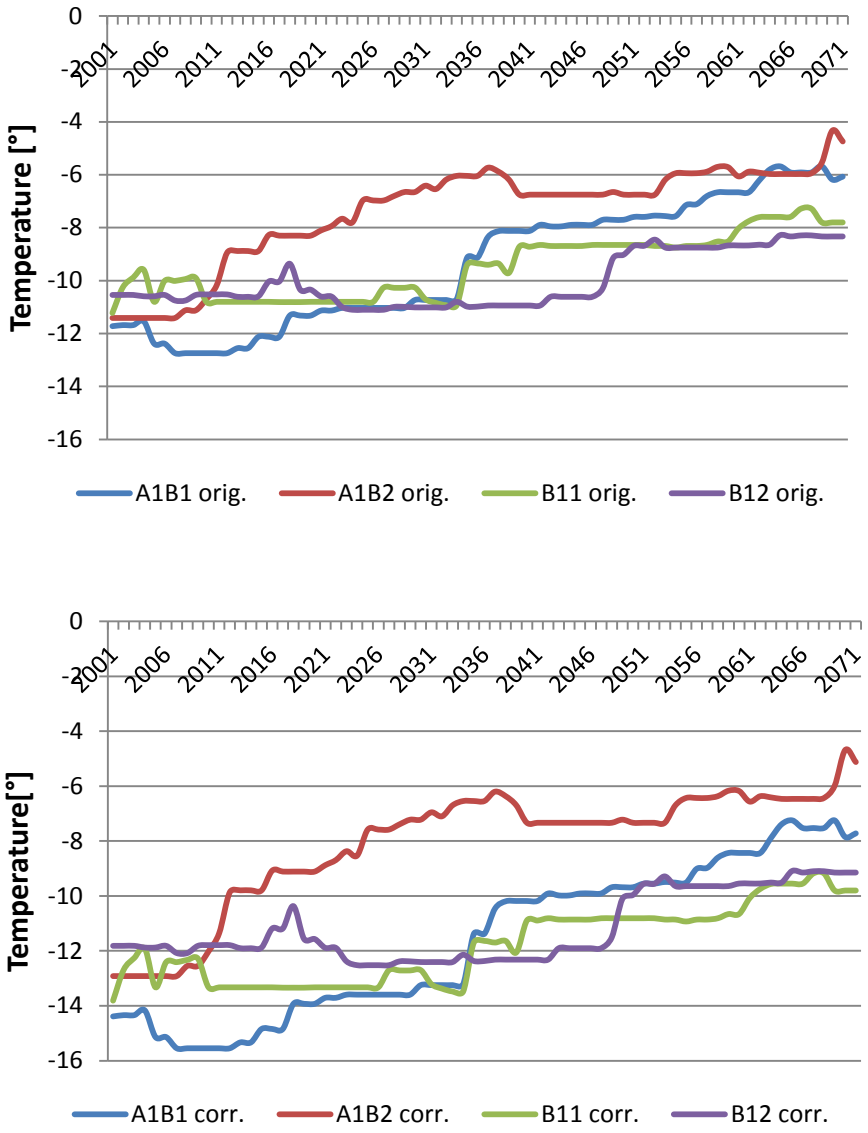

Figure 4.17 Correction comparison of 5P extreme low temperature (5P T) in Cottbus 2001-2100

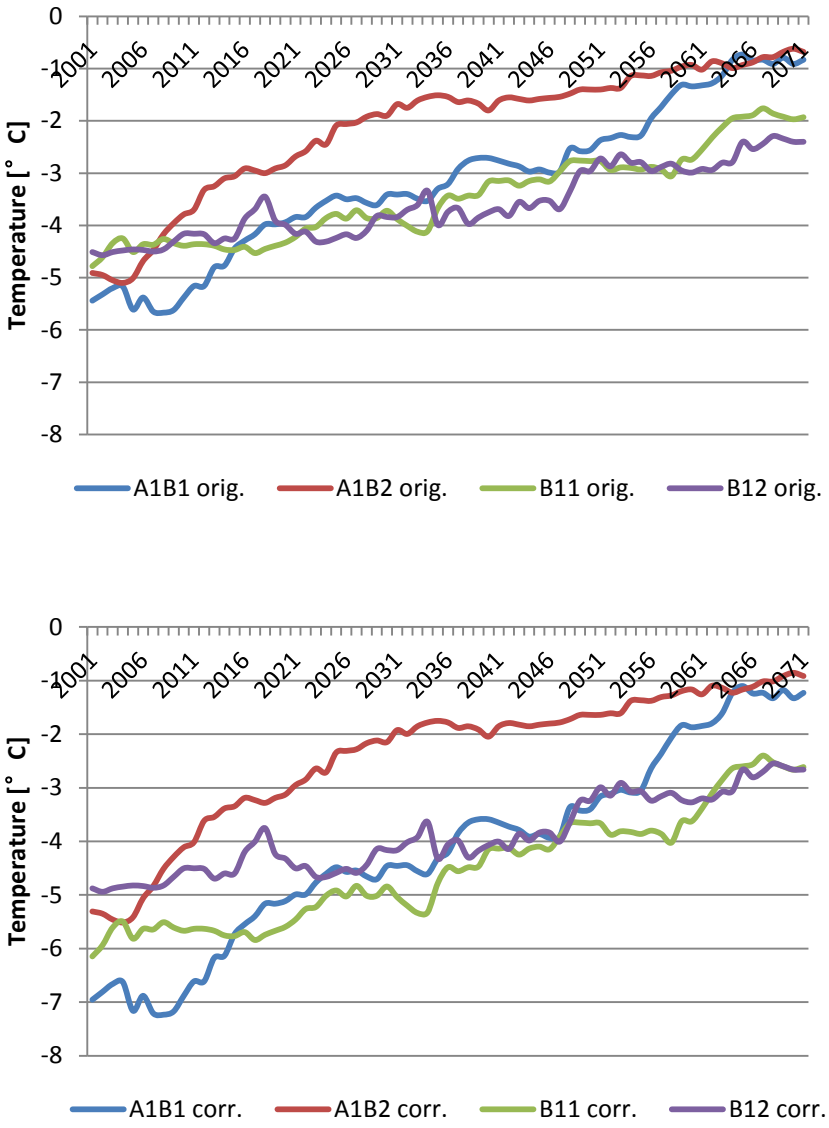

Figure 4.18 Correction comparison of 50P extreme low temperature (5P T) in Cottbus 2001-2100

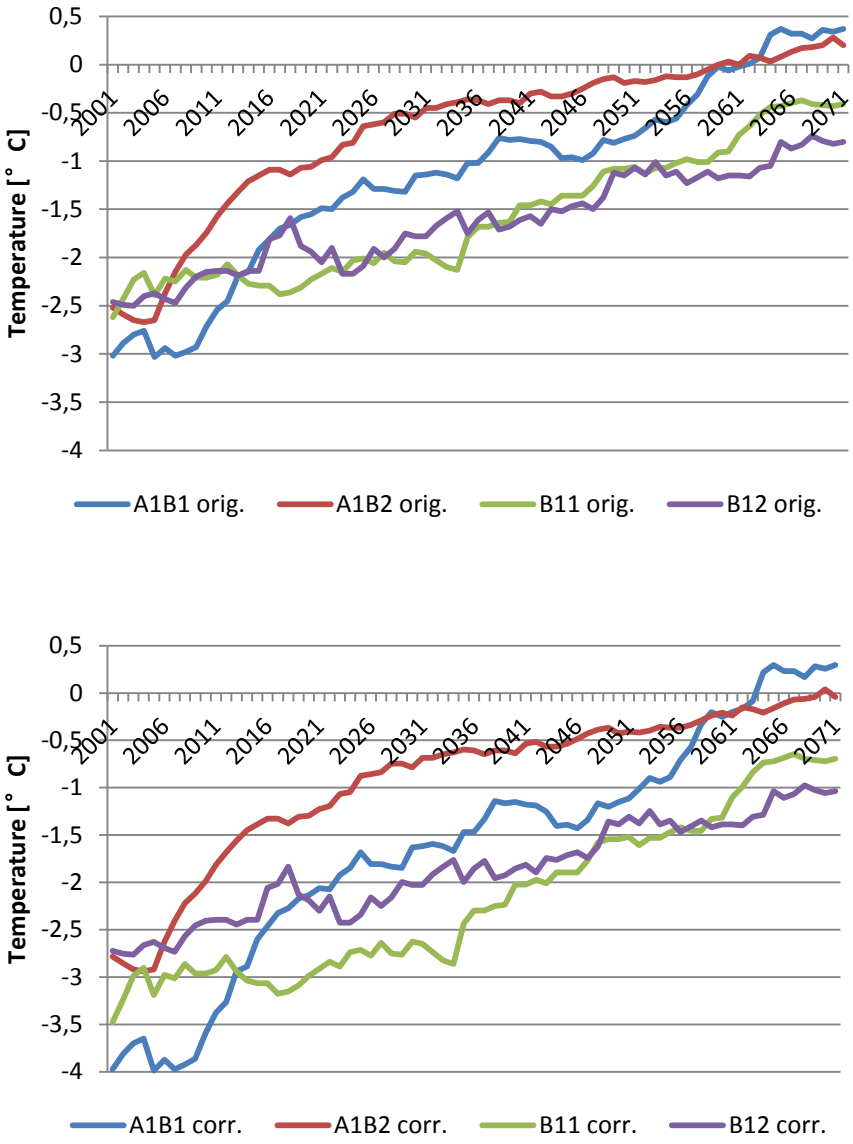

Figure 4.19 Correction comparison of 95P extreme low temperature (5P T) in Cottbus 2001-2100

Meanwhile, the correction also changes the frequency of extreme cold events shown in figure 4.20.

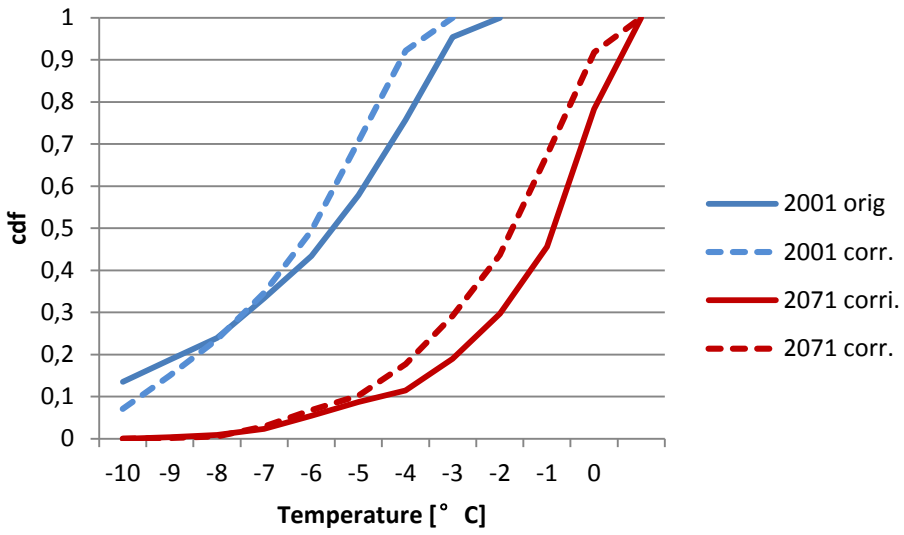

Figure 4.20 Cdf of corrected projections extreme low temperatures (5P T) Cottbus in A1B1 2001 data set and 2071 data set

The same with figure 4.16, the solid and dash lines represent the original and corrected values in the same period. The pair of lines are shifted parallel to the right from 2001 to 2071 periods, indicating that the occurrence possibilities of extreme low temperature will be lower. For example, in 2001 to 2030, the possibility of temperature lower than -5°C is 70% and in 2071 period, this number is reduced to 10%, meaning that there will be more extreme low temperatures as it is now. This change is even amplified after correction.

4.3.2 Daily Temperature Difference Projections

Both original and corrected projections of daily temperature difference do not present any obvious increase or decrease over the next century. The analysis of the cdf distributions also confirms that the frequency of certain events do not change as well. The correction however, elevated the values of the temperatures and also the frequencies of high temperature difference appearance. Figure 4.21 to figure 4.23 show the correction results on daily temperature difference in Lindenberg. The original simulated median daily temperature difference over the century was 5.5K and presented in the two graphs compared in the middle, over the next century, the temperature difference is steady with a small fluctuation and there is also not an

obvious distinction in values between the four projections. This value is modified to an average of 7.3K by the correction with the relationship between projections unchanged. The extreme high and low temperature differences are also raised, respectively 1.8K to 2.4K and 12.5K to 14.5K. As most of the other temperature corrections, the higher the original values are, the bigger the corrections increase. After correction, the daily temperature is higher than the original and will be more than 14.5K in the next century.

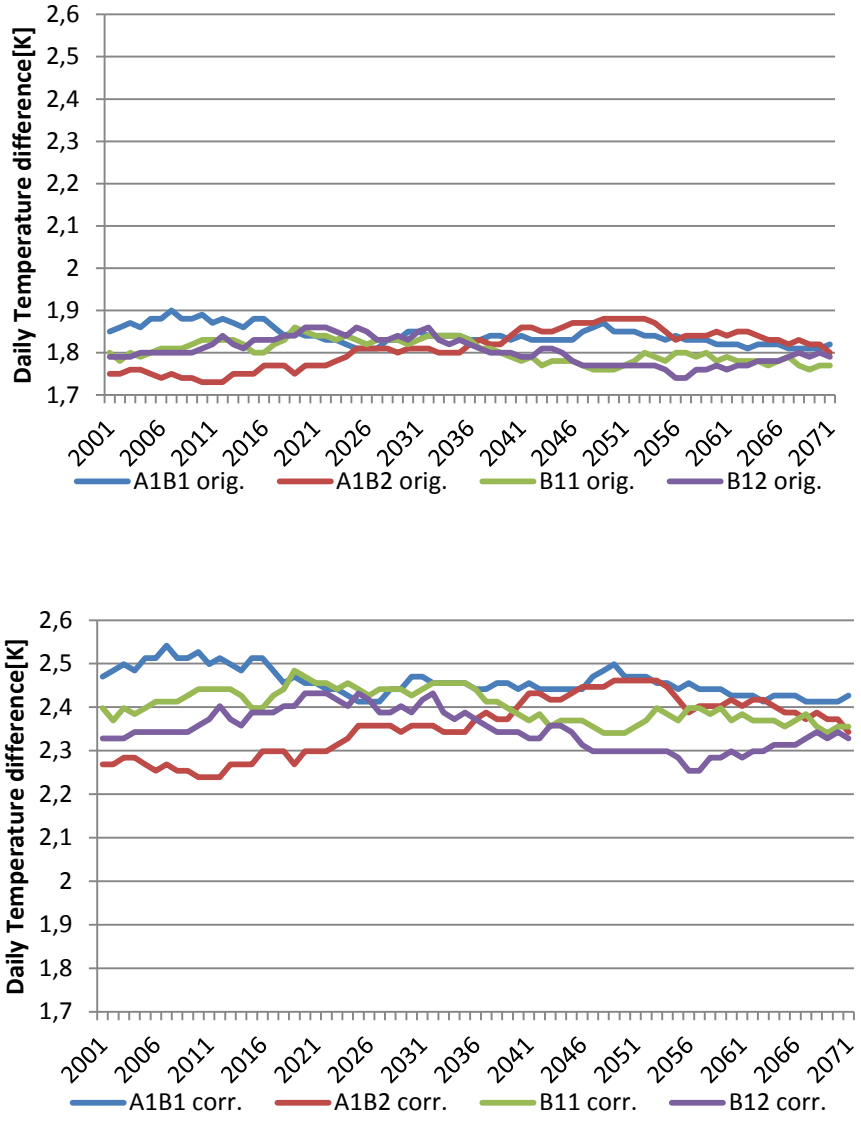

Figure 4.21 Correction comparison of 5P extreme precipitation (95P prec.) in Lindenberg 2001-2100

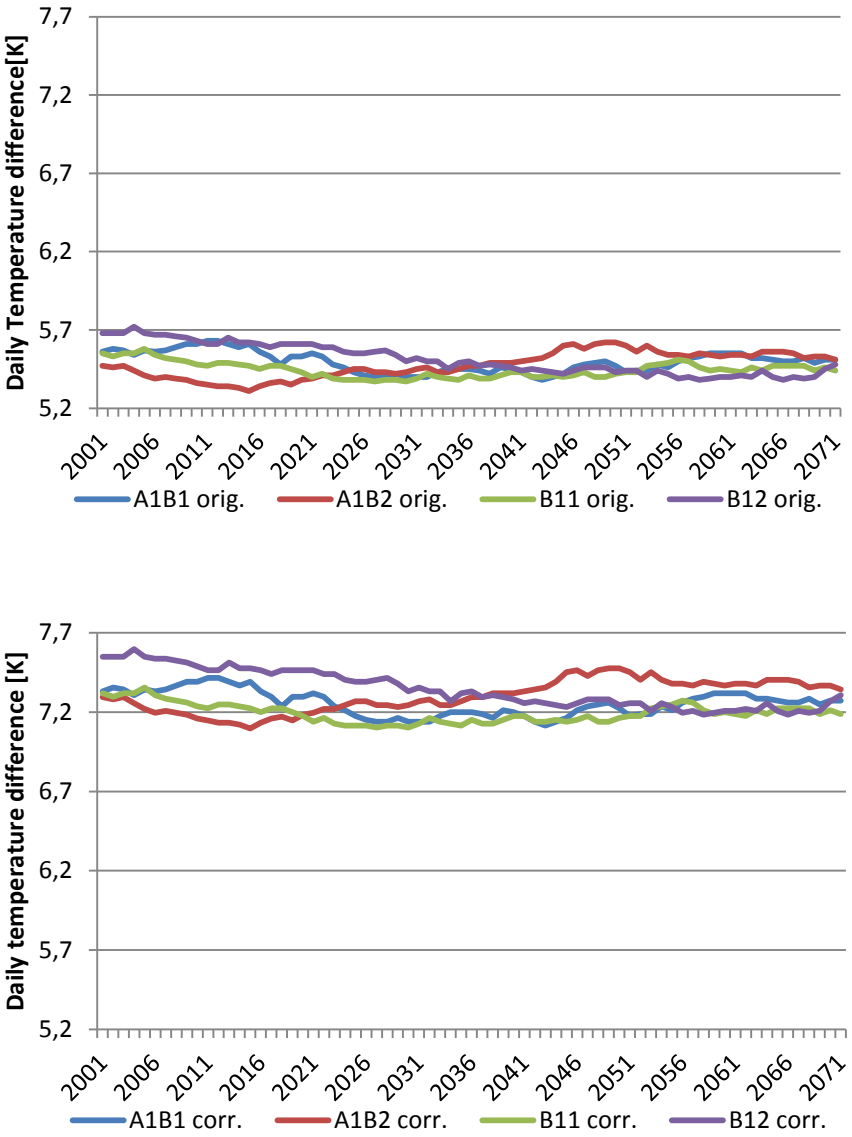

Figure 4.22 Correction comparison of 50P extreme precipitation (95P prec.) in Lindenberg 2001-2100

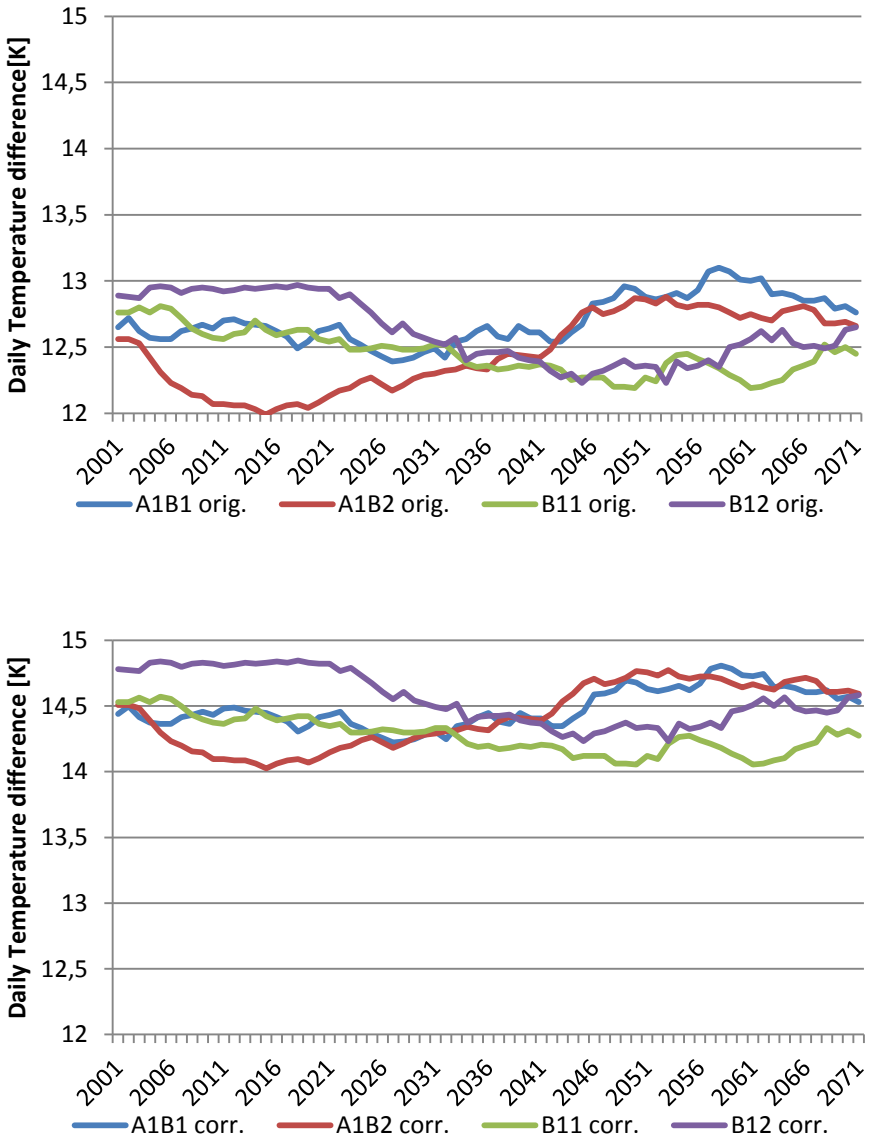

Figure 4.23 Correction comparison of 95P extreme precipitation (95P prec.) in Lindenberg 2001-2100

The frequency of high temperature difference is altered as well. Figure 4.24 describes the cumulative density function of daily temperature difference in Neuruppin. As the other figures, the 2001-2030 data set and the 2071-2100 data seta are marked in different colors, however, in the graph below, these two lines are overlapping, indicating the distribution of different time periods almost identical. This means that in the next century, although the daily mean temperature of the daily max or minimum temperature will be elevated, according to the simulations, the difference

between the highest and lowest temperature will remain the same and great daily temperature difference will not occur more frequently. Nevertheless, the correction increases the frequency. In the original simulations, the value higher or equal to 13K in a day has a probability of 4% (439 days in 30 years) and in the corrected simulations this high daily temperature difference event has a frequency of 11% (1206 days), 767 days more than the original. The new corrected simulations suggest that the phenomenon of higher daily temperature differences is expected.

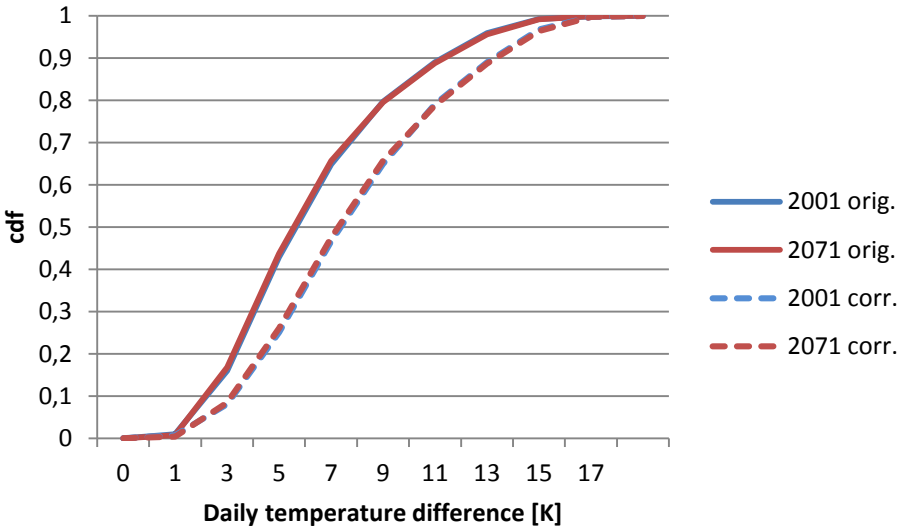

Figure 4.24 Cdf of daily temperature difference in Neuruppin A1B1

4.3.3 Seasonal Temperature

The simulations of summer and winter temperatures indicate a clear signal of increasing over the next century on all the projections. Due to the underestimation shown in the historical runs, the corrections enlarge the temperature values. Figure 4.25 to figure 4.27 show an example of the results comparisons of summer Temperature projections in Lindenberg from 2001 to 2100.

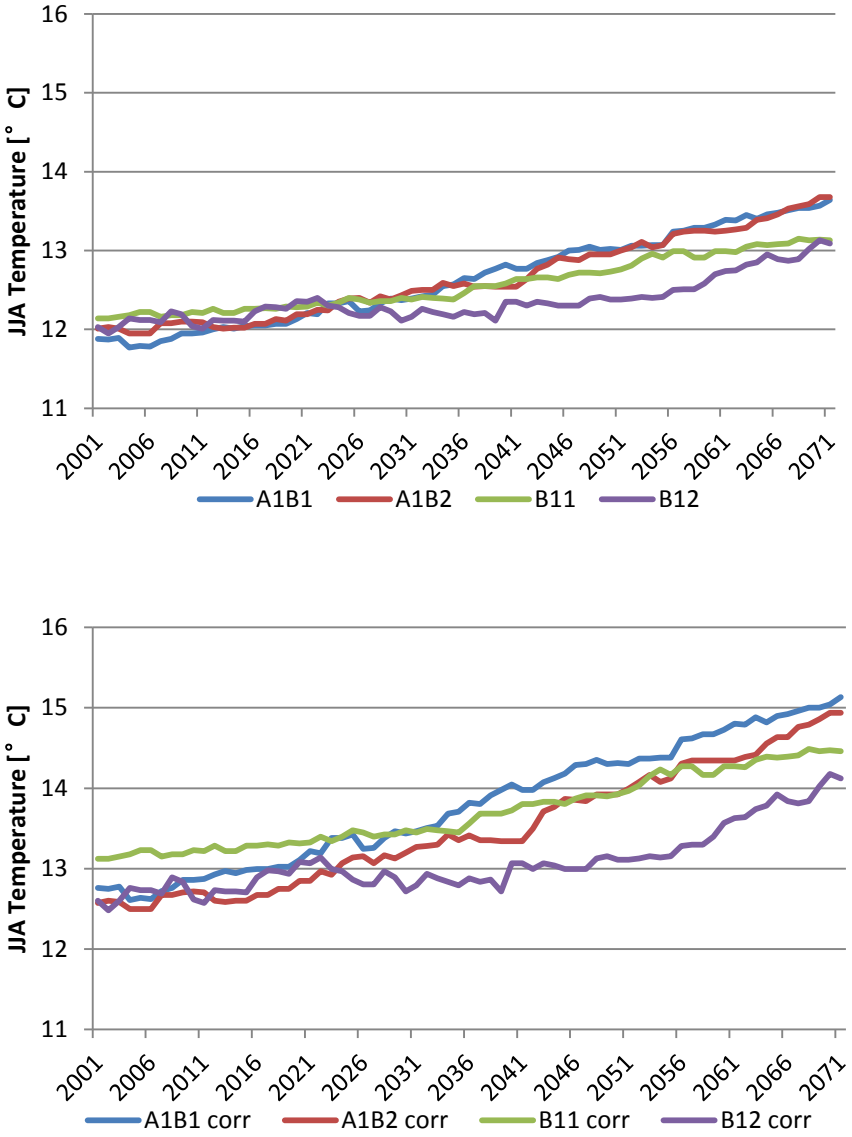

Figure 4.25 Correction comparison of 5P of Summer Temperature in Lindenberg 2001-2100

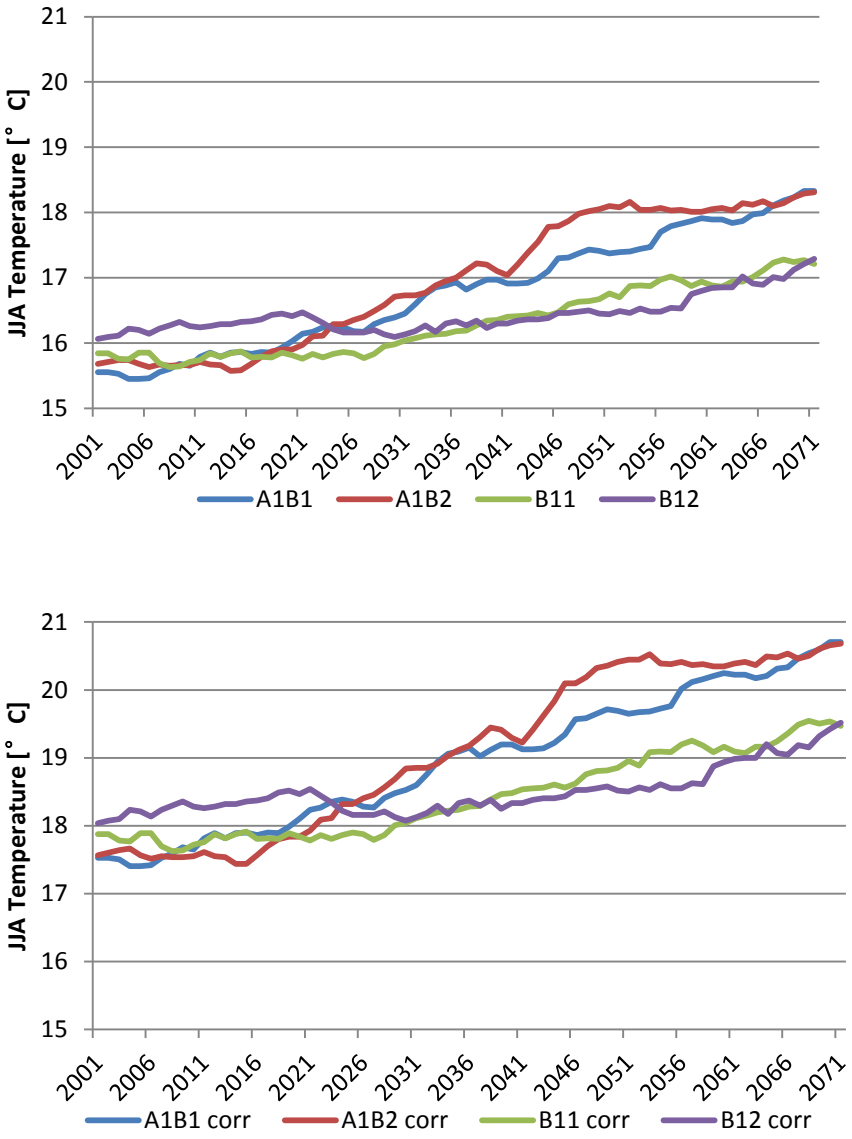

Figure 4.26 Correction comparison of 50P of Summer Temperature in Lindenberg 2001-2100

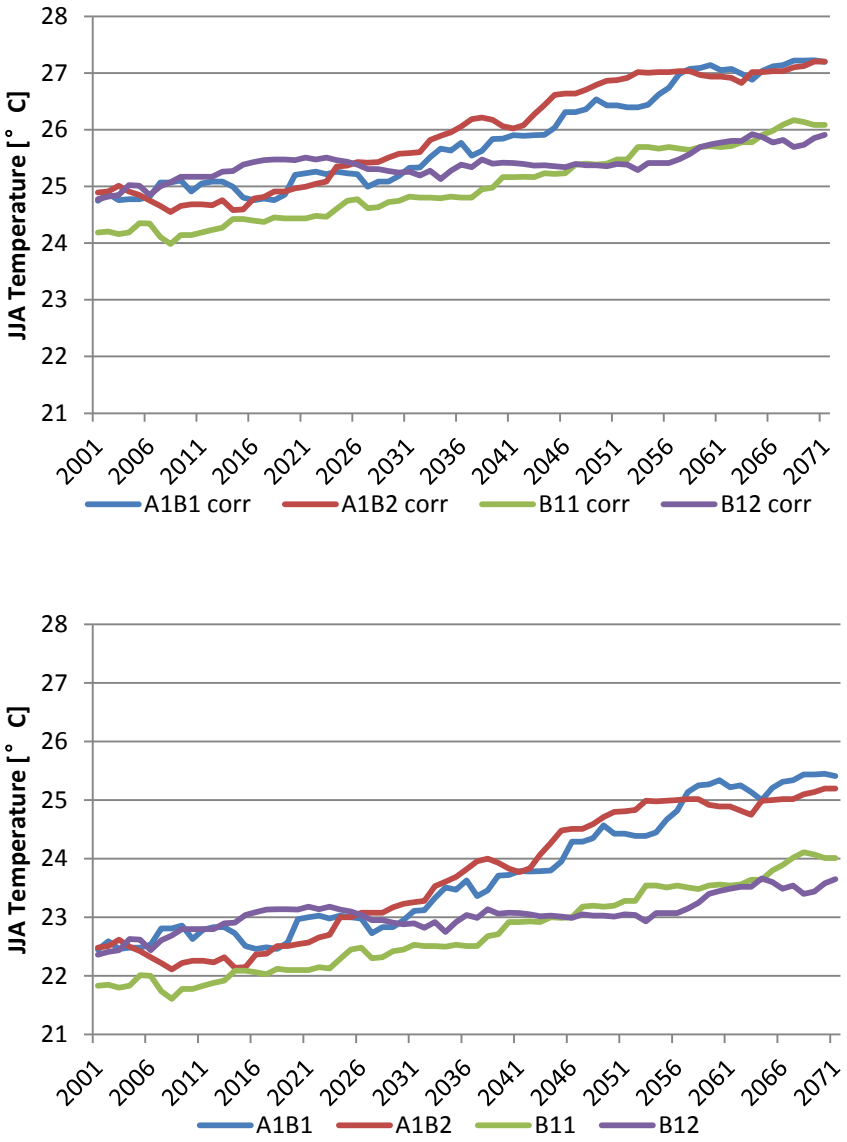

Figure 4.27 Correction comparison of 95P of Summer Temperature in Lindenberg 2001-2100

The extreme low temperatures (5P T) in JJA in Lindenberg are simulated to be around 12°C in 2001-2030. After correction, it is elevated to 12.5-13°C. The 5P summer temperature tend to grow by the end of the century and the projections of A1B1 and A1B2 increase faster than the other two, and after corrected this growing speed is even higher than original. The extreme low summer temperature will increase by 2.5K. With the median range and top range of temperatures, the pattern remains the same, the extreme high temperatures in summer will be elevated by 2K and up to more than

27°C. Table 4.9 presents the correction results for 6 stations with the temperature difference between data set of 2001 to 2071, where the "2001" does not mean the temperature of the single year, but the median temperature in the period of 2001-2030. In the original projection of A1B1 in Lindenberg for example, the median value of summer temperature in the period of 2001-2030 is 15.55°C which increases by 2.78K to 18.33°C in the period of 2071-2100. The corrected median value however, is elevated to 17.53°C and increase by 3.17K to 20.7 degrees, which is 0.39K higher than original simulated growth. The change of 0.39K in growth rate is an extreme example, but most of the cases the growth rates are changed by smaller grades, 0.1-0.2K. The same changing pattern occurs with the lower part of summer temperatures as well, the temperature growths in values are enlarged slightly. This indicates that the correction alters the values and magnifies the climate signal as well.

Table 4.9 Correction results on JJA temperature for 6 stations ("2001" means data set 2001-2030; "2041" means data set 2041-2070; "2071" means data set 2071-2100; Δ means the temperature change between the 2 data sets of 2001-2030 and 2071-2100)

ANGERMUEDE						COTTBUS				LINDENBERG			
		2001[°c]	2041[°c]	2071[°c]	*Δ [K]*	2001[°c]	2041[°c]	2071[°c]	*Δ [K]*	2001[°c]	2041[°c]	2071[°c]	*Δ [K]*
A1B1	Orig.	16.26	17.44	18.96	*2.70*	16.86	18.15	19.65	*2.79*	16.16	17.36	18.78	*2.62*
	Corr.	17.50	18.61	19.92	*2.42*	18.30	19.60	20.98	*2.68*	18.01	19.38	20.88	*2.88*
A1B2	Orig.	16.44	17.66	18.90	*2.47*	16.94	18.28	19.67	*2.72*	16.26	17.47	18.75	*2.48*
	Corr.	17.65	18.80	19.95	*2.30*	18.42	19.79	21.16	*2.74*	18.01	19.40	20.85	*2.84*
B11	Orig.	16.40	17.11	17.84	*1.44*	17.03	17.66	18.52	*1.49*	16.28	16.94	17.70	*1.42*
	Corr.	17.65	18.33	18.98	*1.33*	18.50	19.12	19.95	*1.45*	18.17	18.93	19.75	*1.58*
B12	Orig.	16.54	16.97	17.78	*1.24*	17.17	17.61	18.51	*1.34*	16.46	16.85	17.67	*1.21*
	Corr.	17.75	18.16	18.95	*1.20*	18.68	19.12	20.05	*1.37*	18.27	18.71	19.68	*1.41*
NEURUPPIN						POTSDAM				TEMPELHOF			
		2001[°c]	2041[°c]	2071[°c]	*Δ [K]*	2001[°c]	2041[°c]	2071[°c]	*Δ [K]*	2001[°c]	2041[°c]	2071[°c]	*Δ [K]*
A1B1	Orig.	15.45	16.80	18.22	*2.77*	15.90	17.33	18.76	*2.86*	16.11	17.54	19.22	*3.12*
	Corr.	17.24	18.64	19.99	*2.74*	17.65	19.30	20.82	*3.17*	18.30	19.77	21.38	*3.07*
A1B2	Orig.	15.62	16.94	18.23	*2.62*	16.05	17.46	18.86	*2.81*	16.25	17.81	19.14	*2.89*
	Corr.	17.44	18.84	20.10	*2.66*	17.76	19.29	20.70	*2.94*	18.46	20.13	21.44	*2.98*
B11	Orig.	15.73	16.36	17.13	*1.40*	16.23	16.77	17.66	*1.43*	16.47	17.12	17.97	*1.51*
	Corr.	17.55	18.20	18.96	*1.41*	17.96	18.56	19.50	*1.54*	18.68	19.35	20.20	*1.52*
B12	Orig.	15.94	16.19	17.03	*1.09*	16.43	16.68	17.54	*1.11*	16.73	16.88	17.87	*1.14*
	Corr.	17.79	18.06	18.93	*1.14*	18.28	18.56	19.53	*1.25*	18.99	19.15	20.19	*1.20*

The changes on the extreme and low values will affect the occurrence probability of certain events as well. Figure 4.28 is a graph of cdf distributions for different time period with comparisons of original and simulated values, where solid lines are the original projections and dashed lines are the corrected ones.

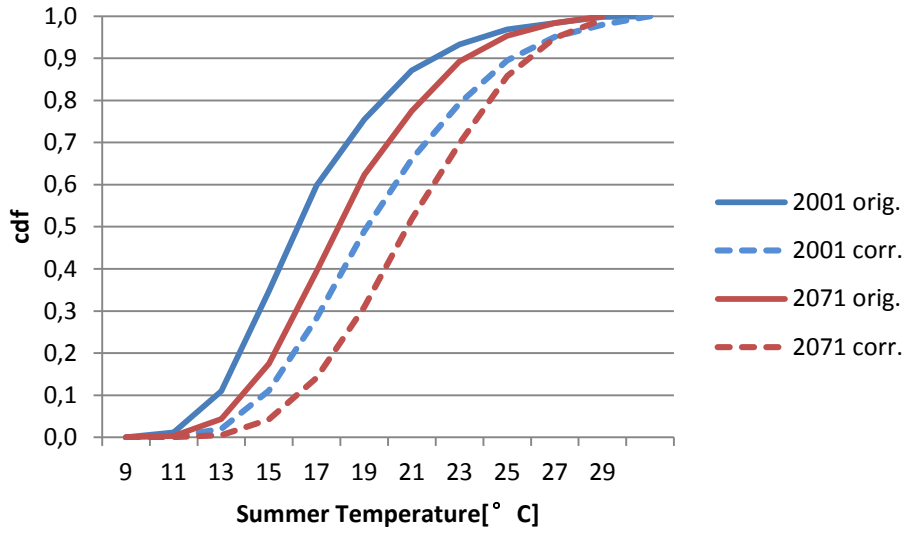

Figure 4.28 Cdf of JJA temperature in Cottbus, projection of A1B1

First of all, the distributions of 2071-2100 locate in the right side of the distributions of 2001-2030, indicating that the in the next century, the extreme high temperature events will happen more frequently, which is coincided with the current prospective. The corrected distribution lines are shifted to the right, indicating the occurrence probability of certain event is higher than before. For example, according to the original simulated data, in the projection of A1B1 in 2001-2030, the chance of temperature higher than 23°C is 7% (1-93%), whereas the corrected probability is 21% (1-79%). Comparing the same data distribution of 2071-2100, the chance of this event is 11% and 30% respectively. Therefore, according to the corrected data, the occurrences of high temperature events will be 9% more over the century. More specifically, of the 2760 days of summer, in 2001-2030, there are 580 days when the daily mean temperature will achieve higher than 23°C, thus in 2071-2100, 633 days will have a temperature this high. This 9% more days of high temperatures were 4% in the original simulations, which means, the correction elevated the frequency of extreme climate events.

Figure 4.29 to figure 4.31 present the comparison of correction on winter temperature in Lindenberg from 2001-2100.

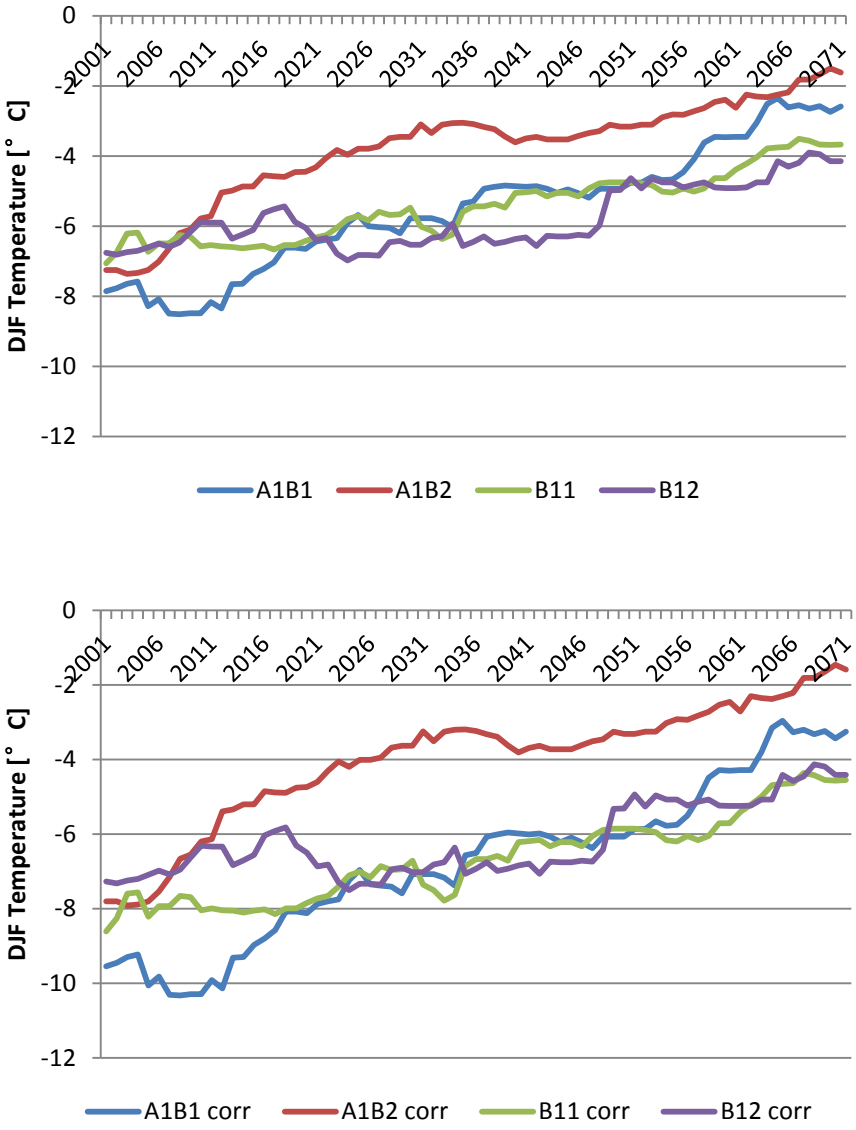

Figure 4.29 Correction comparison of 5P of winter Temperature in Lindenberg 2001-2100

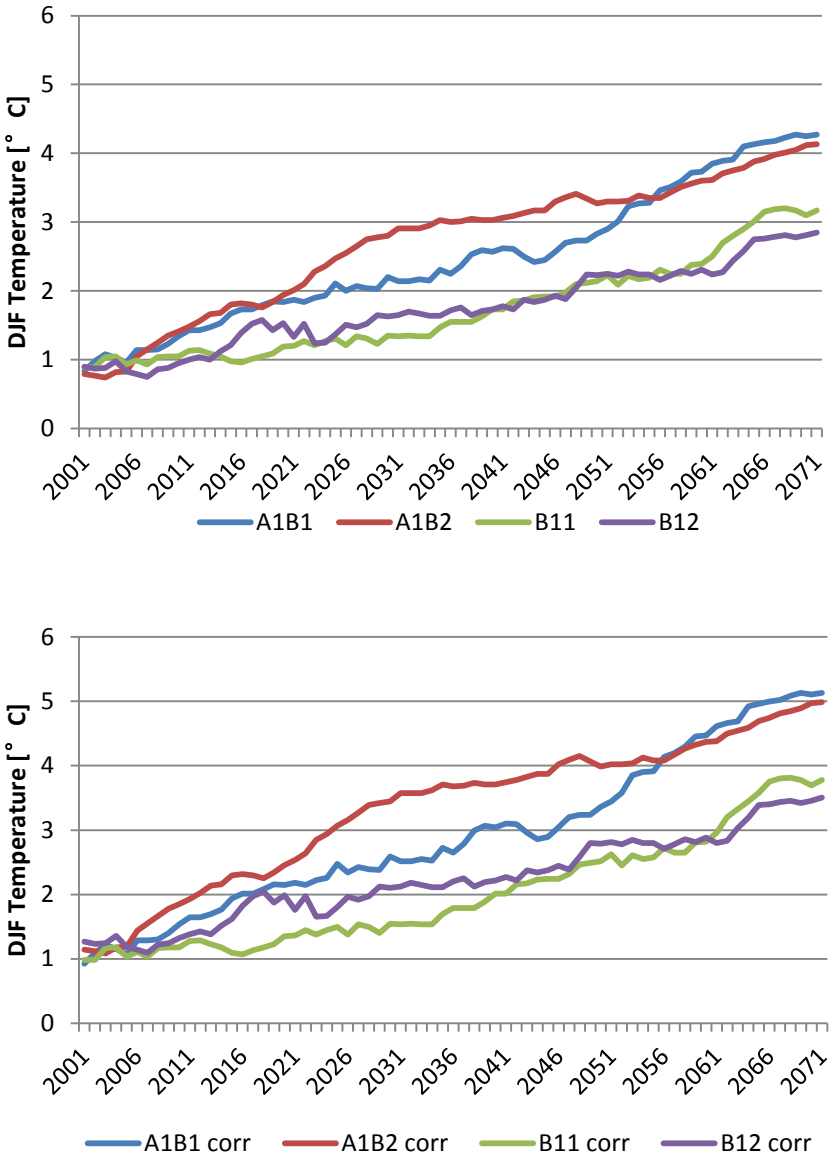

Figure 4.30 Correction comparison of 50P of winter Temperature in Lindenberg 2001-2100

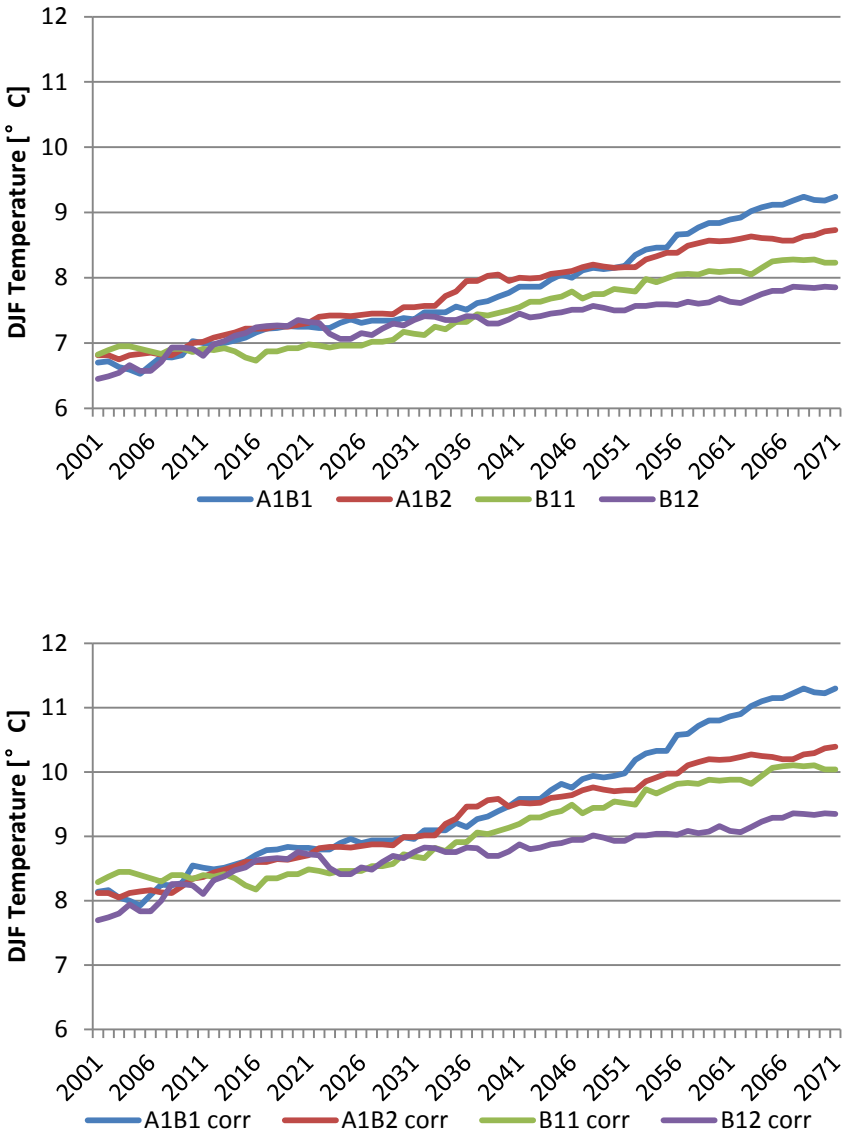

Figure 4.31 Correction comparison of 95P of winter Temperature in Lindenberg 2001-2100

For winter Temperatures corrections, the altered pattern is the same. The temperature values are elevated by 2-3K; middle range values are modified more than the extreme values; the growth rate of the next century is altered 0.5K compared to the original rate (seen in table 4.10); and the frequency of extreme high temperature events are higher and the frequency of extreme low temperature events are lower by 8-9%, Eg. the temperature lower than -5°C in the period of 2001-2030 is corrected to 2%, 9% lower than the original value of 11% (seen in figure 4.32).

Table 4.10 Correction results on DJF temperature projections 7 stations ("2001" means data set 2001-2030; "2041" means data set 2041-2070; "2071" means data set 2071-2100; Δ means the temperature change between the 2 data sets of 2001-2030 and 2071-2100)

ANGERMUEDE					COTTBUS				LINDENBERG			
	2001[°c]	2041[°c]	2071[°c]	*Δ [K]*	2001[°c]	2041[°c]	2071[°c]	*Δ [K]*	2001[°c]	2041[°c]	2071[°c]	*Δ [K]*
A1B1 orig.	0.50	2.33	3.96	*3.46*	0.95	2.69	4.34	*3.39*	0.85	2.63	4.27	*3.42*
A1B1 corr.	1.17	3.49	5.56	*4.39*	1.46	3.66	5.74	*4.28*	0.93	3.12	5.13	*4.20*
A1B2 orig.	0.43	2.68	3.79	*3.36*	0.96	3.18	4.28	*3.32*	0.80	3.07	4.13	*3.33*
A1B2 corr.	1.36	3.99	5.30	*3.94*	1.74	4.35	5.65	*3.92*	1.15	3.76	4.99	*3.83*
B11 orig.	0.44	1.24	2.85	*2.41*	1.04	1.86	3.20	*2.16*	0.89	1.73	3.17	*2.28*
B11 corr.	1.09	2.11	4.15	*3.06*	1.58	2.61	4.30	*2.73*	0.98	2.01	3.78	*2.80*
B12 orig.	0.58	1.42	2.48	*1.90*	0.99	1.95	2.93	*1.94*	0.90	1.79	2.85	*1.95*
B12 corr.	1.53	2.52	3.76	*2.22*	1.77	2.90	4.06	*2.29*	1.27	2.28	3.50	*2.24*
NEURUPPIN					POTSDAM				TEMPELHOF			
	2001[°c]	2041[°c]	2071[°c]	*Δ [K]*	2001[°c]	2041[°c]	2071[°c]	*Δ [K]*	2001[°c]	2041[°c]	2071[°c]	*Δ [K]*
A1B1 orig.	0.82	2.58	4.24	*3.42*	1.23	3.10	4.64	*3.41*	0.78	2.60	4.31	*3.53*
A1B1 corr.	2.02	3.94	5.75	*3.73*	1.20	3.45	5.31	*4.11*	1.64	3.87	5.97	*4.34*
A1B2 orig.	0.79	3.04	4.07	*3.28*	1.23	3.47	4.51	*3.28*	0.78	3.05	4.15	*3.37*
A1B2 corr.	1.71	4.39	5.61	*3.90*	1.34	3.83	4.99	*3.64*	1.87	4.46	5.73	*3.86*
B11 orig.	0.83	1.60	3.08	*2.25*	1.36	2.15	3.47	*2.11*	0.83	1.73	3.15	*2.32*
B11 corr.	1.76	2.68	4.44	*2.68*	1.35	2.30	3.89	*2.54*	1.70	2.80	4.54	*2.84*
B12 orig.	0.88	1.74	2.77	*1.89*	1.34	2.27	3.24	*1.90*	0.86	1.79	2.85	*1.99*
B12 corr.	2.08	3.02	4.15	*2.07*	1.47	2.49	3.57	*2.11*	1.96	3.02	4.23	*2.27*

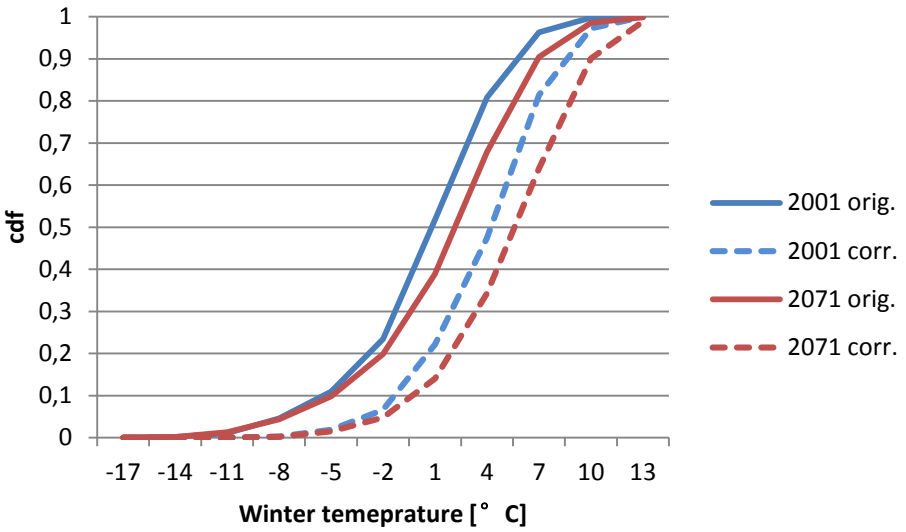

Figure 4.32 Cdf of DJF temperature in Cottbus, projection of A1B1

4.3.4 Extreme Precipitation

According to the analysis of historical runs, the simulations tend to have an overestimation for extreme precipitation and at some of the highest values, the simulated values could appear to be lower than the observed ones. The corrected values of projections therefore are altered to be smaller than original. Table 4.11 is the corrected results of 6 stations in the data set of 2071-2100 in simulation run of A1B1. For the lower parts of the extreme precipitation, the correction makes reduction adjustments on original values in a degree of 1-2mm. These reductions continue until the values get bigger. For the higher 10-20 percentile, the correction alters the simulation values in the other direction. For extreme high values, for example, 99 percentile of Cottbus and Angermuende, the values are increased as before in a grade of 10mm. In general, the correction modifies the projections in the way that a reduction for the lower values and an increase for extreme high values. In this sense, after correction, the extremes of the extreme precipitation events will come in higher grades.

Table 4.11 Corrected results of Extreme precipitation A1B1 2071-2100

	Lindenberg		Neuruppin		Cottbus	
Percentile	orig.	corr.	orig.	corr.	orig.	corr.
1%	9.6	7.6	9.4	7.9	9.0	8.3
5%	9.8	7.9	9.6	8.1	9.2	8.6
10%	10.2	8.4	9.8	8.3	9.5	9.0
50%	13.1	12.1	12.0	10.3	12.5	12.7
90%	23.4	24.6	22.5	19.3	23.9	27.1
95%	27.9	29.9	32.4	27.0	28.6	33.1
99%	44.4	48.9	60.4	46.6	64.0	78.4
	Potsdam		Angermuende		Tempelhof	
Percentile	orig.	corr.	orig.	corr.	orig.	corr.
1%	8.5	8.3	9.1	7.7	9.5	7.9
5%	8.7	8.5	9.2	7.8	9.7	8.1
10%	8.9	8.7	9.5	8.0	10.0	8.5
50%	12.0	11.5	11.9	10.1	12.8	12.1
90%	22.8	21.5	23.3	21.8	22.6	24.8
95%	31.8	29.8	30.2	30.1	27.8	31.7
99%	48.8	45.6	55.4	67.9	41.0	49.7

To reveal the climate change signal, graphs compare original and corrected values with the same percentile are created and shown in figure 4.33 to figure 4.35. The changing trend of extreme precipitation remains the same, which is extreme daily precipitation, will continue to be stronger and higher in the next century, especially the extreme high precipitation events and after correction, this trend is even amplified. As mentioned, the correction makes a reduction on values for lower parts of 95p precipitation, and an increase in extreme high precipitation, leaving the relationships between projections unchanged. In the example of Cottbus, except that the projection of A1B2 does not have a strong indication of precipitation increasing, the other 3 projections show the change in different levels. A1B1 and B12 present a steady increase over the century in the whole distribution, and the gradient of increasing are bigger for higher values. In the lower percentile of 5p, the extreme daily precipitation

increased from 8mm in the beginning to the 8.7mm in 2071-2100 and for median values, this increase is 1mm from 12-13, but for the extreme percentiles, the change in values are much elevated to 5-10mm. B11 simulations show an even rapider growing for extreme events; after correction, the 95p of 95p precipitation increased from 30mm to 45mm, which compared to the original simulation is enlarged. All these results indicate that the correction magnify the climate change signals on extreme daily precipitations.

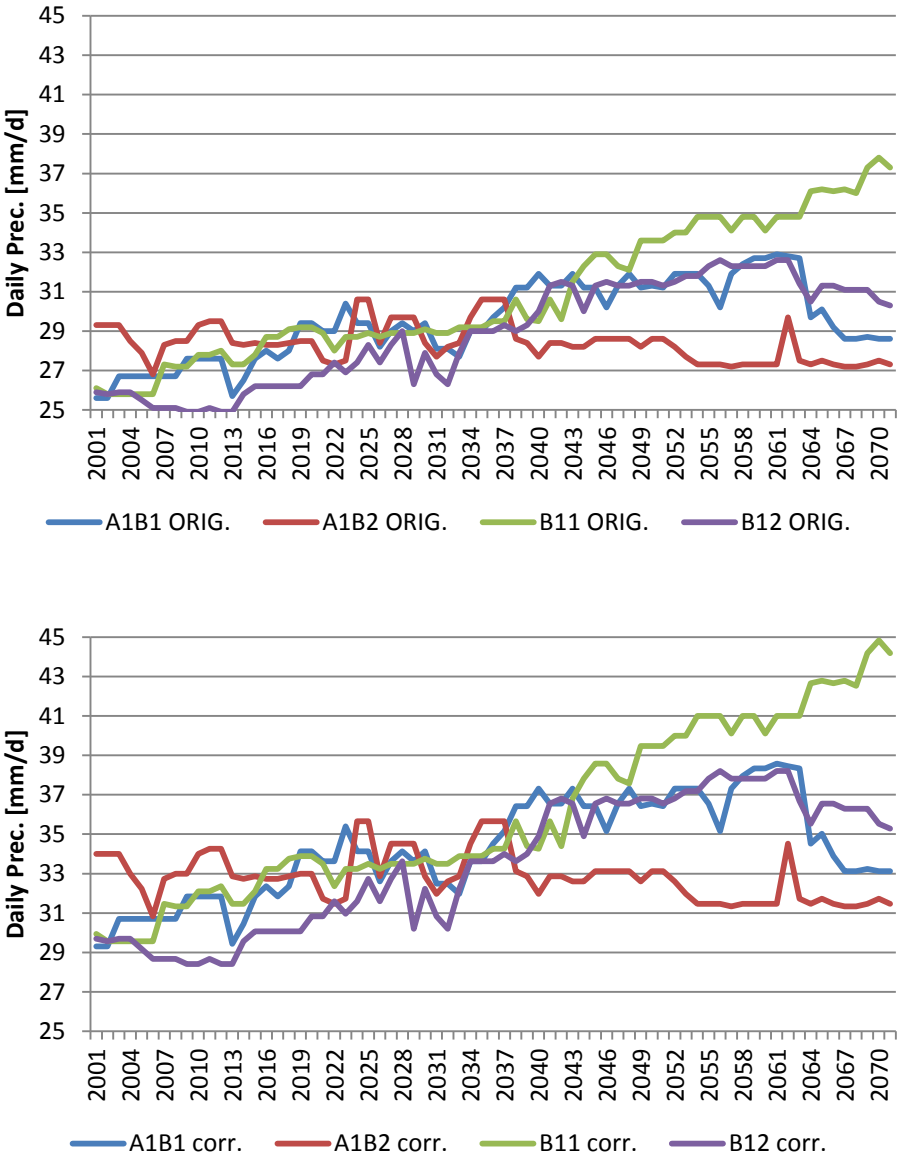

Figure 4.33 Correction comparison of 95P of extreme precipitation in Cottbus 2001-2100

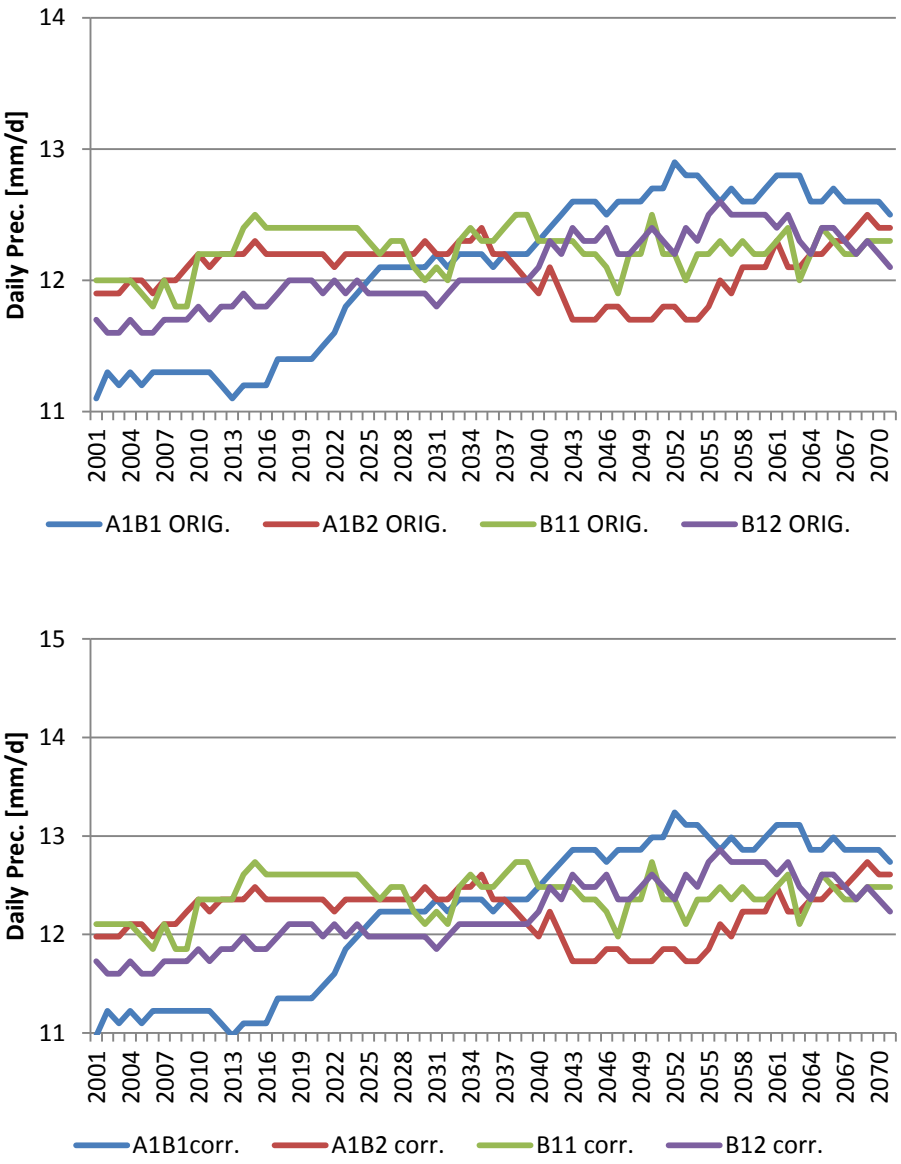

Figure 4.34 Correction comparison of 50P of extreme precipitation in Cottbus 2001-2100

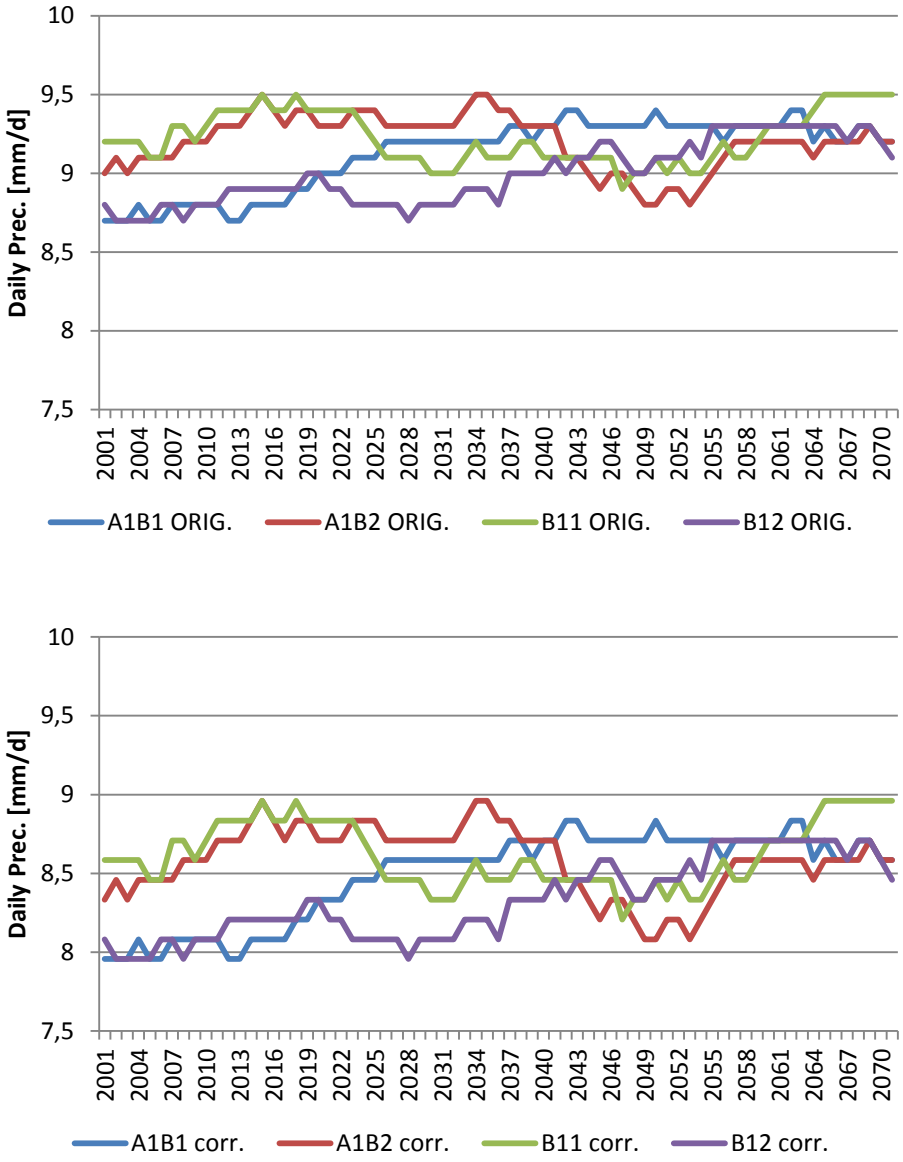

Figure 4.35 Correction comparison of 5P of extreme precipitation in Cottbus 2001-2100

Unlike the strongly increasing temperature, the- monthly precipitations over the next century do not present an obvious changing pattern. The correction on monthly precipitation merely altered the values at the same percentage smaller, seen in table 4.12. However, at different percentile, the correction does not reduce the values in the same amount. For example the data set of 2001-2030 of A1B1, comparing the original and corrected values, the reductions at 1%,5%,10%,50%, 90% and 95% are 5.4, 9.2, 11, 26.8, 18.2, 16.6, 10.2 respectively. The reductions are neither constant nor linear

with the increase of values, but experienced an increase and then decrease course. When the original values are smaller, the reductions are smaller, and increase with the original values up to a high percentile. And after 90%, at extreme values, the reductions are not as strong as before.

Table 4.12 Original and corrected monthly precipitations in A1B1.

	A1B1 (2001-2030)		A1B1 (2041-2070)		A1B1 (2071-2100)	
Percentile	Orig.[mm]	Corr.	Orig.	Corr.	Orig.	Corr.
1%	10.7	5.3	10.4	5.1	11.8	6.0
5%	19.7	11.5	23.3	14.1	19.7	11.5
10%	29.6	18.6	28.4	17.8	25.5	15.6
50%	58.7	41.9	62.0	44.8	59.3	42.4
90%	97.0	78.8	105.8	88.4	103.2	85.5
95%	110.8	94.2	127.9	115.1	119.9	105.1
99%	135.7	125.5	162.9	166.0	160.4	162.0

As for the changing pattern over the century, the signal is not very clear. With some fluctuations during some periods, the general pattern is that the monthly precipitation will not experience a dramatic change even after the correction seen in figure 4.36 to figure 4.38.

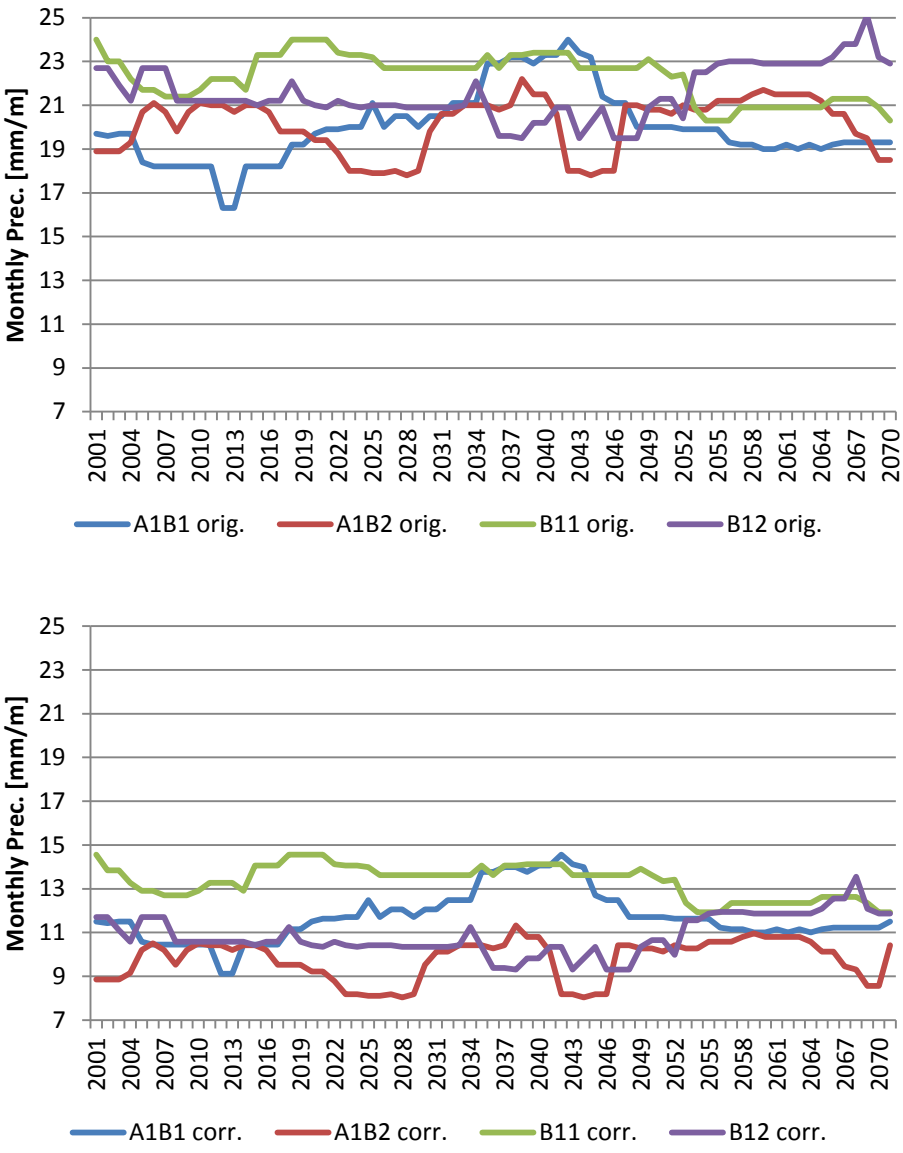

Figure 4.36 Correction comparison of 5P of monthly precipitation in Cottbus 2001-2100

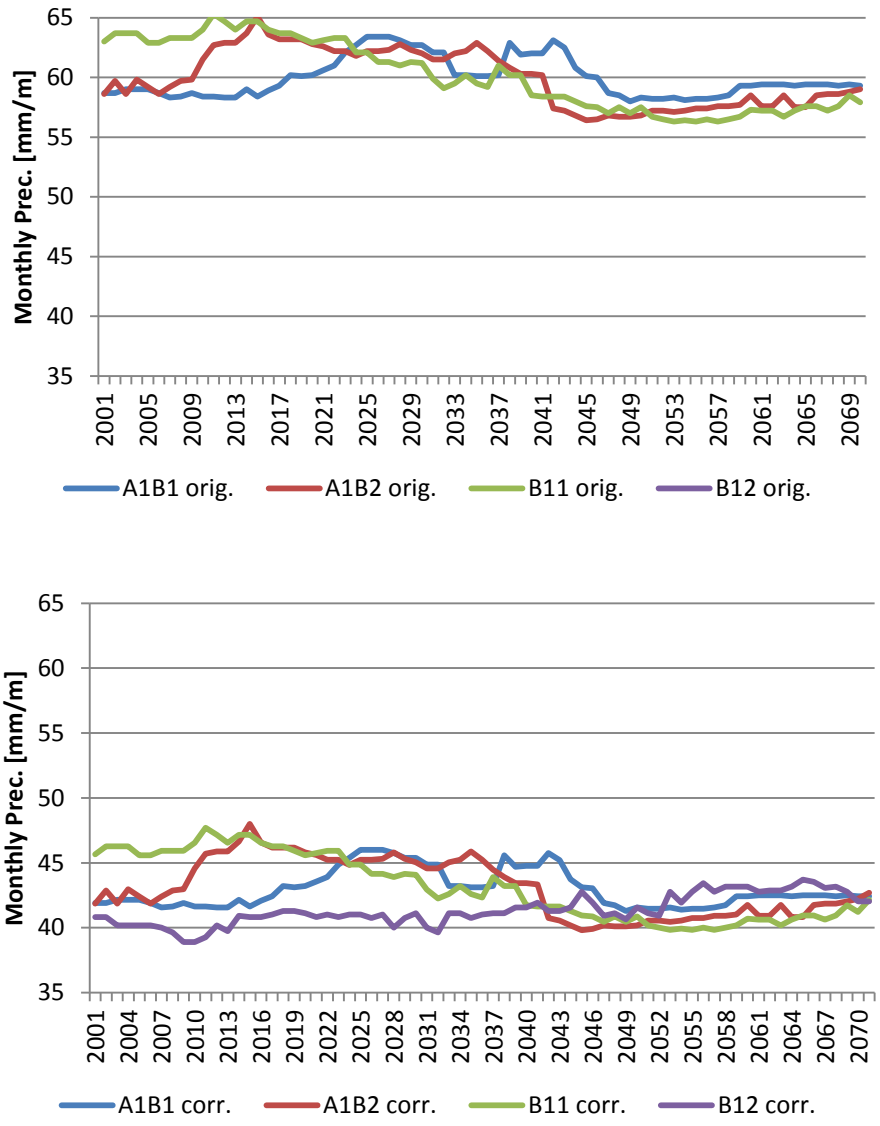

Figure 4.37 Correction comparison of 50P of monthly precipitation in Cottbus 2001-2100

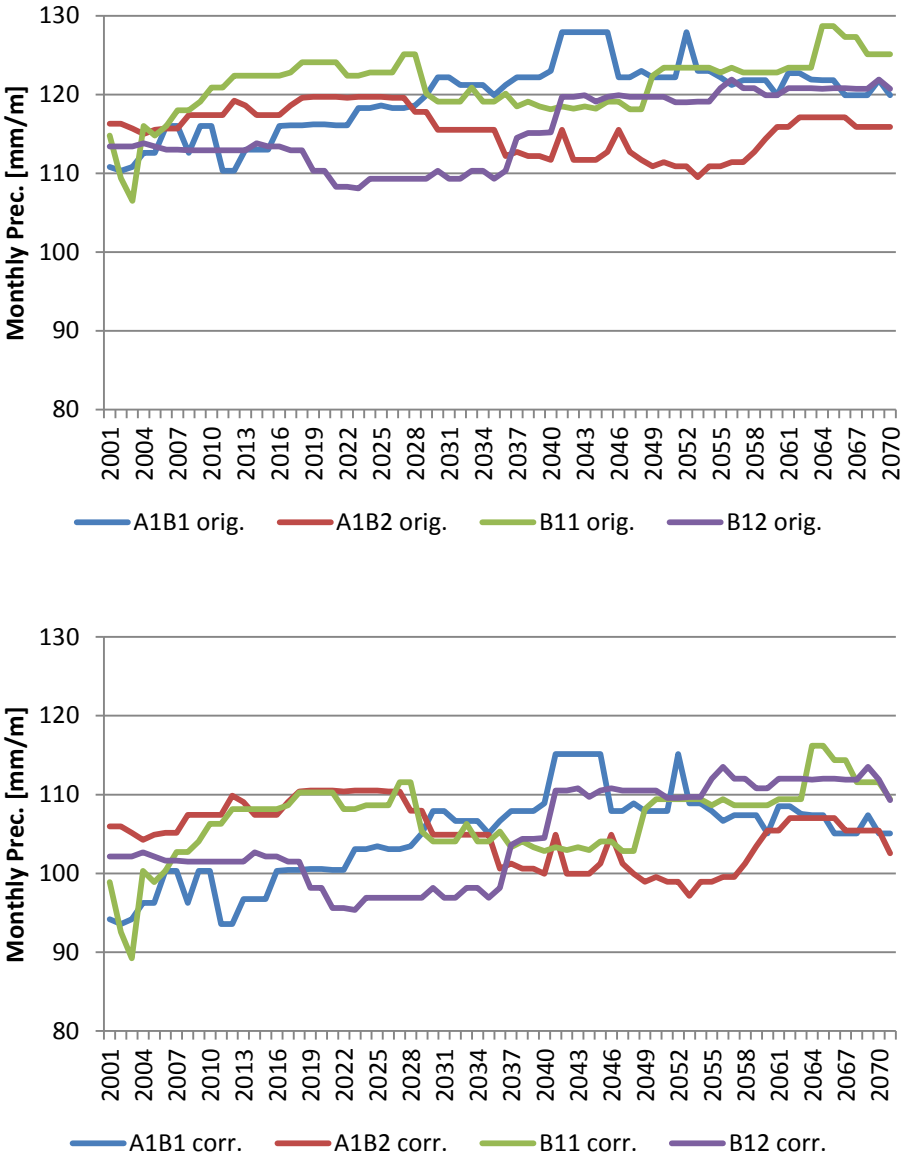

Figure 4.38 Correction comparison of 95P of monthly precipitation in Cottbus 2001-2100

The average of 5p monthly precipitation is around 20-25mm, and after correction, the values are reduced to 10-15mm. This reduction is stronger by 50 percentile, which is 55-65mm to 40-45mm.

In summary, monthly precipitation do not appear to increase in the future, which is not changed by the correction. The correction changes the intensity of the precipitation to a lower level. After correction, there will not be as much precipitation as originally simulated.

5 Conclusion

The analysis shows that the CLM model overestimates the precipitation and a cold bias on extreme high temperature (95P T) and a warm bias on extreme low temperature (5P T). The distribution oriented bias correction method is able to reduce these biases into satisfying results. The extreme daily temperature bias is reduced from 1-2K to less than 0.1K and the extreme daily precipitation bias is reduced from more than 2 mm/d to less than 0.75mm/d. The monthly precipitation and summer temperature have achieved the expected results as well: the former bias is reduced from more than 10mm to less than 2mm and latter is also reduced to less than 0.1K. For the winter temperature, the correction is not as effective for some stations, due to the small original biases. The daily temperature difference simulations are successfully corrected in a similar result, that the bias afterwards is less than 0.5K. The corrections made on the runs of 1972-2008 also confirm the effectiveness on the simulations involved projections.

The corrected projection simulations suggest that the extreme temperatures are about to increase both in intensity and in frequency. Compared to the original simulations, the corrected results indicate that the extreme temperatures are elevated by 1-2K based on the original simulated values and by the end of this century, compared to the period of 2001-2030, the average of extreme temperature will be increased by 2K up to more than 26°C. The occurrence probabilities of extreme events are largely elevated as well. The summer temperature will be higher, compared to the original simulated data of average temperature of 18°C, the corrected data on the end of the century is almost 21°C. The daily temperature difference however, does not appear to be increasing over the century, but the correction does elevate the values of the differences. On the aspect of precipitation, the extreme precipitation after correction is meant to be more severe and frequent as well.

This correction method is able to achieve positive results on the bias correction and possess the advantages that other methods do not have, such as the potential to analyze on future projections, the ability to correct all kinds of parameter simulations, and the correction customized to distinctive distribution behavior. The correction has however its limitation as well. The difficulty of determining the best fitted distribution for each kind of parameter is counted as one disadvantage, which can be simplified by the help of Easyfit software. The other one is the unsatisfying results on some samples

which the original biases are low. When the limitations are dealt with cautions, the bias correction method is worth consideration in other simulations and parameters analysis.

Literature

Ahrens, B., 2003: Rainfall downscaling in an alpine watershed applying a multiresolution approach. Journal of Geophysical Research 108: doi: 10.1029/2001JD001485. issn: 0148-0227.

Beniston, M., Stephenson, D., Christensen, O., Ferro, C., Frei, C., Goyette, S., Halsnaes, K., Holt, T., Jyllhae, K., Koffi, B., Palutikof, J., Schoell, R., Semmler, T., and Woth, K., 2006: 'Current and future extreme climatic events in Europe: observation and modeling studies conducted within the EU "PRUDENCE" project'.

Berg, P., Panitz, H.-J., Schaedler, G., Feldmann, H.,Kottmeier, Ch., 2011: Modelling Regional Climate Change in Germany. In: High Performance Computing in Science and Engineering '10 [W. E. Nagel, D. Kroener, M. Resch (Eds.)]. DOI 10.1007/978-3-642-15748-6_34, Springer Berlin Heidelberg New York 2011, pp. 467-478.

Boberg, F., Berg. P., Thejll, F., Gutowski,W.J., and Christensen, J.H., 2008: Improved confidence in climate change projections of precipitation evaluated using daily statistics from the PRUDENCE ensemble, Clim. Dyn., doi:10.1007/s00382-008-0446-y.

Boehm, U., Kuechen, M., Ahrens, W., Blocj, A., Hauffe, D., Keuler, K., Rockel, B. and Will, A., 2006: CLM-The Climate Version of LM: Brief Description and Long-Term Applications. – COSMO Newsletter No 6, German Weather Service (DWD), P.O. Box 100465, 63004 Offen-bach, Germany, 225–235.

Bronstert A., 2003: Floods and climate change: interactions and impacts. Risk Anal 23(3):545–557

Christensen, J. H., Hewitson, B., Busuioc, A., Chen,B., Gao. X., Held,I., Jones, R., Kolli, R.K., Kwon,W.T., Laprise,R., Magana Rueda, L., Mearns, C.G., Menendez, A., Rinke, A., and Whetton, P., 2007: Regional Climate Projections, in: Climate Change 2007: The Physical Science Basis. Contribution of Working Group I to the Fourth Assessment Report of the Intergovernmental Panel on Climate Change. Eds. S. Solomon, D. Qin, M. Manning, Z. Chen, M. Marquis, K.B. Averyt, and M. Tignor, Cambridge University Press, Cambridge, United Kingdom and New York, NY, USA

Coles, S., 2001: An Introduction to Statistical Modeling of Extreme Values. Springer Series in Statistics. Springer Verlag London. 208p

Disse, M. and Engel, H., 2001: Flood events in the Rhine basin: genesis, influences and mitigation, Nat. Hazards, 23, 271–290, doi:10.1023 /a:1011142402374, 2001.

Dobler, A. and Ahrens, B., 2010: Analysis of the Indian summer monsoon system in the regional climate model COSMO-CLM, Journal of Geophysical Research-Atmosphere, 115, D16, D16101, doi: 10.1175/2010JAS3359.1

Doms, G., 2009: A Description of the Nonhydrostatic Regional COSMO-Model, Printed at Deutscher Wetterdienst, P.O. Box 100465, 63004 Offenbach, Germany. available

Dragic, A., Anicin, I., Banjanac, R., Udovicic, V., Jokovic, D., Maletic,D. and Puzovic, J., 2011: Forbush decreases – clouds relation in the neutron monitor era, Astrophysics and Space Sciences Transactions, Published: 31 August 2011

Hay, L. E., Wilby, R. J. L., and Leavesley, G. H., 2000: A comparison of delta change and downscaled GCM scenarios for three mountainous basins in the United States, J. Am. Water Resour. As., 36, 387–397, doi:10.1111/j.1752-1688.2000.tb04276.

Hay, L. E. and Clark, M. P., 2003: Use of statistically and dynamically downscaled atmospheric model output for hydrologic simulations in three mountainous basins in the Western United States, J. Hydrol., 282, 56–75, doi:10.1016/s0022-1694(03)00252.

Hendl, M., 1994: Das Klima des Norddeutschen Tieflandes. In: H. Liedtke, J. Marcinek (Hrsg.): Physische Geographie Deutschlands. 559 S., Gotha 1994, ISBN 3-623-00840-0

Hollweg, H.J., Boehm, U., Fast, I., Hennemuth, B., Keuler, K., Keup-Thiel, E., Lautenschlager, M., Legutke, S., Radtke, K., Rockel, B., Schubert, M., Will, A., Woldt, M. and Wundram, C., 2008: Ensemble simulations over Europe with the regional climate model CLM forced with IPCC AR4 global scenarios. Technical Report No. 3, Model and Data Group at the Max Planck Institute for Meteorology, Hamburg.ISSN printed: 1619-2249, ISSN electronic: 1619–2257

Holsten, A., Vetter, T., Vohland, K. and Krysanova, V., 2009: Impact of climate change on soil moisture dynamics in Brandenburg with a focus on nature conservation areas. Ecological Modelling, Volume 220, Issue 17, 10 September 2009, Pages 2076–2087

Huang, SC., Hattermann, FF., Krysanova, V. and Bronstert, A., 2013: Projections of climate change impacts on river flood conditions in Germany by combining three different RCMs with a regional eco-hydrological model, Climate Change, 116, 3-4, pp. 631-663, doi: 10.1007/s10584-012-0586-2

Katz, R.W., 1999: Extreme value theory for precipitation: sensitivity analysis for climate change. Adv Water Resour 23:133

Kjellstroem, E., Baerring, L., Jacob, D., Jones, R., Lenderink, G. and Schaer, C., 2007, Modelling daily temperature extremes: Recent climate and future changes over Europe, Clim. Change, 81, 249–265, doi:10.1007/s10584-006-9220-5.

Kreibich, H. and Thieken, A. H., 2009: Coping with floods in the city of Dresden, Germany. - Natural Hazards, 51, 3, 423-436

Leander, R. and Buishand, T.A., 2007: Re-sampling of regional climate model output for the simulation of extreme river flows. J Hydrol 332(3–4):487–496

Lutz, J., Volkholz, J. and Gerstengarbe, F.W., 2013: Climate projections for southern Africa using complementary methods, International Journal of Climate Change Strategies and Management, 5, 2, 130-151, doi: 10.1108/17568691311327550

Meng, Y., Jiang, T., Su, B. and Zhang, J., 2013: Temperature Simulation Assessment by High-resolution Regional Climate Model(CCLM)in Poyang Lake Basin, Chinese Journal of Agrometeorology, 34, 2, pp. 123-129.
Meehl GA, Tebaldi C, 2004: More intense, more frequent, and longer lasting heat waves in the 21st century. Science 305:994–997

Moron, V., Robertson, A. W., Ward, M. N. and Ndiaye, O., 2008: Weather types and rainfall over Senegal. Part II: Downscaling of GCM simulations, J. Climate, 21, 288–307

Nakicenovic, N. and Swart, R., 2000: Special Report on Emissions Scenarios: A SpecialReport of Working Group III of the Intergovernmental Panel on Climate Change, Cambridge University Press, Cambridge, U.K., 599 pp. Available online at: http://www.grida.no/climate/ipcc/emission/index.htm

Orlanski, I., 1975: A rational subdivision of scales for atmospheric processes. Bulletin of the American Meteorological Society 56 (5): 527–530.

Panitz, H.-J., Schaedler, G. and Feldmann, H., 2010: Modelling Regional Climate Changes in Southwest Germany, pp. 429 - 441, in: High Performance Computing in Science and Engineering '09. Transactions of the High Performance Computing Center Stuttgart (HLRS) 2009 (Eds. : W. E. Nagel, D. B. Kroener, M. M. Resch); Springer Verlag Berlin Heidelberg 2010; DOI 10.1007/978-3-642-04665-0 ISBN 978-3-642-04664-3

Panitz, H.-J., Dosio, A., Buechner, M., Luethi, D. and Keuler, K., 2013: COSMO-CLM (CCLM) Climate Simulations over CORDEX Africa Domain: Analysis of the ERA-Interim Driven Simulations at 0.44° and 0.22° Resolution. Climate Dyn., DOI 10.1007/s00382-013-1834-5

Piani, C., Haerter, J. O. and Coppola, E., 2007: Regional probabilistic forecasts from a multithousand, multi-model ensemble of simulations. J Geophys Res 112:D24108. doi:10.1029/2007JD008712

Piani C., Haerter. J. O. and Coppola, E, 2009: Statistical bias correction for daily precipitation in regional climate models over Europe. Theor Appl Climatol (2010) 99:187–192 DOI 10.1007/s00704-009-0134-9

Ritzema, H.P., 1994: Subsurface Flow to Drains. In: Ritzema, H.P (Ed.), Drainage Principles and Applications, 2nd edition, International Institute for Land Reclamation and Improvement, Wageningen, pg. 263-303.

Rockel, B. and Geyer, B., 2008: The performance of the regional climate model CLM in different climate regions, based on the example of precipitation, Meteorol. Z., 17 (4), 487-498

Schoenwiese, C.D., 2006: Praktische Statistik fuer Meteorologen und Geowissenschaftler. Gebrueder Borntraeger, Berlin, Stuttgart,. ISBN 978-3-443-01057-7.

Song, G., Chen, G., Jiang, L., Zhang, Y., Zhao, N., Chen, B. and Kan, H., 2008, Diurnal temperature range as a novel risk factor for COPD death. Respirology, 13: 1066–1069. doi: 10.1111/j.1440-1843.2008.01401.x

Tang, H., Eronen, JT., Micheels, A. and Ahrens, B., 2012: Strong interannual variation of the Indian summer monsoon in the Late Miocene, Climate Dynamics, 41, 1, pp. 135-153.

Themessl, M. J., Gobiet, A., and Leuprecht, A., 2011: Empirical-statistical downscaling and error correction of daily precipitation from regional climate models, Int. J. Climatol., 31, 1530–1544, doi:10.1002/joc.2168.

Tiedtke, M., 1989: A Comprehensive Mass Flux Scheme for Cumulus Parameterization in Large-Scale Models. Mon. Wea. Rev., 117, 1779–1800. doi: http://dx.doi.org/10.1175/1520-0493(1989)117<1779:ACMFSF>2.0.CO;2

Wood, A. W., Leung, L. R., Sridhar, V. and Lettenmaier, D. P., 2004: Hydrologic implications of dynamical and statistical approaches to downscaling climate model outputs, Climatic Change,62, 189–216

Zhong, J., Su, B., Zhai, J. and Jiang, T., 2013: Distribution Characteristics and Future Trends of Daily Precipitation in China, Progressus Inquisitiones de Mutatione Climatis, 9, 2, pp. 89-95.